The Phylogeny of Carangiform Fishes: Morphological and Genomic Investigations of a New Fish Clade

Authors: Girard, Matthew G., Davis, Matthew P., and Smith, W. Leo

Source: Copeia, 108(2) : 265-298

Published By: The American Society of Ichthyologists and Herpetologists

URL: https://doi.org/10.1643/CI-19-320

Copeia

Copeia 108, No. 2, 2020, 265–298

STOYE AWARD CONTRIBUTION

The Phylogeny of Carangiform Fishes: Morphological and Genomic Investigations of a New Fish Clade

Matthew G. Girard[1,2], Matthew P. Davis[3], and W. Leo Smith[1,2]

Surveys and analyses of anatomical characters have allowed researchers to describe a wealth of anatomical features and contribute to our evolutionary understanding of fishes for centuries. However, most of these studies have focused on specific lineages or families rather than the broader evolutionary relationships. As such, there has been a lack of progress inferring higher-level relationships among percomorphs. With the use of large-scale DNA-based methods in multiple studies over the past two decades, the backbone of the phylogeny of fishes is becoming increasingly understood. Taking this DNA-based phylogenetic backbone into account, we have the opportunity to integrate discrete morphological characters and DNA sequence data to test earlier topologies and provide new and improved hypotheses of relationships. The carangiform fishes, which include approximately 1,100 species in 29–34 families, were initially recovered as a clade in DNA-based studies. Subsequent to its initial recovery, many molecular phylogenies have been published assessing carangiform relationships, but these studies present a conflicting array of hypotheses on the intrarelationships of this clade. In addition to this diversity of hypotheses, no studies have explicitly diagnosed the clade or its major subgroups from a morphological perspective or conducted a simultaneous analysis to put forth synapomorphies for relationships across the Carangiformes using a combination of molecular and morphological data. In this study, we performed combined analyses of new and previously identified discrete morphological characters and new and previously published genome-scale data to characterize the evolutionary history and anatomical variation within this clade of fishes. Our novel morphological dataset included 201 hard and soft tissue characters, and it was combined with a novel dataset of 463 ultraconserved element loci. Our combined analysis of these data resulted in a monophyletic Carangiformes, with a series of subclades nested within. We put forth a series of subordinal names based on the recovered branching pattern, morphological character evidence, and relative stability in large-scale studies. These suborders are the Centropomoidei, which includes Centropomidae, Lactariidae, Latidae, and Sphyraenidae; Polynemoidei, which includes Polynemidae and the infraorder Pleuronectoideo; Toxotoidei, which includes Leptobramidae and Toxotidae; Nematistioidei, which includes Nematistiidae; and Menoidei, which includes Menidae and Xiphioidea. Furthermore, we highlight and discuss morphological characters that support the relationships between two or more lineages of carangiform fishes. Finally, we highlight patterns of morphological convergence among some carangiform fishes and their previously hypothesized sister lineages.

FOR centuries, studies on the evolution of fishes were based on surveys and analyses of anatomical characters. Comparisons among wet and dry skeletons (e.g., Olney et al., 1993; Holcroft and Wiley, 2015), and surveys of characters through different visualization techniques, such as scanning electron microscopy and histology (e.g., Webb, 1989a; Ghedotti et al., 2018), x-ray computed tomography (e.g., Schaefer, 2003; Webb et al., 2006; Schwarzhans et al., 2018), and magnetic resonance imaging (e.g., Chakrabarty et al., 2011; Graham et al., 2014), have helped identify a wealth of anatomical features that have facilitated our interpretation of fish evolution (e.g., Potthoff et al., 1986; Springer and Johnson, 2004; Hilton et al., 2015). These techniques have helped us discover, differentiate, and assess the homology and phylogenetic significance of particular anatomical features (e.g., Johnson, 1975; Gemballa and Britz, 1998), were critical for identifying characters that suggested novel placements of taxa within the broader phylogeny of fishes (e.g., Rosen and Parenti, 1981; Johnson and Patterson, 1993; Stiassny, 1993), allowed researchers to assess the intrarelationships of lineages of fishes hypothesized to be closely related (e.g., Parenti, 1981; Baldwin and Johnson, 1996; Harold and Weitzman, 1996), or aided the search for the sister group of well-established clades (e.g., Gill and Mooi, 1993; Johnson and Brothers, 1993). Despite this breadth of studies, relatively few explicit anatomical studies have focused on the broader evolutionary relationships of fishes (exceptions include: Johnson and Patterson, 1993; Patterson and Johnson, 1995; Springer and Orrell, 2004), at least compared to the large number of broad-scale DNA-based studies (e.g., Chen et al., 2003; Miya et al., 2003; Smith and Wheeler, 2006; Near et al., 2012; Betancur-R. et al., 2013a; Smith et al., 2016). The limited taxonomic scope common with anatomical phylogenetic studies likely results from the difficult and time-consuming effort needed to examine and distinguish homologous morphological characters across a wide diversity of taxa. The overwhelming diversity of taxa and striking anatomical convergences among the perch-like

[1] Biodiversity Institute, 1345 Jayhawk Boulevard, University of Kansas, Lawrence, Kansas 66045; Email: (MGG) mgirard@ku.edu. Send reprint requests to MGG.
[2] Department of Ecology and Evolutionary Biology, University of Kansas, Lawrence, Kansas 66045.
[3] Department of Biological Sciences, St. Cloud State University, St. Cloud, Minnesota 56301.
Submitted: 1 November 2019. Accepted: 12 February 2020. Associate Editor: M. T. Craig.
 DOI: 10.1643/CI-19-320 Published online: 8 May 2020

fishes (Percomorpha), in particular, has played a substantial role in our delayed inference of the phylogenetic relationships of the clade (Johnson, 1984, 1993; Smith, 2010). Two of the most important papers in the systematics of percomorph fishes are Rosen (1973) and Johnson and Patterson (1993), who spent more of their writing delimiting the Percomorpha rather than resolving relationships within the species group. Rosen (1973) first defined the Percomorpha, and Johnson and Patterson (1993) altered the taxonomic composition of Percomorpha by including the Atherinomorpha (*sensu* Parenti, 1993) and removing their Beryciformes, Lampriformes, Polymixiiformes, Stephanoberyciformes, and Zeiformes. While Johnson and Patterson (1993) supported their revised Percomorpha by the presence of eight anatomical synapomorphies, there have been few subsequent explorations of percomorph anatomy since. As such, the phylogeny of Percomorpha remains unresolved based on morphological data alone.

Beginning in the early 1990s, DNA-based phylogenetic methods allowed researchers to hypothesize novel sets of relationships among fishes (e.g., Normark et al., 1991; Tang et al., 1999; Wiley et al., 2000). More recently, the use of large-scale DNA-based methods (e.g., Chen et al., 2003; Miya et al., 2003; Smith and Craig, 2007; Near et al., 2012, 2013; Betancur-R. et al., 2013a, 2013b, 2017; Rabosky et al., 2018) has allowed researchers to identify novel hypotheses of relationships among fishes, to revise the composition of clades (e.g., Paracanthopterygii; Grande et al., 2013), and to recognize new percomorph subclades (e.g., Ovalentaria, Wainwright et al., 2012; Pelagia, Miya et al., 2013). While the relationships within these new and revised clades, and what to call them, remains contentious, the composition of many of these clades and the backbone of the phylogeny of fishes is becoming increasingly stable in these molecular studies. Recent genomic large-scale molecular datasets that include ultraconserved elements, transcriptomes, and exon capture (e.g., Alfaro et al., 2018; Hughes et al., 2018) are inferring similar phylogenetic hypotheses to prior large Sanger-DNA-based studies (e.g., Near et al., 2012, 2013; Betancur-R. et al., 2013b; Rabosky et al., 2018), but conflict remains as we get closer to the tips of the tree. With a DNA-based phylogenetic backbone providing an order-level framework for how fishes are related, we have the exciting opportunity to integrate different types of data, such as discrete morphological characters and DNA sequence data. We can use these data to test newly proposed sister groups and to provide new hypotheses of relationships based on the simultaneous analysis and study of molecular and morphological data. Exploring morphological features within a clade identified by the analysis of DNA sequence data can lead to the discovery of new anatomical synapomorphies that are a combination of novel morphological features as well as previously described characters that are investigated in the context of the revised taxonomic sampling. This combination of molecular and morphological data provide the data needed to propose new and more holistic phylogenies and classifications of fishes that include diagnostic anatomical features. Although these types of studies have been conducted for some of the newly recognized orders and larger groups (e.g., Grande et al., 2013, 2018; Smith and Busby, 2014; Smith et al., 2018a), few of these newly recovered clades have been studied morphologically and are in need of investigation.

There are many new clades identified by DNA-based analyses that need anatomical assessment or re-assessment, but few of these order-level clades are as morphologically diverse as the one that includes trevally jacks (Carangidae), moonfishes (Menidae), barracudas (Sphyraenidae), billfishes (Istiophoridae and Xiphiidae), and flatfishes (traditional Pleuronectiformes), among other families (Chen et al., 2003; Harrington et al., 2016; Campbell et al., 2019). This diverse clade has had numerous names proposed since its initial grouping (e.g., Clade L, Carangimorpha, Carangiformes, Carangimorphariae, Carangaria). Herein, this clade will be referred to as the Carangiformes. Carangiform fishes include approximately 1,100 species in 29–34 families and exhibit a number of notable evolutionary traits, such as modifications to the dorsal fin (Britz and Johnson, 2012; Friedman et al., 2013) and alterations of the feeding apparatus (Gregory and Conrad, 1937). Traditionally, most carangiform families were classified within the perciform suborder Percoidei (*sensu* Nelson, 2006), such as Carangidae, Centropomidae, Coryphaenidae, Echeneidae, Lactariidae, Latidae, Leptobramidae, Menidae, Nematistiidae, Polynemidae, Rachycentridae, and Toxotidae. The remainder of carangiform families were either placed in the Scombroidei (Istiophoridae, Sphyraenidae, Xiphiidae; Nelson, 2006) or the Pleuronectiformes (Achiridae, Achiropsettidae, Bothidae, Citharidae, Cynoglossidae, Paralichthodidae, Paralichthyidae, Pleuronectidae, Poecilopsettidae, Psettodidae, Rhombosoleidae, Samaridae, Scophthalmidae, and Soleidae; Nelson, 2006). Since its initial recovery as a clade in DNA-based studies (Clade L, Chen et al., 2003), many phylogenies have been published assessing carangiform relationships (e.g., Campbell et al., 2014a; Harrington et al., 2016; Rabosky et al., 2018), and these studies present a conflicting array of hypotheses of this clade. Comparing previous phylogenies highlights the conflicting relationships among families within the carangiform radiation, with only a few families consistently recovered as sister groups (Fig. 1; Smith and Wheeler, 2006; Li et al., 2011; Near et al., 2013; Betancur-R. and Ortí, 2014; Harrington et al., 2016; Mirande, 2016; Smith et al., 2016; Rabosky et al., 2018). In addition to this array of hypotheses, no studies have explicitly diagnosed the clade or its major subgroups from a morphological perspective. Furthermore, no studies have performed a simultaneous analysis to put forth synapomorphies for relationships across the Carangiformes using a combination of molecular and morphological data. In this study, we highlight anatomical features that support the carangiform fishes as a clade and the subclades within the carangiform radiation. Our approach includes combined analyses of new and previously identified discrete morphological characters and new and previously published genome-scale data to characterize the evolutionary history and anatomical variation within this clade of fishes.

MATERIALS AND METHODS

Hereafter, family-, subfamily-, and genus-level terminology follows Fricke et al. (2019) with the following exceptions: Percomorpha or "percomorph" refers to Percomorpha *sensu* Miya et al. (2003); Carangoidei or "carangoids" includes the families Carangidae, Coryphaenidae, Echeneidae, and Rachycentridae; the infraorder Pleuronectoideo or "pleuronectoids" includes all flatfish families, including

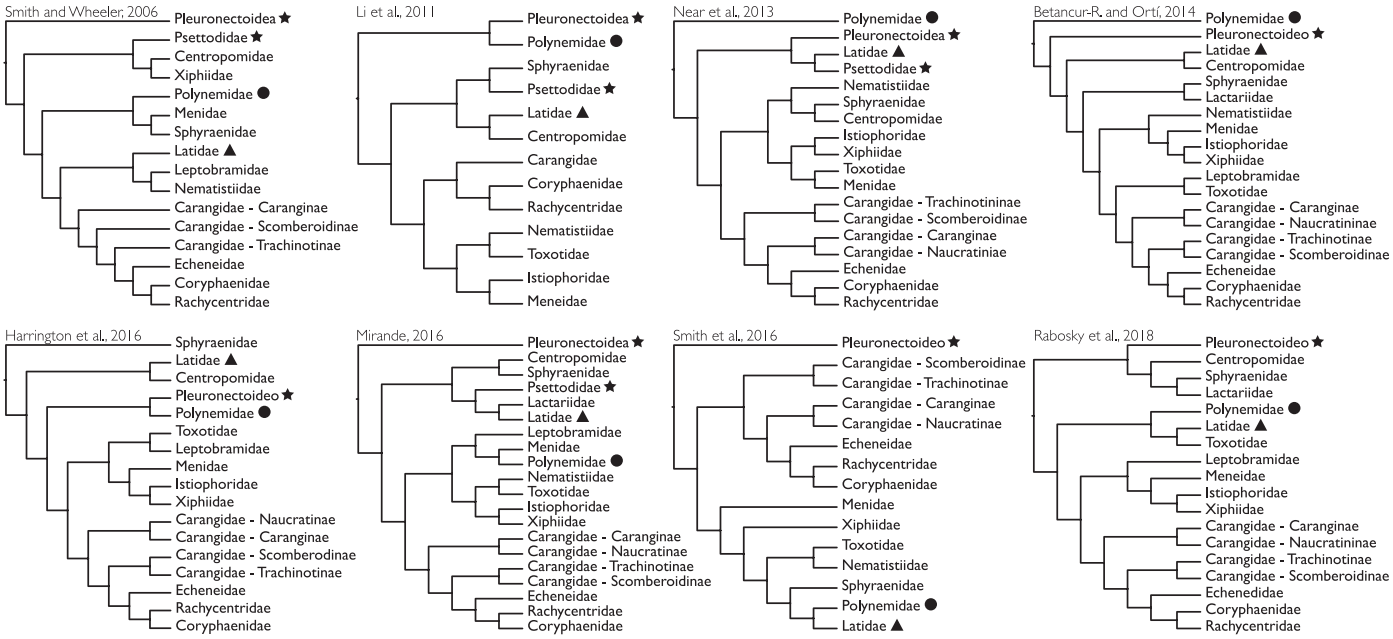

Fig. 1. Hypotheses of relationships among the Carangiformes based on the following molecular studies: Smith and Wheeler, 2006; Li et al., 2011; Near et al., 2013; Betancur-R. and Ortí, 2014; Harrington et al., 2016; Mirande, 2016; Smith et al., 2016; Rabosky et al., 2018. Latidae, Polynemidae, and members of the infraorder Pleuronectoidea are denoted by a triangle, a circle, and one or more stars, respectively, to highlight the conflicting hypotheses of carangiform relationships across previous DNA-based studies.

Psettodidae; Percoidei or "traditional percoids" refers to Percoidei *sensu* Johnson (1984); Scombroidei or "traditional scombroids" refers to Scombroidei *sensu* Collette et al. (1984); Echeneoidea includes the families Coryphaenidae, Echeneidae, and Rachycentridae *sensu* O'Toole (2002); Pleuronectoidea includes all flatfish families except Psettodidae; the subfamilies of Carangidae: Caranginae, Naucratinae, Scomberoidinae, and Trachinotinae follow Hilton and Johnson (2007).

Taxon sampling.—The choice of taxa is a critical component of any phylogenetic study, particularly for one focusing on a species-rich and morphologically diverse group like the Carangiformes. Many researchers have argued that the "groundplan" or "exemplar" approach is most appropriate when conducting a study such as the one herein, particularly when morphological data are included (e.g., Yeates, 1995; Prendini, 2000, 2001). Our focus is the interrelationships of the families of carangiform fishes exclusive of the species-rich flatfishes (≈73% of carangiform species diversity). As the monophyly of the Pleuronectoidea has been consistently recovered in morphological and molecular analyses (e.g., Chapleau, 1993; Harrington et al., 2016; Byrne et al., 2018), we only sampled two families from this clade to reduce the noise in the morphological matrix that would be created by densely sampling the asymmetric and highly aberrant flatfishes. Therefore, we took an exemplar approach when selecting taxa for our study, emphasizing morphological diversity and taking previous studies into account. Once selected, taxa were used in two matrices: one matrix composed of discrete morphological characters and a second matrix comprising DNA sequences of ultraconserved element loci (e.g., Harrington et al., 2016; hereafter, UCEs).

A total of 35 taxa, which includes eight outgroup taxa and 27 representatives of the carangiform fishes, were included in our morphological matrix. To provide a thorough test of carangiform monophyly and relationships, eight outgroup taxa were chosen based on the results of previous morphology-based (Starks, 1899; Johnson, 1984, 1993; Kang et al., 2017) and DNA-based studies (e.g., Wainwright et al., 2012; Betancur-R. et al., 2013a, 2013b; Near et al., 2013; Harrington et al., 2016; Rabsoky et al., 2018). These outgroups included taxa from the Centrarchidae, Channidae, Mugilidae, Nandidae, Percidae, Polycentridae, Sciaenidae, and Scombridae. Within the Carangiformes, all non-flatfish carangiform families, which include Carangidae, Centropomidae, Coryphaenidae, Echeneidae, Istiophoridae, Lactariidae, Latidae, Leptobramidae, Menidae, Nematistiidae, Polynemidae, Rachycentridae, Sphyraenidae, Toxotidae, and Xiphiidae, were sampled in our study. We included at least one representative of each of the four subfamilies of Carangidae to provide a limited test of the monophyly of the family, as members of the Echeneoidea have been found nested within the Carangidae in previous DNA-based hypotheses (e.g., Smith and Wheeler, 2006; Harrington et al., 2016; Rabosky et al., 2018). However, the limits and relationships within the Carangidae (*sensu* Nelson, 2006) were beyond the focus of this study. Additionally, many studies have recovered the non-monophyly of flatfishes (e.g., Smith and Wheeler, 2006; Li et al., 2009; Near et al., 2012, 2013; Betancur-R. et al., 2013b; Campbell et al., 2013), recovering Psettodidae as a separate and non-sister lineage from the Pleuronectoidea. Despite the recovery of flatfish non-monophyly, recent analyses based on either morphology (Chapleau, 1993; Hoshino, 2001) or DNA-sequence data (e.g., Betancur-R. et al., 2013a; Betancur-R. and Ortí, 2014; Campbell et al., 2014a; Harrington et al., 2016; Byrne et al., 2018; Rabosky et al., 2018) have recovered flatfishes as monophyletic. We sampled three flatfish families in our study, including members of the Achiridae, Psettodidae, and Scophthalmidae to provide a limited test of the monophyly of the Pleuro-

nectoideo, but, as noted above, testing the relationships within the Pleuronectoidea was outside of the focus of this study.

The molecular dataset in this study sampled 33 taxa, including eight outgroup taxa and 25 carangiform fishes. Tissue samples of *Lactarius lactarius* and *Psammoperca waigiensis* were not available for analysis and were represented in the combined matrix by morphological data exclusively. Every effort was made to match morphological and molecular vouchers at the species level. However, some congeners were used when building these datasets due to the difficulties in obtaining species-specific samples. Four congener taxa, two among the outgroup taxa (*Nandus, Scomber*) and two among carangiform fishes (*Trachinotus*, *Sphyraena*), were represented by different species of the same genus between the morphological and molecular matrices. Taxa represented by congeners were listed by only their genus in the analysis and resulting phylogeny. Lists of taxa used in both the morphological and molecular components of this study can be found in the Material Examined section and Supplemental Tables 1 and 2 (see Data Accessibility), respectively, with symbolic codes for institutional resource collections following Sabaj (2016). Both the morphological and molecular datasets were rooted on the scombroid *Scomber*.

Collection of morphological data.—We constructed a novel morphological dataset for this study that included 201 hard and soft tissue characters coded for carangiform and outgroup taxa sampled. Of the 201 characters included in the morphological dataset, approximately 80 characters were either explicitly coded from or modified from the following sources: Bridge, 1896; Gregory and Conrad, 1937; Smith and Bailey, 1962; Gosline, 1968; Smith-Vaniz and Staiger, 1973; Johnson, 1975; Greenwood, 1976; Freihofer, 1978; Fink, 1981; Nakamura, 1983; Collette et al., 1984; Johnson, 1984; Smith-Vaniz, 1984; Feltes, 1986; Johnson, 1986; Bannikov, 1987; Van Neer, 1987; Gushiken, 1988; Chapleau, 1993; Johnson and Patterson, 1993; Roberts, 1993; Leis, 1994; O'Toole, 2002; Otero, 2004; Springer and Smith-Vaniz, 2008; Hilton et al., 2010; Bräger and Moritz, 2016; Harrington et al., 2016; and Kang et al., 2017. An abbreviated version of these character descriptions is listed in Appendix 1, with a more detailed version listed in the Supplemental Appendix (see Data Accessibility). The final morphological matrix (Supplemental Table 1; see Data Accessibility) includes 6,922 of 7,035 possible entries and is thus 98% complete at the level of individual character states. Morphological characters were coded from whole ethanol specimens, disarticulated dry skeletons, and dissected cleared and stained specimens. Cleared and stained specimens prepared by the authors of this study were cleared and double-stained for bone and cartilage following the methods of Potthoff (1984) with the following modifications: Our cartilage staining solutions contained 10 mg of alcian powder per 100 mL of solution for specimens under 80 mm SL and 15 mg of alcian powder per 100 mL of solution for specimens over 80 mm SL. We also used 0.5 g of trypsin powder per 100 mL of solution for digestion. Cleared and doubled stained specimens were dissected following the protocol of Weitzman (1974) as it pertains to the circumorbital series, suspensorium, branchial basket, and shoulder girdle. All specimens coded in the morphological dataset, including specimen preparations and associated catalog numbers, can be found in the Material Examined section.

Imaging of morphology.—Morphological features were examined primarily with a Leica M205 C microscope, but were occasionally examined with a Nikon SMZ-18 stereomicroscope that has a P2-SHR plan apo 0.5X objective lens. Specimens and morphological features were visualized via digital photography using a variety of imaging techniques. Images were taken using a Nikon D500 with either a Venus Optics Laowa 60 mm f/2.8 2X Ultra-Macro lens or a Venus Optics Laowa 25 mm f/2.8 2.5–5X Ultra-Macro lens. Lighting for imaging was provided by either daylight LED lighting ($\leq$5000 K) or high-energy Royal Blue lighting (440–460 nm) emitted from two NIGHTSEA BlueStar flashlights. To view the stained autofluorescing anatomical features under Royal Blue lighting, we followed the protocol established by Smith et al. (2018b) with the following modification: a 60 mm B+W Dark Red MRC 091M filter was attached to the camera and 60 mm lens combination noted above in order to view the alizarin-stained autofluorescing features. In order to overcome difficulties in positioning specimens for photography and the small depth of field in high magnification images, several images were photographed via z-stacking (also known as focus stacking; see Smith et al., 2018b). Images for z-stacking were taken using the camera, lens, and optional filter combinations listed above with the camera attached to a WeMacro 100 mm focus stacking rail controlled by a Cognisys Stackshot Controller and Helicon Remote v3.9.5. Digital images at different focal distances were then algorithmically combined into a single composite image using Helicon Focus v6.7.1.

DNA extraction, locus amplification, and sequence alignment.—Prior to the extraction of DNA sequenced for UCE loci, muscle or fin clips were preserved in 95% ethanol, RNAlater Stabilization Solution (Thermo Fisher Scientific), or frozen (fresh) and stored at either –20°C, –80°C, or in liquid nitrogen. Either a DNeasy Tissue Extraction Kit (Qiagen) or a Maxwell RSC Blood DNA Kit and Instrument (Promega) was used to extract DNA from tissue samples following manufacturers' extraction protocols (with the exception of the replacement of the Blood DNA Kit's lysis buffer with Promega's tissue lysis buffer). For Qiagen DNeasy Kit extractions only, the first and second elution from a Qiagen filter were combined and dried to a volume of 102 µL using a Savant DNA120 SpeedVac Concentrator (Thermo Fisher Scientific). For Maxwell RSC extractions only, extractions were eluted into a volume of 102 µL. For both types of preparations, 2 µL of the raw DNA extracts were quantified using a Qubit Fluorometer 2.0 (Thermo Fisher Scientific) using the dsDNA BR Assay Kit (Thermo Fisher Scientific). When insufficient DNA was collected, multiple samples from the same specimen were extracted, combined, dried, and quantified again using the same methods stated above. Final quantified samples (100 µL in volume) were sent to Arbor Biosciences for library preparation (e.g., DNA shearing, size selection, cleanup), target capture, enrichment, sequencing on an Illumina HiSeq 2500 (Illumina), and demultiplexing. Target capture for UCE loci used the 500 UCE actinopterygian-loci probe set (Faircloth et al., 2013).

Demultiplexed sequence data from multiple runs were received in compressed FASTQ format from Arbor Bioscienc-

es. These data were uncompressed and combined into two read files per taxon. Data were then cleaned of adapter contamination and low-quality bases using the parallel wrapper illumiprocessor v2.0.7 (Faircloth, 2013) around trimmomatic v0.36 (Bolger et al., 2014). These cleaned sequencing reads were submitted to GenBank and have been assigned SRA Accession Numbers SRR11016325–SRR11016348 under BioProject PRJNA604383 (Supplemental Table 2; see Data Accessibility). Cleaned reads were then combined with previously published UCE data obtained from Harrington et al. (2016; BioProject Accession Number PRJNA341709; Supplemental Table 2; see Data Accessibility) and Alfaro et al. (2018; BioProject Accession Number PRJNA348720; Supplemental Table 2; see Data Accessibility). Assembly of all clean reads was completed using a python script (assemblo_abyss.py) within PHYLUCE v1.5.0 (Faircloth et al., 2012; Faircloth, 2016) in conjunction with ABySS v1.3.7 (Simpson et al., 2009). The *k*-mer parameter in ABySS was set to a value of 60. In order to identify taxon-specific contigs within the assembled UCE loci, contigs were aligned and assembled into a relational database containing all probes using a python script (match_contigs_to_loci.py, PHYLUCE) and LASTZ v1.02.00 (Harris, 2007). Minimum coverage and minimum identity for identifying UCEs were set to 80%. The PHYLUCE script get_match_counts.py was then used to search the relational database and generate a list of UCE loci shared among all taxa. This list was input into the PHYLUCE script get_fastas_from_match_counts.py to create a single FASTA file containing all UCE sequence data for all taxa. The data in this file were divided by locus using explode_get_fastas_file.py within PHYLUCE and then aligned using MAFFT v7 (Katoh and Standley, 2013). Each locus alignment that contained data from a minimum of 21 taxa (≈65% complete) was converted into PHYLIP-format files and prepared for analyses.

Partitioning schemes and nucleotide substitution models.—A total of 463 aligned UCE loci were analyzed in our study. Across all UCE loci, mean sequence fragment length was approximately 1,000 bp, with a range of 110–5,649 bp (Supplemental Table 2; see Data Accessibility). All UCE loci were concatenated into a single matrix. The resulting matrix was minimally 65% complete at the locus level with a final length of 409,406 bps, including 76,837 parsimony informative sites. This matrix was partitioned using the Sliding-Window Site Characteristics–Entropy method (hereafter, SWSC-EN; Tagliacollo and Lanfear, 2018) to split each UCE locus into left and right flanking regions and the ultraconserved core (i.e., center segment) by rate of evolution. The resulting left, central, and right UCE segments from SWSC-EN were then used as input for PartitionFinder v2.1.1 (Lanfear et al., 2014, 2017; Stamatakis, 2014) to find the best-fitting nucleotide substitution model for each data partition. PartitionFinder selected among models using AICc and the rclusterf search method with the setting -raxml (Lanfear et al., 2014). PartitionFinder designated 515 subsets with associated models for these regions. A list of the subsets of UCEs, partitions, and associated models can be found in Supplemental Table 3 (see Data Accessibility).

Combined analysis of morphological and molecular data matrices.—Once the morphology-based and UCE-based matrices were assembled and partitioned, tree inference was performed by simultaneously analyzing both matrices using IQ-Tree v1.6.11 (Nguyen et al., 2015; Chernomor et al., 2016). Both the morphology-based and UCE-based matrices, along with an independent partition model file, were used as inputs for executions of the IQ-Tree software. The model file consisted of the 515 PartitionFinder designated subsets and associated models for the UCE regions and a single partition and model designated for the morphological data (see Supplemental Table 3; see Data Accessibility). The total number of partitions used in the combined analysis was 516. Tree inference was performed by ten independent executions of the software with the settings perturbation strength (-pers) set to 0.2 and number of unsuccessful iterations to stop (-nstop) set to 1,000 using the above inputs and partitioning scheme. Support for the resulting topology with the highest likelihood score was assessed by generating and analyzing 500 standard bootstrap replicates (-bc). Taxa represented by exclusively morphological data (i.e., *Lactarius, Psammoperca*) were excluded from the support analysis due to their lack of sequence data. The best-fitting phylogeny (Fig. 2) was then reconciled with the resulting bootstrap replicates (Supplemental Fig. 1; see Data Accessibility). The resulting phylogeny was visualized with FigTree v1.4.3 (Rambaut, 2012).

Character optimization.—With the inferred phylogeny of carangiform fishes, we used the resulting tree topology and our morphological matrix (Supplemental Table 1, Supplemental Fig. 1; see Data Accessibility) as input data for WinClada v1.00.08 (Nixon, 2002) and Mesquite v3.6 (Maddison and Maddison, 2018) to view the evolution of morphological transformations. In WinClada, only unambiguous morphological character state optimizations were visualized using parsimony, and in Mesquite, morphological character-state transformations were optimized using parsimony. The optimization of these characters from WinClada is shown in Figure 3 and Supplemental Figure 2 (see Data Accessibility) and will be discussed in the following sections.

RESULTS

The hypothesis of relationships for the combined analysis is shown in Figure 2 and Supplemental Figure 1 (see Data Accessibility). Of the 30 nodes that were recovered in the support analysis, 27 nodes (≈90%) were supported by a bootstrap value ≥95% and 29 nodes (≈96%) were supported by a bootstrap value ≥70% (Supplemental Fig. 1; see Data Accessibility). The resulting topology from the combined analysis showed a monophyletic Carangiformes, with a series of six named suborders nested within (Fig. 2, Supplemental Fig. 1; see Data Accessibility). These suborders are: Centropomoidei including Centropomidae, Lactariidae, Latidae, and Sphyraenidae; Polynemoidei including Pleuronectoideo and Polynemidae; Toxotoidei including Leptobramidae and Toxotidae; Nematistioidei including Nematistiidae; Menoidei including Menidae and Xiphioidea; and Carangoidei including Carangidae and Echeneoidea. Centropomoidei is recovered as the earliest diverging clade of the Carangiformes. Within Centropomoidei, Lactariidae and Sphyraenidae are recovered as sister lineages, with Centropomidae and then Latidae recovered in a grade. The earliest diverging clade among Carangoidei, Menoidei, Nematistioidei, Polynemoi-

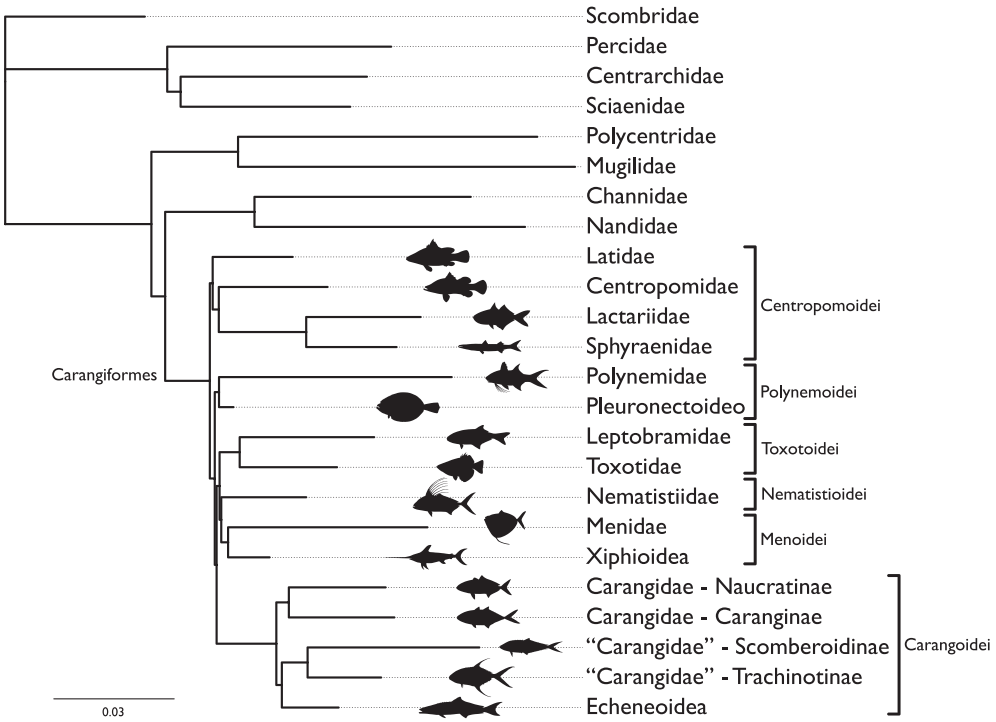

Fig. 2. Hypotheses of relationships from partitioned likelihood analysis of carangiform fishes and outgroup taxa. The dataset included 201 discrete morphological characters and 463 ultraconserved element loci. Cladogram condensed to show the relationships among families and larger groups sampled. See Data Accessibility for tree file.

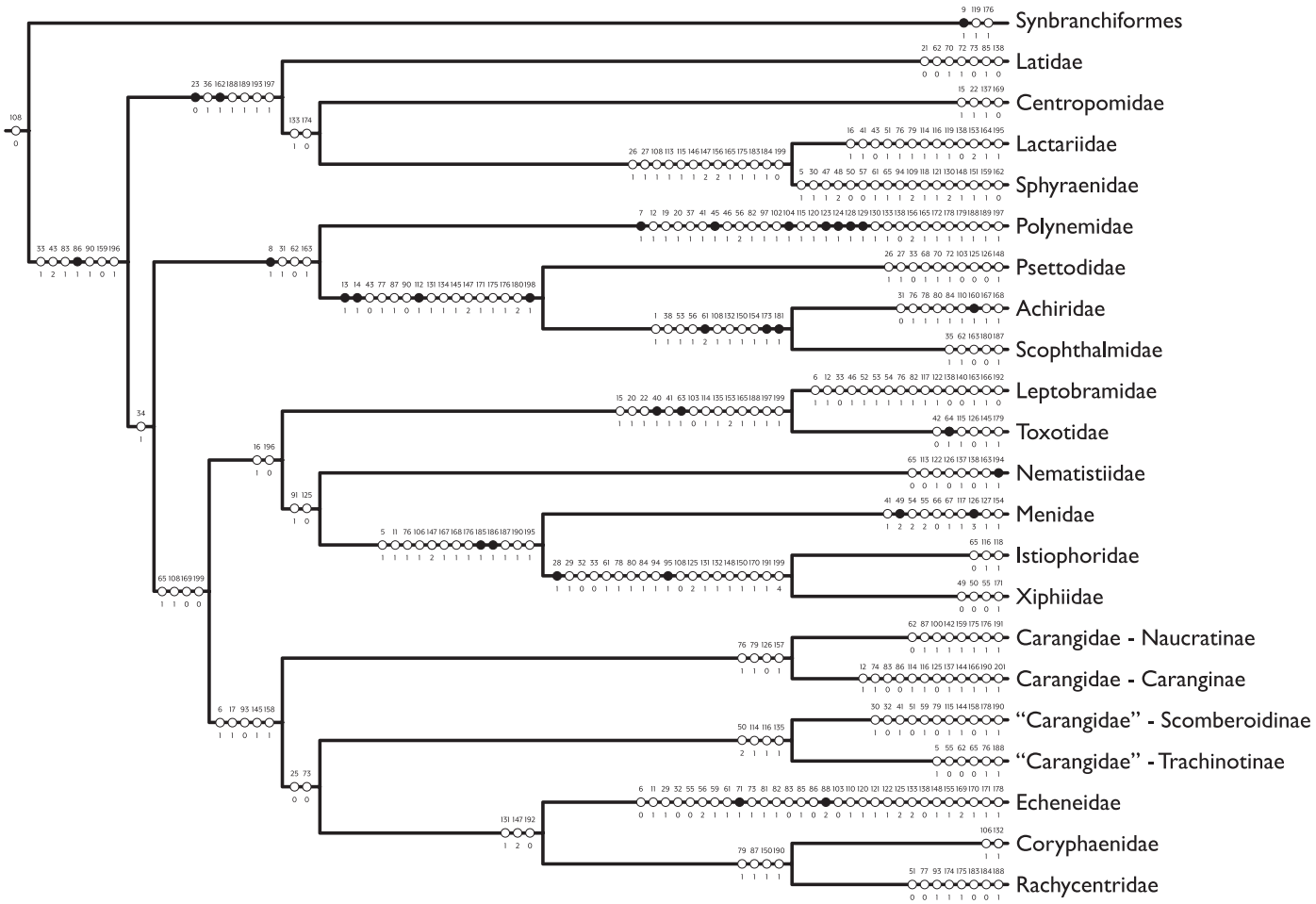

Fig. 3. Cladogram from partitioned likelihood analysis of carangiform fishes. Dataset included 201 discrete morphological characters and 463 ultraconserved element loci. Cladogram restricted to only the Carangiformes and Synbranchiformes. Morphological characters optimizing onto each node are represented by a circle with the corresponding character number listed above and corresponding character state below. Circles with black fill-in are unique and unreversed characters. Circles with white fill-in are inferred to have evolved multiple times in the cladogram.

dei, and Toxotoidei is the Polynemoidei, which includes Polynemidae sister to Pleuronectoideo. Toxotoidei is recovered sister to a clade composed of Nematistioidei and Menoidei. Within Toxotoidei, Leptobramidae is recovered sister to Toxotidae. Within Menoidei, Xiphioidea (Istiophoridae + Xiphiidae) is recovered sister to Menidae. This menoid clade is recovered sister to Nematistioidei. The final clade is Carangoidei. Within Carangoidei, Echeneoidea is composed of Coryphaenidae sister to a clade composed of Rachycentridae and Echeneidae. Echeneoidea is recovered sister to a clade composed of the traditional carangid subfamilies Trachinotinae and Scomberoidinae. The remaining two traditional carangid subfamilies, Caranginae and Naucratinae, are recovered as the sister lineage to Echeneoidea plus Trachinotinae and Scomberoidinae.

To examine character evolution within the carangiform fishes, the morphological characters were optimized onto the resulting topology (Fig. 3, Supplemental Fig. 2; see Data Accessibility). When optimizing the morphological characters onto the recovered relationships from the combined analysis, it is notable that at least one morphological character optimizes onto each node of the phylogeny. Of these characters, 34 (≈6%) are unique and unreversed (Fig. 3, Supplemental Fig. 2; see Data Accessibility). The following section will discuss a subset of characters that support the relationships between two or more families of carangiform fishes. Characters that support the monophyly of a single family or represent terminal changes will not be discussed as their phylogenetic implications fall outside of the goals of this study. All characters that unambiguously optimized onto the recovered topology can be seen in Supplemental Figure 2 (see Data Accessibility).

DISCUSSION

Our study was designed to look at the relationships among the carangiform fishes by taking an integrative and exemplar approach. In particular, we combined discrete morphological characters and genome-scale data of exemplar taxa to recover a hypothesis of relationships for the Carangiformes and highlight anatomical features that support not only the carangiform fishes as a clade, but also multiple subclades within the carangiform radiation. Our combined analysis recovers a monophyletic carangiform fishes, sister to members of the synbranchiform fishes (i.e., *Channa* and *Nandus;* =Anabantaria *sensu* Betancur-R. et al., 2017). This relationship is supported by one unambiguously optimized morphological character and DNA-sequence data. The Synbranchiformes have been recovered as the sister lineage of the Carangiformes in most large-scale DNA-based datasets (e.g., Near et al., 2013; Davis et al., 2016; Smith et al., 2016; Betancur-R. et al., 2017; Rabosky et al., 2018). While one character (108_0, long supracleithrum; Fig. 3; Supplemental Fig. 2; see Data Accessibility) did optimize in support of a carangiform–synbranchiform relationship, we did not set out to explicitly test the sister-group relationship between carangiform and synbranchiform fishes in this study. Additional morphological work will be needed to test the relationship between the carangiform and synbranchiform clades.

The monophyly of the Carangiformes is supported by seven morphological characters and DNA-sequence data, including, but not limited to, presence of the external process on maxilla (character 33_1), accessory gill rakers present on the lateral and medial aspects of the branchial arches (characters 83_1 and 86_1), and the presence of an epibranchial two toothplate that is serially associated with the second pharyngobranchial toothplate (character 90_1). The presence of an epibranchial two toothplate that is serially associated with the second pharyngobranchial toothplate (character 90_1) was found to diagnose all members of the Carangiformes, with losses occurring in *Istiophorus*, *Mene*, and Pleuronectoideo. Dentition was present on the second epibranchial of *Istiophorus,* but the dentition was scattered throughout the branchial element, rather than restricted to a defined toothplate. Because of this, we questioned the homology of this dentition and elected to code this character as absent (character 90_0) in *Istiophorus* until developmental work and/or additional specimens help resolve the state of this character in this taxon. While the presence of an epibranchial two toothplate supports the monophyly of the carangiform fishes among the included taxa, this toothplate can also be found in other distantly related lineages within Percomorpha. Members of the Centrarchiformes (e.g., *Lepomis,* Supplemental Table 1; see Data Accessibility) and Scorpaeniformes (e.g., Hoplichthyidae, Platycephalidae, Triglidae; Smith et al., 2018a) possess an epibranchial two toothplate. In contrast, lineages that have been closely allied to the carangiform fishes do not possess a second epibranchial toothplate. In our study, character 90_1, among others, optimizes as a synapomorphy for the carangiform fishes. Additional instances of these features among distantly related percomorphs are the result of convergent evolution.

In the following paragraphs, we will discuss the intrarelationships of the carangiform fishes. These sections are organized by the topology we recovered in our combined analysis and include the historical placement(s) of these families based on morphology and DNA-sequence data. One prior study with a broad sampling of carangiform fishes included a combined approach with molecular and morphological data (Mirande, 2016); however, that study did not explicitly search for new morphological characteristics and emphasized molecular data. As such, we decided to treat it with other DNA-based studies for convenience. Following a discussion of the historical placement of groups based on morphological and molecular data, we will then discuss some of the morphological features that support the relationships we recover.

Centropomoidei.—The first and earliest diverging clade of carangiform fishes includes Centropomidae, Lactariidae, Latidae, and Sphyraenidae. The families Centropomidae and Latidae have a complex history of being considered as a single family or in distinct, somewhat related, lineages in morphology-based and DNA-based studies (e.g., Otero, 2004; Li et al., 2011). The traditional Centropomidae (*sensu* Greenwood, 1976) included four genera, *Centropomus, Lates, Psammoperca,* and †*Eolates,* which were allied together based on two anatomical synapomorphies: expansion of the second abdominal neural spine and pored lateral-line scales extending onto the caudal fin. Since Greenwood's (1976) study, the monophyly of the Centropomidae (*sensu* Greenwood, 1976) has been refuted in both morphology-based (e.g., Mooi and Gill, 1995; Otero, 2004) and DNA-based (e.g., Li et al., 2011; Near et al., 2013) studies. Mooi and Gill (1995) separated *Lates* and *Psammoperca* into the Latidae based on

differences in the association between the epaxial musculature and the skeletal supports of the dorsal fin. Mooi and Gill (1995) also suggested that *Hypopterus* and †*Eolates* are members of the Latidae, but their epaxial musculature was not examined in that study. Subsequently, Otero (2004) supported the separation of Centropomidae and Latidae, noting multiple osteological differences between the taxa in these two families. In addition to these anatomical studies, multiple DNA-based studies have recovered the non-monophyly of Centropomidae (*sensu* Greenwood, 1976), with Latidae being recovered sister to Lactariidae (Mirande, 2016), Leptobramidae + Nematistiidae (Smith and Wheeler, 2006), Polynemidae (Campbell et al., 2014a), Psettodidae (Near et al., 2013), and Toxotidae (Li et al., 2009; Rabosky et al., 2018). However, a majority of DNA-based studies have found a sister-group relationship between Centropomidae (*sensu stricto*) and Latidae (e.g., Li et al., 2011; Near et al., 2012; Campbell et al., 2013; Betancur-R. et al., 2013a, 2013b, 2017; Betancur-R. and Ortí, 2014; Harrington et al., 2016). In light of these studies, the Centropomidae is currently regarded as the family of snooks, with all species of *Centropomus* occurring in waters off the New World. In contrast, the Latidae is composed of the extant Old World genera: *Hypopterus*, *Lates,* and *Psammoperca*.

We recover the Latidae as the earliest diverging lineage of Centropomoidei sister to Centropomidae, Lactariidae, and Sphyraenidae in our combined analysis. While the recovery of these four families in a clade is a novel finding, a subset of these families have been hypothesized as close allies in both morphological (e.g., Greenwood, 1976) and molecular (e.g., Betancur-R. and Ortí, 2014; Harrington et al., 2016; Rabosky et al., 2018) hypotheses. Centropomoidei is supported by seven morphological characters and DNA-sequence data. Some morphological characters supporting this node include: fewer than six spines on horizontal arm of the preopercle (character 23_0), rostral extension of external process on maxilla (character 36_1; Fig. 4A–D), enlargement of the second abdominal neural spine (character 162_1; Fig. 4E–G), procurrent spur present with proximal base of caudal-fin ray preceding procurrent ray shortened (characters 188_1 and 189_1), the presence of a bifurcated gas bladder with anterior extensions (character 193_1), and an enlarged pelvic axial 'scale' at the point of insertion of the pelvic fin (character 197_1). When present, the external process lies on the dorsal or lateral aspect of the maxilla, originating posteriorly to the rostral head of the maxilla. While we believe that this process serves as a contact point for up to three ligaments, which have been discussed in great detail by Datovo and Vari (2013), little information about the process itself was found in previous studies. Not only does this process vary in its presence or absence among the taxa examined, but it also varies in its size and direction of extension. In a subset of taxa with an external process on the maxilla, the process extends rostrally, forming a shelf-like projection that merges with the rostral head of the maxilla (Fig. 4A–D). We observed this rostral extension of the external process in all of the taxa included in Centropomoidei (*Centropomus* [Fig. 4A, B], *Lactarius, Lates, Psammoperca*, and *Sphyraena* [Fig. 4C, D]), as well as two other included taxa, *Lepomis* and *Mene*. The morphology exhibited by *Lepomis* is similar to what is observed among centropomoids; however, the shelf-like extension of the external process in *Mene* is directed dorsally in comparison to what is observed in *Lates* and allies. This shelf-like expansion of the external process is a complex character, particularly in light of the variation in size and orientation of the external process of the maxilla, and deserves a more broad assessment among percomorph fishes to fully assess the distribution of this feature. Another morphological character that optimizes in support of the Centropomoidei is the presence of an enlarged second abdominal neural spine (character 162_1; Fig. 4E–G), which was observed in *Centropomus* (Fig. 4F), *Lactarius* (Fig. 4G), *Lates* (Fig. 4E), and *Psammoperca* but absent in *Sphyraena*. This character was first noted in centropomids and latids by Greenwood (1976) and was used as one of the two characters supporting the monophyly of the Centropomidae (*sensu lato*). In 1995, Mooi and Gill refuted the homology of this character, noting that the second neural spine of *Centropomus* is broadly expanded over most of its length while the second neural spine of latid species is not closely applied to the first neural spine and is only expanded proximally. We interpreted this character differently or our material varies from that of Mooi and Gill (1995) as it relates to latids. We find that the second neural spine is enlarged throughout its length and closely applied to the first neural spine among latids examined in this study (Fig. 4E). We also observed this expanded second abdominal neural spine in *Lactarius* (Fig. 4G). Leis (1994) was the first to note the enlargement of the second abdominal neural spine in *Lactarius*, also noting the close application between the enlarged first and second neural spines. Despite being present in *Centropomus*, *Lactarius*, *Lates,* and *Psammoperca*, an enlarged second neural spine was not observed in *Sphyraena*. Sphyraenids do exhibit a robust and enlarged first neural spine, but the second neural spine is not any more enlarged than the neural spine on the third or more posterior abdominal vertebrae. We interpret this as a reversal in this character for the sphyraenids. Despite this reversal in one genus, our analysis recovers the presence of an enlarged second abdominal neural spine supporting the monophyly of Centropomoidei. A final morphological feature optimizing in support of Centropomoidei is the presence of a bifurcated gas bladder with anterior extensions (193_1), which are present in all centropomoid taxa examined except *Centropomus armatus*. Meek and Hildebrand (1923) were the first to note a bifurcated gas bladder in all five members of *Sphyraena* they examined, but they did not note the nature of this bifurcation among these taxa. We observed one pair of robust anterior gas bladder extensions, each positioned between the shoulder girdle and the base of the neurocranium, in *Sphyraena idiastes*. While anterior extensions were observed in *S. barracuda*, they were less robust than those observed in *S. idiastes*. Meek and Hildebrand (1925) also surveyed the gas bladder shape in eight species of *Centropomus*, finding anterior extensions of the gas bladder in half of the centropomids surveyed. They reported that these extensions varied in length from rudimentary, flanking the posterior aspect of the neurocranium (e.g., *C. robalito*), to elongated appendages, curving posteriorly, lying along lateral sides of the gas bladder (e.g., *C. undecimalis*). Among the remaining taxa recovered in Centropomoidei, anterior extensions of the gas bladder were found in *Lates* and *Psammoperca,* as noted by Greenwood (1976), and *Lactarius,* as noted by Leis (1994). Anterior gas bladder extensions have been observed in other carangiform and outgroup taxa sampled in this study (i.e., *Micropogonias, Mene,* and *Nematistius*) as well as many other taxa we did not sample (see

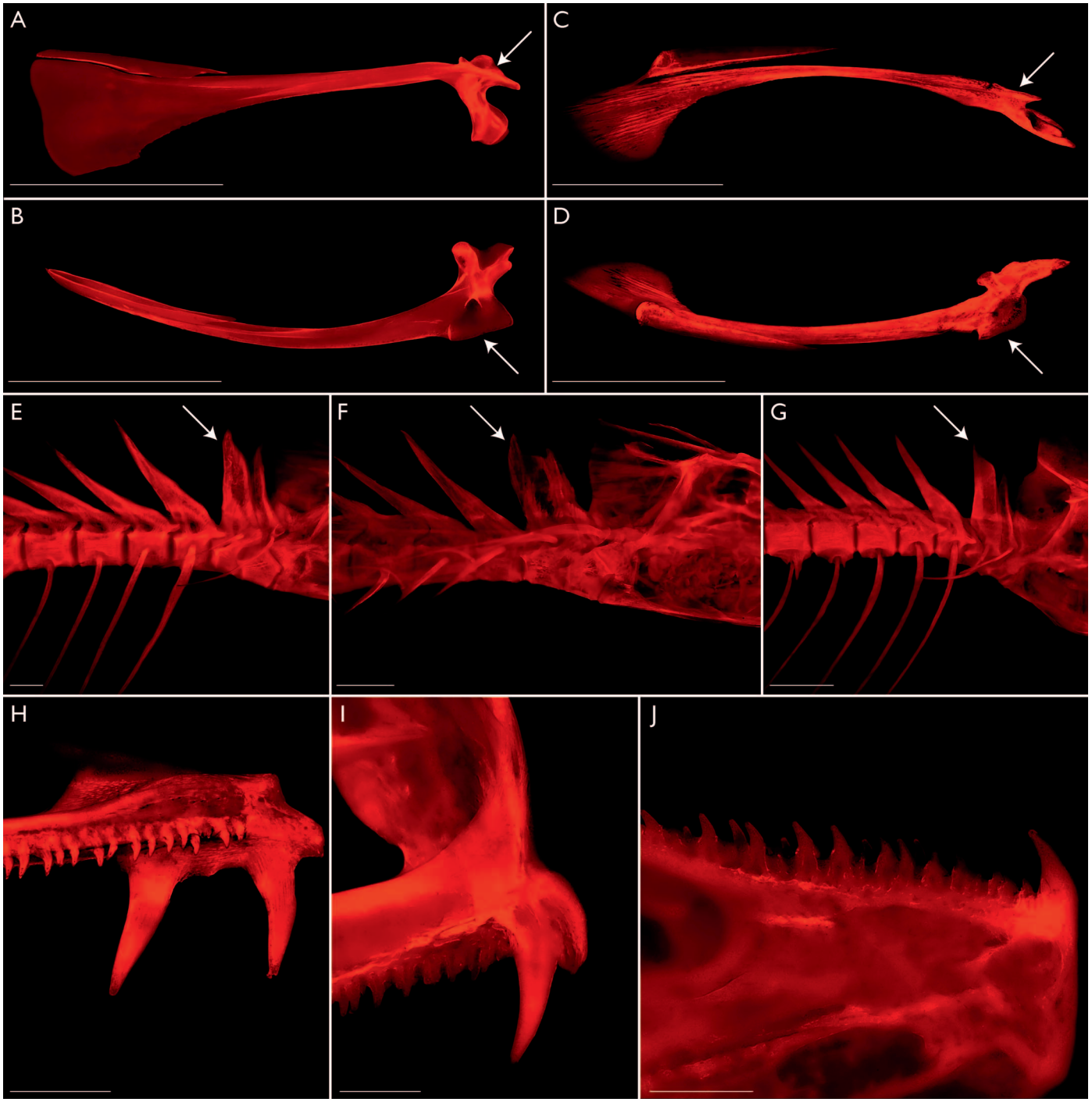

Fig. 4. Morphological variation in support of the relationships among the Centropomoidei. Images of cleared and stained specimens fluorescing under royal blue light. Presence of rostral extension of external process on maxilla (character 36_1)—(A) *Centropomus undecimalis* (FMNH 77806), arrow, lateral view of right maxilla, scale bar = 5 mm; (B) *Centropomus undecimalis* (FMNH 77806), arrow, dorsal view of right maxilla, scale bar = 5 mm; (C) *Sphyraena barracuda* (FMNH 74209), arrow, lateral view of right maxilla, scale bar = 5 mm; (D) *Sphyraena barracuda* (FMNH 74209), arrow, dorsal view of right maxilla, scale bar = 5 mm. Enlargement of the second abdominal neural spine (character 162_1)—(E) *Lates calcarifer (*AMNH 37839), arrow, right lateral view, scale bar = 1 mm; (F) *Centropomus undecimalis* (FMNH 77806), arrow, right lateral view, scale bar = 2.5 mm; (G) *Lactarius lactarius* (KUI 41405), arrow, right lateral view, scale bar = 5 mm. Possession of elongated, fang-like teeth in the oral jaws (character 26_1) and oral teeth that are ankylosed to the premaxilla and dentary (character 27_1)—(H) *Sphyraena idiastes* (SIO 15–182), lateral view of right premaxilla, scale bar = 1 mm; (I) *Lactarius lactarius* (KUI 41405), lateral view of right premaxilla, scale bar = 1 mm; (J) *Lactarius lactarius* (KUI 41405), lateral view of right dentary, scale bar = 1 mm.

Tominaga et al., 1996; Webb et al., 2006). While anterior gas bladder extensions have likely evolved numerous times across teleosts, the presence of these extensions supports the relationship among taxa in the Centropomoidei.

Within Centropomoidei, the recovery of Lactariidae sister to Sphyraenidae is novel from a morphological perspective, but the relationship was recovered in two previous DNA-based studies (Betancur-R. and Ortí, 2014; Rabosky et al.,

2018). Also known as the False Trevally, Lactariidae is a monotypic family native to coastal Indo-Pacific waters (Leis, 1994). While this family has been traditionally regarded as a percoid, it has garnered little attention overall in systematic studies. Only one comparative study has focused on this species (Leis, 1994), finding it a difficult taxon to place based on morphological characters. Leis (1994) listed eight larval and adult characters that suggested a close relationship between a subset of carangoids and *Lactarius*, as well as four additional characters that suggested a close relationship between a subset of carangoids, *Mene*, and *Lactarius*. Leis (1994) also noted that, while these morphological characters were not unique, unreversed synapomorphies, they were strong indicators allying *Lactarius* to these fishes. Since the initial study by Leis (1994), *Lactarius* has been included in only a few DNA-based studies, which have recovered *Lactarius* sister to Menidae (Sanciangco et al., 2016; Betancur-R. et al., 2017), Sphyraenidae (Betancur-R. and Ortí, 2014; Rabosky et al., 2018), or a clade consisting of eight carangiform families (Campbell et al., 2013). The barracudas (Sphyraenidae) have had a comparatively rich systematic history across morphology-based and DNA-based hypotheses. All 27 species of *Sphyraena* are found in tropical to temperate marine waters throughout the world. Traditional morphological hypotheses have allied the Sphyraenidae with the Mugilidae and Polynemidae (e.g., Starks, 1899; Regan, 1912), with some studies also including the Atherinidae and Phallostethidae as close allies (e.g., Myers, 1928; Hubbs, 1944; Gosline, 1962). These studies primarily ally sphyraenids with these other families based on the posterior displacement of the pelvic girdle and the lack of an interaction between the elements of the pectoral and pelvic girdles. This hypothesis largely persisted in ensuing investigations by Cockerell (1913), Myers (1935), Hubbs (1944), Gosline (1962, 1968, 1971), Rosen (1964), Greenwood et al. (1966), and McAllister (1968) until an alternative hypothesis was suggested by Johnson (1986). In his study, Johnson (1986) allied Sphyraenidae with Scombroidei, based on five characters from the neurocranium, upper branchial arches, oral jaws, and hyoid arch. Following these morphological studies, hypotheses based on DNA-sequence data have consistently recovered Sphyraenidae as a member of the carangiform fishes (e.g., Li et al., 2011; Near et al., 2013; Harrington et al., 2016). However, these DNA-based studies have recovered a number of sister groups to the Sphyraenidae, including all other carangiform fishes (Harrington et al., 2016), Centropomidae (Near et al., 2013; Mirande, 2016; Alfaro et al., 2018), Menidae (Smith and Wheeler, 2006; Campbell et al., 2014a), and Psettodidae (Li et al., 2011).

We recovered Lactariidae sister to Sphyraenidae in our combined analysis. This relationship was supported by 13 morphological characters, including, but not limited to, the ventral process of the coracoid reaching to a similar point or past the ventral plane of cleithrum (character 113_1), the ventral process of coracoid being broadened by laminae at the ventral aspect (character 115_1), and more than two anal-fin pterygiophores anterior to first hemal spine (character 147_2), among others. Additionally, two morphological characters that optimize onto this node relate to the characteristics of the oral teeth: possession of elongated, fang-like teeth in the oral jaws (character 26_1; Fig. 4H, I) and oral teeth that are ankylosed to the premaxilla and dentary (character 27_1; Fig. 4H–J). We define a fang as an elongated and distally tapered caniniform tooth present in the oral jaws. Fangs are found across a diversity of teleosts (e.g., *Anoplogaster*, *Esox, Meiacanthus, Stomias;* Springer, 1968; Fink, 1981), but the distribution of fang-like teeth was limited among taxa examined in this study. One of the most striking features of sphyraenids is the series of fangs in the oral jaws, which have been noted by numerous authors in both extant and extinct species of sphyraenids (e.g., Meek and Hildebrand, 1923; Nishimoto and Ohe, 1982; de Sylva, 1984a; Johnson, 1986; Santini et al., 2015; Fig. 4H). A few authors have also characterized the overall shape of the fangs (de Sylva, 1984a), fang attachment to the oral jaw (Fink, 1981), and replacement of these fangs (Johnson, 1986) in previous studies. In his survey of tooth attachment types across actinopterygians, Fink (1981) found that the attachment of sphyraenid fangs to the oral jaws was dissimilar to the modes of attachment commonly found among percomorphs. The functional part of the fang was directly connected to the attachment bone on the oral jaws (i.e., ankylosed; Type 1; Fig. 4H) in sphyraenids rather than separated from the attachment bone in the oral jaws by a band of collagen that vary in shape (Types 2–4 [Fink, 1981]). Johnson (1986) characterized this morphology further within acropomatids, sphyraenids, and some scombroids, finding the replacement of sphyraenid fangs similar to the replacement of oral teeth in scombroids and allies. Fangs with a type 1 tooth attachment are also found in the oral jaws of False Trevally (*Lactarius*; Fig. 4I, J) and spiny turbot (*Psettodes*) among carangiform fishes (characters 26_1 and 27_1). Leis (1994) noted a cluster of two or three enlarged canine teeth surrounding the symphyses of both the dentary and premaxilla in larval and adult stages of *Lactarius*. He noted that these fang-like teeth are attached to the oral jaws via a type 1 attachment, with the posterior, non-fang-like teeth attached via a type 2 tooth attachment (Leis, 1994). However, Leis (1994) did not note if a type 2 tooth attachment was found in exclusively the larval or adult stages or found throughout the ontogeny of *Lactarius*. In the adult specimens of *Lactarius* we examined, we did not observe a collagen band between the functional and attachment parts of the non-fang-like oral teeth of *Lactarius* and classify all of the oral teeth as attaching via a type 1 tooth attachment (Fig. 4I, J). As larval stages were not examined in this study, we cannot rule out that type 2 tooth attachment occurs prior to the adult stage of *Lactarius,* and further investigation is needed. Fang-like teeth with a type 1 tooth attachment were also observed in *Psettodes* among taxa sampled in this study. While fang-like teeth and a type 1 tooth attachment have evolved numerous times throughout the evolution of fishes (Fink, 1981), the distribution of these characters is limited among carangiform fishes. Both the presence of fang-like oral teeth and a type 1 attachment between oral teeth and oral jaws are some characters supporting a relationship between Lactariidae and Sphyraenidae.

All carangiform fishes except Centropomoidei.—The clade recovered sister to Centropomoidei includes members of the Carangoidei, Menoidei, Nematistioidei, Polynemoidei, and Toxotoidei, which is supported by one morphological character and DNA-sequence data. While previous DNA-based studies have recovered a subset of these families in a clade (e.g., Betancur-R. and Ortí, 2014; Harrington et al., 2016; Alfaro et al., 2018), the recovery of this clade is a novel

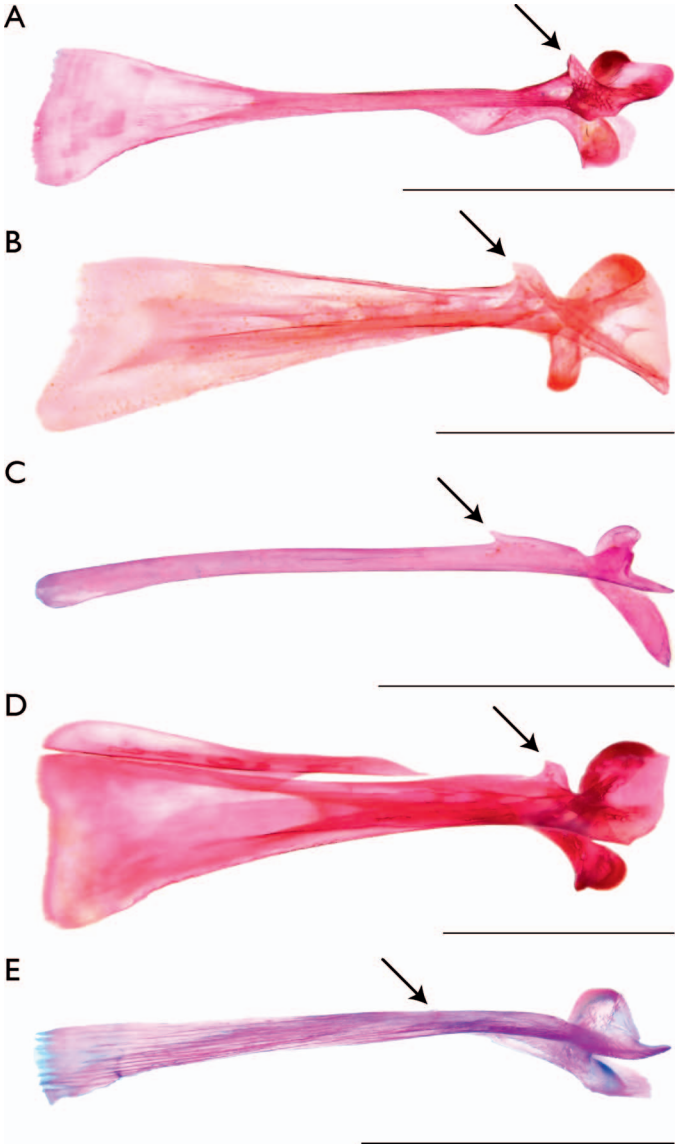

Fig. 5. Morphological variation in support of the relationships among carangiform taxa not included in the Centropomoidei. Images of cleared and stained specimens under white or daylight LED light. Dorsally directed external process on maxilla (character 34_1)—(A) *Polydactylus sexfilis* (CAS 50911), arrow, lateral view of right maxilla, scale bar = 5 mm; (B) *Scophthalmus aquosus* (KUI 30388), arrow, lateral view of right maxilla, scale bar = 5 mm; (C) *Toxotes jaculatrix* (KUI 42174), arrow, lateral view of right maxilla, scale bar = 5 mm; (D) *Caranx hippos* (KUI 30383), arrow, lateral view of right maxilla, scale bar = 5 mm; (E) *Coryphaena hippurus* (FMNH 48561), arrow, lateral view of right maxilla, scale bar = 5 mm.

hypothesis. Despite the extensive amount of external and internal morphological variation seen across the carangiform families not included in Centropomoidei, one morphological character, a dorsally directed external process on the maxilla (character 34_1; Fig. 5A–E), supports this clade. As noted above, the external process may be present on the dorsal or lateral aspect of the maxilla, originating posteriorly to the element's rostral head. Variation occurs in the orientation of this process as it relates to the maxilla, with some fishes exhibiting an external process directed towards the lateral aspect of the maxilla (Fig. 4A–D). Notably, the external process was dorsally directed in all carangiform taxa not included in the Centropomoidei (Fig. 5A–E) with the exception of Xiphioidea, *Leptobrama,* and *Psettodes*, which did not possess an external process (character 34_1). Outside of this lineage, a dorsally directed external process was only found in a distantly related sciaenid (*Micropogonias*). Additional investigations of this process are needed to fully understand the phylogenetic significance and distribution of this character.

Polynemoidei.—Despite pleuronectoids being the species-dominant lineage when compared to Polynemidae, there is a long history of the family Pleuronectidae serving as the root for the order-, suborder- and suprafamily-level designations, referring to all or a subset of flatfish families (i.e., Pleuronectiformes, Pleuronectoidei, Pleuronectoidea). Because of this, and the recovery of Polynemidae as sister to all or a subset of flatfishes in this and other studies (e.g., Harrington et al., 2016; Alfaro et al., 2018; Shi et al., 2018), we have elected to use Polynemoidei to refer to the pleuronectoid–polynemid clade so it is differentiated from other exclusively-flatfish clade names. Accordingly, we have designated Pleuronectoideo to refer to all flatfish families at the infraordinal level following the infraorder endings used by Tyler (1980).

There are approximately 800 species of flatfishes in roughly 15 families that are notable for the migration of either the left or right eye onto or across the dorsal midline of the neurocranium, resulting in an asymmetric baüplan. Despite this striking character, the monophyly of flatfishes has been debated. Early morphological studies by Kyle (1923) were some of the first to suggest multiple origins of flatfishes, allying members of *Symphurus* with members of the rattails (Macrouridae) and ribbonfishes (Trachipteridae), "Rhomoids" allied with pomfrets (*Pampus*), and "bothids" placed near the Psettodidae (Kyle, 1923). Similar suggestions of independent flatfish origins have also been made by Chabanaud (1949) and Amaoka (1969). In contrast, most authors (e.g., Rosen and Patterson, 1969; Rosen, 1973; Hensley and Ahlstrom, 1984) have included all flatfishes in the monophyletic Pleuronectiformes (*sensu* Hensley and Ahlstrom, 1984). Flatfish monophyly has been recovered in recent morphology-based studies as well, with the cladistic study of flatfishes conducted by Chapleau (1993) recovering a monophyletic flatfishes based on three characters: migration of one eye across the midline, anterior extension of the dorsal fin above the neurocranium, and presence of the *recessus orbitalis*. Three subsequent studies by Hoshino (2001), Chanet (2003), and Chanet et al. (2004) also recognized the monophyly of flatfishes based on morphological data. Studies based on DNA sequence data have also recovered flatfishes as a clade (e.g., Berendzen and Dimmick, 2002; Betancur-R. and Ortí, 2014; Campbell et al., 2014a; Harrington et al., 2016; Byrne et al., 2018; Rabosky et al., 2018). However, the non-monophyly of flatfishes has been hypothesized in a number of DNA-based studies (Chen et al., 2003; Smith and Wheeler, 2006; Li et al., 2009; Near et al., 2012, 2013; Betancur-R. et al., 2013b; Campbell et al., 2013; Shi et al., 2018). These DNA-based hypotheses typically recover flatfishes in two independent clades (Psettodoidea and Pleuronectoidea) among carangiform taxa.

We recover flatfishes in a monophyletic group, supported by 16 morphological characters and DNA-sequence data. Many of the morphological features supporting flatfish

monophyly are those that have been described in previous studies, namely asymmetry of the neurocranium (our character 13_1; Chapleau, 1993 character 1), presence of the pseudomesial bar (our character 14_1; Hoshino, 2006; Harrington et al., 2016, character 3), and asymmetric lateral pigmentation (our character 198_1; Harrington et al., 2016 character 4). One additional morphological character supporting the monophyly of flatfishes is the absence of posterior expansion on the dorsalmost element of the postcleithrum (character 112_1). In all other members of the carangiform fishes sampled, the dorsalmost element of the postcleithrum possessed a posterior lamellar expansion that was limited to the dorsoposterior margin of the element. However, members of the Psettodidae and Scophthalmidae were the only carangiform taxa examined lacking posterior expansion on the dorsalmost element of the postcleithrum. The postcleithrum is lost in *Achirus* and was coded as inapplicable (-) for this character. While further examination is needed to assess the distribution of this character among the diversity of pleuronectoids, we find the absence of posterior expansion on the dorsalmost element of the postcleithrum to be another morphological feature supporting the monophyly of Pleuronectoideo.

In addition to the recent debate regarding flatfish monophyly, the placement of Pleuronectoideo as a clade has been difficult from a morphological perspective due to the unique morphological features found in these fishes (Munroe, 2015). While flatfishes have been traditionally placed in their own order, Pleuronectiformes, the placement of this order within the evolution of acanthomorphs has been debated. Kyle (1923) placed a subset of flatfishes with other families of fishes (e.g., Stromateidae, Macrouridae) and Psettodidae as an ancestor of an extinct percoid. Rosen (1973), Hensley and Ahlstrom (1984), Chapleau (1993), and others have placed flatfishes either sister to or nested among the percoids. Studies based on DNA-sequence data have consistently recovered flatfishes among the carangiform fishes (e.g., Betancur-R. et al., 2013a, 2013b; Near et al., 2013; Harrington et al., 2016; Rabosky et al., 2018), finding a number of carangiform lineages sister to the clade. Previous allies of a monophyletic flatfishes include all other members of the Carangiformes (Campbell et al., 2014a; Smith et al., 2016), Centropomidae (Sanciangco et al., 2016), and Polynemidae (Harrington et al., 2016; Alfaro et al., 2018).

Fishes in Polynemidae (42 species) are a morphologically distinctive group commonly called threadfins for their numerous, elongated, and thread-like fin rays positioned on a ventral expansion of their pectoral girdle. Similar to sphyraenids, traditional hypotheses of threadfin interrelationships were primarily influenced by the posterior placement of their pelvic fins relative to other perch-like fishes (e.g., Starks, 1899; Gosline, 1962, 1968, 1971). Interestingly, Gill (1861) not only classified Polynemidae based on this posterior placement of the pelvic fins, but he also put forth an alternative hypothesis which allied polynemids with the drums and croakers (Sciaenidae) based on squamation, weakness of fin spines, and other characters. Later, Freihofer (1978) allied polynemids and sciaenids together based on both groups possessing an anterior extension of the nasal canal rarely observed in other fishes. De Sylva (1984b) noted similarities between the larvae of threadfins and drums, specifically in eye size and myomere count. Later, Johnson (1993) provided corroborative evidence for this relationship noting that polynemids share five of the 21 putative synapomorphies for sciaenids identified by Sasaki (1989), including a character rarely found in other fishes, the interdigitation between the metapterygoid and quadrate. The most recent morphological work on threadfins (Kang et al., 2017) supported the earlier polynemid–sciaenid grouping based largely on the characters put forth by Johnson (1993). Despite the morphological support for grouping polynemids with sciaenids, DNA-based studies have neither recovered these two families as sister lineages nor found these families near each other. While DNA-based studies have recovered polynemids among the carangiform fishes, numerous sister groups to the Polynemidae have been hypothesized, including Latidae (Campbell et al., 2014a; Smith et al., 2016), Menidae (Betancur-R. et al., 2013b; Mirande, 2016), and Sphyraenidae (Dettaï and Lecointre, 2004, 2005). Among the larger and more recent studies, one of the more commonly recovered sister groups to polynemids has been all or a subset of pleuronectoids (Harrington et al., 2016; Alfaro et al., 2018; Shi et al., 2018); we corroborate this hypothesis in this study.

We recover Polynemidae sister to a monophyletic flatfishes and support this relationship with four morphological characters and DNA sequence data, including, but not limited to, a basihyal that is shorter than hypobranchial one (character 62_0), and distal tips of posterior abdominal parapophyses directed medially and joined with the opposing parapophysis on the same vertebra, often forming a single spine-like projection with a bifurcating distal tip (character 163_1). An additional morphological character supporting this sister-group relationship is a prominent anterodorsal expansion of the parasphenoid found in all polynemids and flatfishes examined (character 8_1; Fig. 6A–C). The polynemid parasphenoid includes a prominent anterodorsal extension that begins underneath the region where the belophragm of the basisphenoid contacts the parasphenoid in the posterior half of the orbit (Fig. 6A, C). This expansion reaches dorsally and rostrally toward the frontal, which is ventrally bent in polynemids, and the lateral ethmoid in the anterior part of the orbit. A variety of expansions may be present in carangiform fishes and outgroup taxa, but we have not found a morphology that was similar to what is observed in polynemids outside of the pleuronectoids. There are slight expansions of the parasphenoid in *Centropomus*, *Lates*, and *Scomber,* but these expansions do not extend to a similar height dorsally or interact with the lateral ethmoids or frontal (Fig. 6D). While a large dorsal expansion of the parasphenoid can be found in *Mene*, this expansion is restricted to the posterior aspect of the parasphenoid, and it does not extend rostrally or interact with the neurocranial elements in the anterior region of the orbit. It should also be noted that various expansions of the parasphenoid, pterosphenoid, and ethmoids can be found among some members of the Sciaenidae (Taniguchi, 1969; Sasaki, 1989, his character 28). However, the limited number of groups that have been found to exhibit these expansions (e.g., *Argyrosomus*, *Johnius, Nibea*) occupy a derived position among the Sciaenidae across morphology-based and DNA-based studies (Sasaki, 1989; Lo et al., 2015). Upon first observation, the prominent parasphenoid extension found in polynemids was thought to be unique among the Carangiformes; however, Chapleau's (1993) study on the relationships among flatfishes showed (his figs. 4 and 5) that the

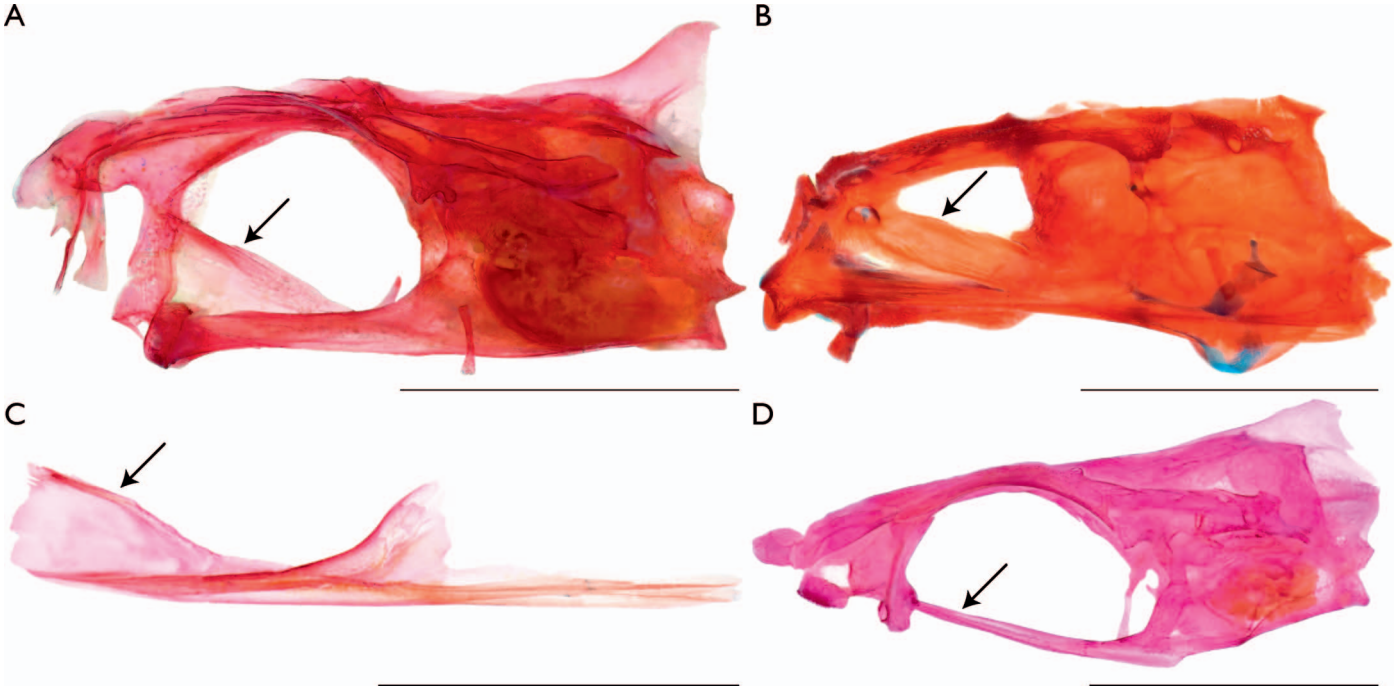

Fig. 6. Morphological variation in support of the relationships among the Polynemoidei. Images of cleared and stained specimens under white or daylight LED light. Anterodorsal expansion of the parasphenoid (character 8_1)—(A) *Filimanus similis* (LACM 38134.017), arrow, left lateral view of neurocranium, scale bar = 1 cm; (B) *Psettodes erumei* (ANSP 214777), arrow, left lateral view of neurocranium, scale bar = 5 mm; (C) *Polydactylus sexfilis* (CAS 50911), arrow, left lateral view of isolated parasphenoid, scale bar = 5 mm. Absence of anterodorsal expansion of the parasphenoid (character 8_0)—(D) *Toxotes jaculatrix* (FMNH 69510), arrow, left lateral view of neurocranium, scale bar = 1 cm.

neurocranium of *Psettodes erumei* (Fig. 6B) has a prominent anterodorsal extension of the parasphenoid that interacts with the blind-side lateral ethmoid. This extension is readily seen in both the ventral view and lateral view of the blind side of the neurocranium. While this prominent anterodorsal expansion of the parasphenoid was seen in all polynemids and flatfishes examined in this study, we did not observe this expansion in any other fishes sampled. This character provides support for the relationship between pleuronectoids and polynemids.

***Carangoidei* + *Menoidei* + *Nematistioidei* + *Toxotoidei*.**—We recover a clade consisting of Carangoidei, Menoidei, Nematistioidei, and Toxotoidei that is supported by four morphological characters and DNA-sequence data. This clade has not been previously recovered in morphology-based studies, with only a few DNA-based studies that have sampled all of these lineages recovering them as a clade (i.e., Betancur-R. et al., 2013b; Betancur-R. and Ortí, 2014). One morphological character in support of the recovered clade relates to the amount of dentition present on the basihyal (character 65_1, Fig. 7) and branchial arches within the oral cavity. With the exception of *Istiophorus, Nematistius*, and *Trachinotus*, all members of this clade exhibit dentition on the basihyal (character 65_1). Basihyal dentition occurs in a number of lineages of fishes, both carangiform (e.g., *Eleutheronema*) and non-carangiform (e.g., Moronidae, Gill and Leis, 2019) alike. Given our analysis, the presence of basihyal dentition, as well as three other morphological characters and DNA-sequence data, supports the monophyly of the Carangoidei, Menoidei, Nematistioidei, and Toxotoidei.

***Menoidei* + *Nematistioidei* + *Toxotoidei*.**—The recovery of a clade consisting of Menoidei, Nematistioidei, and Toxotoidei is novel hypothesis. However, only a few DNA-based studies have included representatives from all of these lineages (i.e., Betancur-R. and Ortí, 2014; Betancur-R. et al., 2017; Rabosky et al., 2018). This clade is supported by DNA-sequence data and two morphological characters, an increased number of circumorbital elements (character 16_1; Fig. 8A–C) and the absence of pored lateral-line scales extending onto the caudal fin (character 196_0). In their review of the subocular shelf of fishes, Smith and Bailey (1962) noted that the number of elements in the circumorbital series is highly conserved throughout teleosts, with six elements typically found in the series. However, these authors also noted that some fishes have undergone reduction or division of these elements, thereby decreasing or increasing the total number of elements in the series, respectively. Evidence of reductions or increases in the number of these elements can be found throughout percomorphs including members of the Carangiformes (e.g., members of Cottidae and Psychrolutidae possess fewer circumorbitals [Yabe, 1985; Girard and Smith, 2016], members of Acanthuridae possess additional circumorbitals [Tyler et al., 1989]). While six or fewer circumorbital elements were found in most of the taxa sampled in this study (character 16_0), the presence of seven or more circumorbital elements (character 16_1; Fig. 8A–C) supports the monophyly of the six families in this clade. Seven circumorbital elements were observed in Toxotoidei (Fig. 8A), while eight or more elements were found in Nematistioidei (Fig. 8B) and Menoidei (Fig. 8C). This is a different condition than what is reported for *Nematistius* by Rosenblatt and Bell (1976), who report six elements in the series. Among our specimens of *Nematistius,* we observed upwards of ten

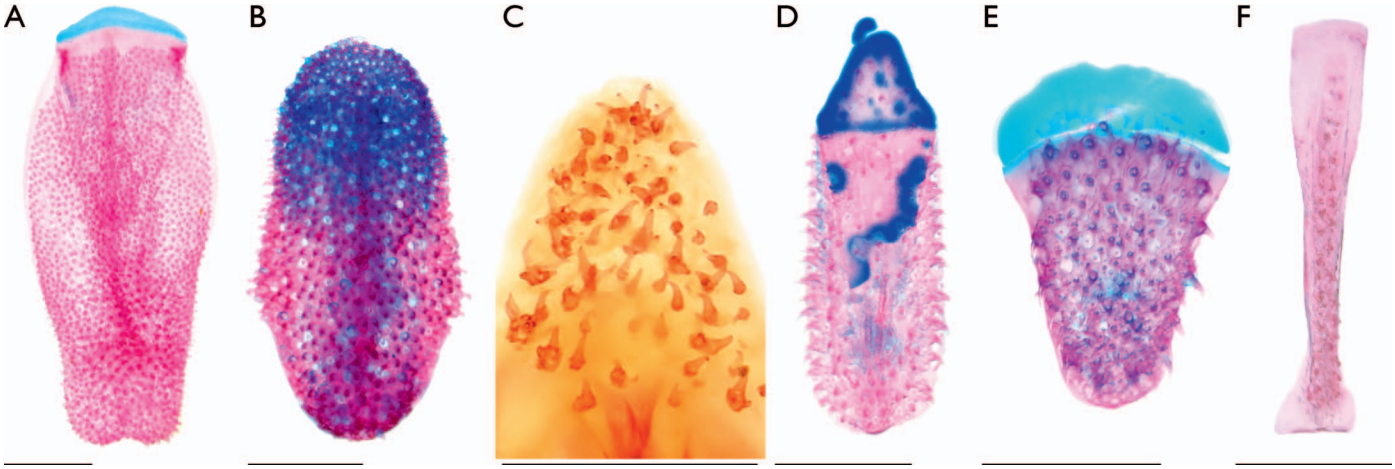

Fig. 7. Morphological variation in support of the relationship among the Carangoidei, Menoidei, Nematistioidei, and Toxotoidei. Images of cleared and stained specimens under white or daylight LED light. Dentition present on the basihyal (character 64_1)—(A) *Toxotes blythii* (KUI 42173), dorsal view of basihyal, scale bar = 1 mm; (B) *Leptobrama muelleri* (KUI 41406), dorsal view of basihyal, scale bar = 1 mm; (C) *Xiphias gladius* (MCZ 55512, Museum of Comparative Zoology, Harvard University, ©2019 President and Fellows of Harvard College), dorsal view of basihyal, scale bar = 1 mm; (D) *Oligoplites saurus* (KUI 17205), dorsal view of basihyal, scale bar = 1 mm; (E) *Coryphaena hippurus* (FMNH 48561), dorsal view of basihyal, scale bar = 1 mm; (F) *Trachurus trachurus* (KUI 19964), dorsal view of basihyal, scale bar = 1 mm.

circumorbital elements in the series. As noted above, there are percomorphs that exhibit more than six circumorbital elements, but this character supports the relationships among the Menoidei, Nematistioidei, and Toxotoidei. In addition to the number of circumorbital elements, the absence of pored lateral-line scales extending onto the caudal fin (character 196_0) supports the monophyly of these three suborders. We observed pored lateral-line scales extending onto the caudal fin in all carangiform families sampled in this study except representatives of the Menoidei, Nematistioidei (H. J. Walker, pers. comm.), and Toxotoidei. The loss of pored lateral-line scales that extend on the caudal fin supports a relationship within the taxa in Menoidei, Nematistioidei, and Toxotoidei.

Toxotoidei.—The beachsalmons (Leptobramidae) include two species, *Leptobrama muelleri* and *L. pectoralis*, which are found in the waters surrounding southern New Guinea and northern Australia (Kimura et al., 2016). These fishes exhibit a set of notable external morphological characters, such as a dorsal-fin base shorter than the anal-fin base, medial fins covered with scales, and a baüplan similar to pempherids and carangids, that has led ichthyologists to ally *Leptobrama* with a number of percoid families in previous morphology-based studies (e.g., Cockerell, 1913; Tominaga, 1965). Early on, Steindachner (1878) noted *Leptobrama* was similar in overall shape to *Lichia* (Carangidae), while dorsal-fin shape and scale characteristics aligned the beachsalmons with the genus *Brama*. In subsequent studies (e.g., Cockerell, 1913; Ogilby, 1913; Greenwood et al., 1966), *Leptobrama* was considered a member of the Pempheridae. In contrast, Tominaga (1968) excluded *Leptobrama* from the Pempheridae and he described a new family, Leptobramidae, that he placed near the Carangidae based on their morphological similarity. Though numerous characters were shared between Carangidae and Leptobramidae, Tominaga (1965) also listed a few other families that exhibited similar morphological traits to *Leptobrama* (e.g., Scombridae, Toxotidae). Since these morphological studies, virtually all hypotheses based on DNA-sequence data that have sampled *Leptobrama* have recovered the family as a member of the carangiform fishes (e.g., Smith and Craig, 2007; Betancur-R. et al., 2013a, 2013b). While these DNA-based studies have recovered a number of sister groups to Leptobramidae, including Menidae and Xiphioidea (Rabosky et al., 2018), Nematistiidae (Smith and Wheeler, 2006), and Sphyraenidae (Smith and Craig, 2007), the most common sister group recovered to the leptobramids are the toxotids (Toxotidae; Betancur-R. et al., 2013a, 2013b, 2017; Betancur-R. and Ortí, 2014; Harrington et al., 2016; Sanciangco et al., 2016).

The ten species of archerfishes (Toxotidae) can be variously found throughout the fresh- and brackish-water environments of southeast Asia, northern Australia, and the Indo-Pacific archipelago (Kottelat and Hui, 2018). These fishes are notable for their ability to shoot water from their mouths, knocking terrestrial prey items off balance and into the water to be consumed (Dill, 1977). Similar to the leptobramids, toxotids exhibit a set of morphological characters that have led authors to ally the family with many other families (e.g., Kyphosidae, Monodactylidae, Mok and Shen, 1983). Günther (1860) suggested a number of allies to Toxotidae, from Chaetodontidae to Microcanthidae, based on a diversity of morphological features. Since Günther's work, two explicit groups have been allied with toxotids based on morphological data: McAllister (1968) and Mok and Shen (1983) allied Toxotidae with various squamipennes (*sensu* Mok and Shen, 1983) based on a number of gill arch and scale characteristics, and the analysis by Springer and Orrell (2004) recovered Ambassidae and Centrolophidae allied to Toxotidae based on dorsal gill-arch musculature. Studies based on DNA-sequence data have consistently recovered Toxotidae among the carangiform fishes (e.g., Chen et al., 2007), with allies ranging from Latidae (Li et al., 2009; Rabosky et al., 2018) to Nematistiidae (Li et al., 2011). However, many DNA-based studies have recovered Leptobramidae as the sister group of Toxotidae (Betancur-R. et al., 2013a, 2013b; Betancur-R. and Ortí, 2014; Harrington et al., 2016; Sanciangco et al., 2016).

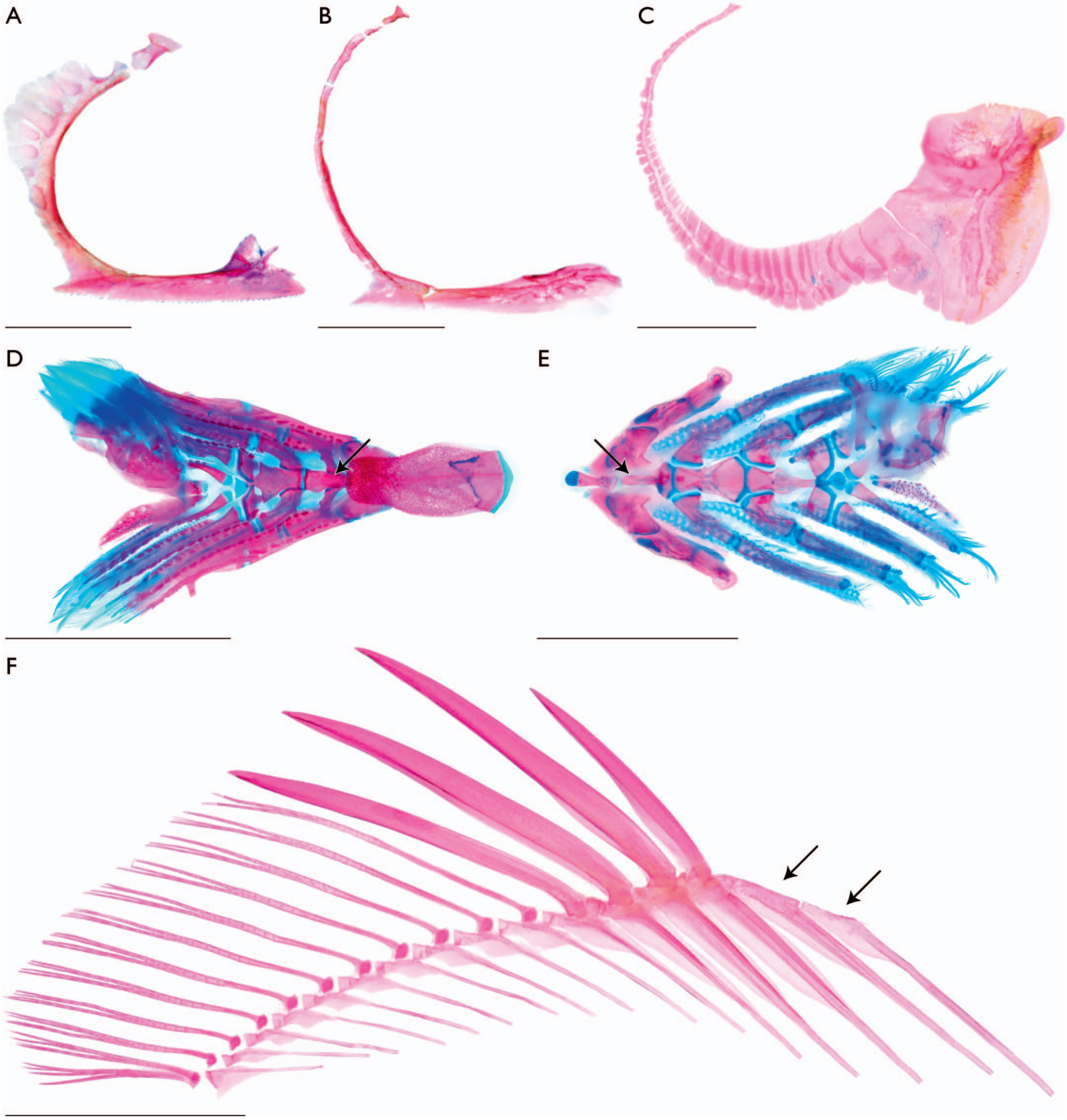

Fig. 8. Morphological variation in support of the relationship among the Menoidei, Nematistioidei, and Toxotoidei. Images of cleared and stained specimens under white or daylight LED light. Increased number of circumorbital elements (character 16_1)—(A) *Leptobrama muelleri* (KUI 41406), right lateral view, scale bar = 5 mm; (B) *Nematistius pectoralis* (SIO 12-3085), right lateral view, scale bar = 5 mm; (C) *Mene maculata* (FMNH 119713), right lateral view, scale bar = 5 mm. Basibranchial two is the anteriormost visible basibranchial when viewed dorsally, as basibranchial one is covered dorsally by the basihyal (character 63_1)—(D) *Toxotes blythii* (KUI 42173), arrow, dorsal view of branchial elements, scale bar = 5 mm. Basibranchial one is the anteriormost visible basibranchial with the basihyal anterior to and in series with basibranchials (character 63_0)—(E) *Achirus lineatus* (FMNH 113137), arrow, dorsal view of branchial elements, scale bar = 5 mm. Dorsal pterygiophore without associated dorsal spine (character 135_1)—(F) *Toxotes jaculatrix* (FMNH 69510), arrows, right lateral view of dorsal-fin elements, scale bar = 5 mm.

Our combined analysis recovers Leptobramidae sister to Toxotidae within the Toxotoidei; this clade is supported by 14 morphological characters and DNA-sequence data. Some morphological characters supporting this relationship include, but are not limited to, ventral margin of lachrymal serrated (character 15_1), posteriorly placed basihyal that inserts dorsal to basibranchial one (character 63_1; Fig. 8D vs. 8E), absence of a medial-extrascapular (character 103_0),

the ventral processes of the coracoid and cleithrum are distinctly separate (character 114_1), and an anterior dorsal pterygiophore without an associated dorsal spine (character 135_1; Fig. 8F). Aside from members of the Toxotoidei, taxa sampled in this study possessed a basihyal placed rostral to the first basibranchial (e.g., *Lates, Echeneis, Sphyraena*) or rostral and slightly dorsal to the first basibranchial element (e.g., *Coryphaena, Polydactylus*, *Trachinotus*; Fig. 8E). However, *Leptobrama* and *Toxotes* exhibit a different condition, where the basihyal lies directly dorsal to basibranchial one, covering the element, and in the case of *Toxotes,* covering the rostral margin of the second basibranchial as well (Fig. 8D). Accompanying the posterior placement, the basihyal has an elevated position when viewing the branchial basket laterally. We did not find any indication in previous studies that this feature has been found in any other lineages of fishes. Given the results of our combined analysis, the posterior placement of the basihyal supports the monophyly of the Toxotoidei. One of the defining characteristics of acanthomorph fishes are the prominent spine(s) in the anterior portions of the dorsal and anal fins (Johnson and Patterson, 1993). In many percomorph fishes, the first two dorsal spines are borne on the anteriormost compound dorsal pterygiophore (e.g., Anthiadidae, Epinephelidae, Serranidae, Johnson, 1983, 1988). In his study of *Leptobrama*, Tominaga (1965) noted nine predorsals in the dorsal fin of leptobramids that did not possess an associated external ray or spine. We find that the nine predorsals listed by Tominaga (1965) correspond to three supraneurals (*sensu* Mabee, 1988) and six spineless pterygiophores in *Leptobrama*. Anterior pterygiophores lacking a spine or ray are rarely found among percomorph fishes. Examples of groups with rayless anterior pterygiophores include *Bathyclupea* (≈6 spineless pterygiophores; Prokofiev, 2014), some members of the carangid subfamilies Scomberoidinae and Trachinotinae (≈1 spineless pterygiophore; Springer and Smith-Vaniz, 2008), *Kurtus* (≤3 spineless pterygiophores; Tominaga, 1965), and *Toxotes* (1–3 spineless pterygiophores, pers. obs.; Fig. 8F). Given the limited distribution of this character among percomorphs and the results of our combined analysis, the presence of one or more spineless anterior pterygiophores that lack an associated spine (character 135_1) is a feature that supports the sister-group relationship between Leptobramidae and Toxotidae.

Menoidei.—The two families of billfishes, Istiophoridae (10 species) and Xiphiidae (1 species), can be found in pelagic environments throughout the oceans (Nakamura, 1983). These fishes exhibit a suite of morphological features that are rarely found in other lineages of fishes, including an elongated premaxillary rostrum and the physiological ability for regional endothermy (Brill, 1996). Studies based on comparative morphology have largely allied the xiphioids among the traditional scombroids, as well as these scombroids plus Acropomatidae, Dinolestidae, Malakichthyidae, Pomatomidae, Sphyraenidae, and Synagropidae (Johnson, 1986). Despite commonly placing these fishes among scombroids, morphological hypotheses have disagreed on the placement of billfishes among these families. Xiphioidea has been placed as the sister group to Scombridae (Collette and Russo, 1984; Collette et al., 1984) or within the Scombridae and sister to *Acanthocybium* (Johnson, 1986; Carpenter et al., 1995). Similar to the morphological hypotheses of Nakamura (1983), Potthoff et al. (1986), and van der Straten et al. (2006), hypotheses based on DNA-sequence data have recovered the xiphioids outside of the Scombroidei (e.g., Orrell et al., 2006; Miya et al., 2013) and among the carangiform fishes (e.g., Smith and Wheeler, 2006; Near et al., 2012; Rabosky et al., 2018). Like most members of the Carangiformes, previous hypotheses have recovered a diversity of lineages sister to the xiphioids (e.g., Smith and Wheeler, 2006; Li et al., 2009). However, a majority of DNA-based hypotheses that have included both xiphioid families have recovered this clade sister to the Menidae (Betancur-R. et al., 2013a; Campbell et al., 2013; Betancur-R. and Ortí, 2014; Harrington et al., 2016; Rabosky et al., 2018; Shi et al., 2018).

Represented by one extant species and numerous extinct species, the moonfishes (Menidae) are easily recognized by their laterally compressed, disc-like bodies, uniquely shaped medial-fin rays, and narrow pelvic fins. The extant species, *Mene maculata*, can be found near the bottom of coastal waters throughout the Indian Ocean, Indo-Pacific archipelago, Taiwan, and Japan (Carpenter et al., 1997). While one early study based on comparative morphology placed *Mene* near a variety of fishes (Beryciformes and Ophidiiformes, Springer and Johnson, 2004; see Friedman and Johnson, 2005 for review), Leis (1994) allied menids with the Carangoidei based on six morphological characters shared between carangoids and menids. Leis (1994) also noted eight additional characters shared by *Lactarius, Mene*, and a subset of carangoids, and he tentatively placed Lactariidae sister to Menidae and a subset of carangoids. While early DNA-based studies recovered Menidae sister to all or a subset of families within Carangoidei (e.g., Chen et al., 2003; Dettaï and Lecointre, 2004, 2005), more recent hypotheses based on DNA-sequence data have recovered Menidae sister to the Xiphioidea (e.g., Harrington et al., 2016; Rabosky et al., 2018; Shi et al., 2018).

Our combined analysis recovers Menidae sister to Xiphioidea supported by 13 morphological characters and DNA-sequence data. Some morphological characters supporting this relationship include the absence of vomerine teeth (character 5_1), lateral flaring of the parasphenoid (character 11_1; Fig. 9), lack of a projection on hypobranchial one (character 76_1), more than one accessory ossification associated with extrascapular bones of supratemporal canal (character 106_1), fusion of hypurals and urostyle into a singular plate in adults (characters 185_1, 186_1, and 187_1; Fig. 10B), and the presence of hypurostegy (character 190_1; Fig. 10A, B). In their survey of xiphioid morphology, Gregory and Conrad (1937, their fig. 8) noted and illustrated that the parasphenoid is a dorsoventrally flattened element with laterally flaring lamellar bone among the xiphioids. Nakamura (1983) described a flattened parasphenoid in all billfishes, noting variation in the width of the anterior part of the parasphenoid in various species (his character 7). The parasphenoid is typically a rod-like medial element that interacts with the base of the neurocranium posteriorly and the vomer anteriorly. While the parasphenoid is typically a simple element, the parasphenoid is dorsoventrally flattened into a plate-like element, with laterally extending lamellar bone in members of the Menoidei (Fig. 9A, B). Flaring of the parasphenoid was not observed in any other fishes examined aside from *Echeneis*, where the parasphenoid was a broad plate merging with the vomer. In the illustrations of Collette

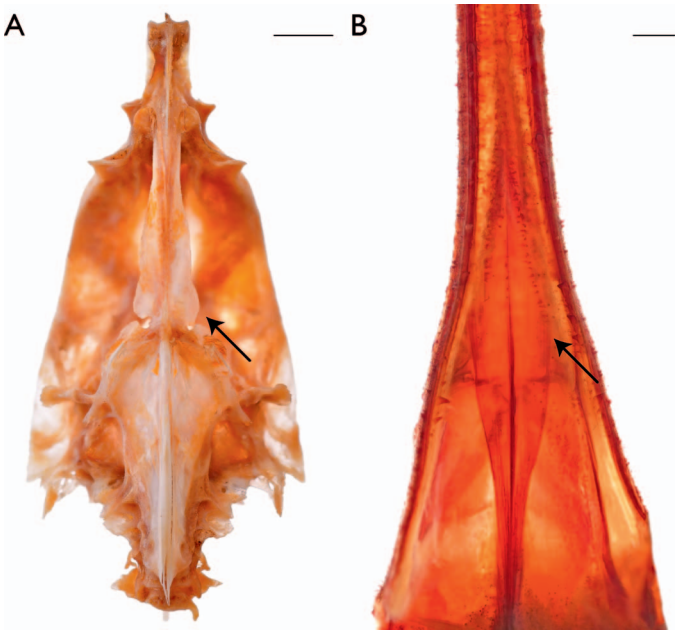

Fig. 9. Morphological variation in support of the relationship among the Menoidei. Lateral flaring of the parasphenoid (character 11_1)—(A) *Mene maculata* (KUI 42175), skeletal specimen imaged under white or daylight LED light, ventral view, scale bar = 5 mm; (B) *Xiphias gladius* (MCZ 55512, Museum of Comparative Zoology, Harvard University, ©2019 President and Fellows of Harvard College), cleared and stained specimen imaged under white or daylight LED light, ventral view, scale bar = 1 mm.

and Russo (1984), *Acanthocybium* and some species of *Scomberomorus* exhibit a wide parasphenoid when viewed ventrally (their figs. 17 and 19). In lateral view, it would appear that the parasphenoid in these fishes is robust throughout, without the lamellar plate-like bone expanding laterally (Collette and Russo, 1984, their figs. 15 and 16). Collette and Russo (1984) noted that the wide parasphenoid appears "independently" in several other lineages of scombroids, including *Cybiosarda*, *Gymnosarda*, *Orcynopsis*, and *Sarda*. While we were limited to viewing the osteology of *Acanthocybium* and *Scomberomorus* from published illustrations, we currently do not find the morphology exhibited by these taxa to be the same as what is observed in menoids. Further examination is needed to clarify the homology of this character across disparate percomorph clades. A number of caudal skeletal characters also support a relationship among the Menoidei, including the fusion of hypurals and urostyle into a singular plate (characters 185_1, 186_1, and 187_1) and the presence of hypurostegy (character 190_1; Fig. 10A, B). The first through fourth hypurals in Xiphioidea and *Mene* are fused into a plate along with the urostyle. As noted by Johnson (1986), most percomorphs possess five autogenous hypural elements, with differential fusion occurring between the upper and lower hypurals in some fishes (e.g., scombroids). Fusions between hypurals have been used to support hypotheses of relationships as they relate to scombroids, with Collette et al. (1984) finding the fusion of the upper and lower hypural plates as a synapomorphy for all scombrids and xiphioids except *Gasterochisma*, *Grammatorcynus*, and his Scombrini. Alternatively, Johnson (1986) found the fusion of the upper and lower hypural plates as a synapomorphy of Xiphioidea, the Sardini and Thunnini of Collette et al. (1984), as well as *Acanthocybium*, *Grammatorcynus*, and *Scomberomorus*. While fusions among the upper and lower hypurals occur in a number of taxa (see characters 183 and 184), the second and third hypurals were fused together, forming a singular plate, in Menoidei (character 185_1). Further, this hypural plate, which consists of hypurals 1–4, was fused to the urostyle in menoid taxa exclusively (characters 186_1 and 187_1). While other taxa sampled did exhibit fusion between the third hypural, fourth hypural, and urostyle (e.g., *Mugil*, *Nandus*, *Scophthalmus*; character 187_1), fusion was not detected between the first hypural, second hypural, and urostyle in any other lineages examined besides Xiphioidea and *Mene*. Hypurostegy is the anterior extension of the proximal bases of the caudal-fin rays such that they partially or completely cover the lateral aspects of the hypurals (Fig. 10A–C). Similar to hypural fusion, hypurostegy was found by Collette et al. (1984) and Johnson (1986) to support a clade of Scombridae + Xiphioidea (Fig. 10A, C). Various amounts of hypurostegy can be found within a diversity of fast-swimming carangiform fishes (e.g., *Caranx*) and percomorphs outside of the Carangiformes (e.g., *Scomber* [Fig. 10C], *Luvarus* [Nakamura, 1983; Johnson, 1986]). Given the distribution of hypurostegy among fishes, it is likely that the presence of this character is the result of convergence among large and fast-swimming acanthomorphs (Nakamura, 1983; Johnson, 1986). While we recognize that this feature has likely evolved in unrelated groups of fishes, the results from our combined analysis suggest that the presence of hypurostegy supports the relationship between taxa in the Menoidei.

Carangoidei.—The amberjacks, trevally, pompanos, leatherjackets, and allies are classified in the diverse family Carangidae, which includes approximately 150 species in four subfamilies. While morphology-based studies have repeatedly recovered the monophyly of Carangidae (e.g., Smith-Vaniz, 1984; Gushiken, 1988) united largely by the posteroventral elongation of the first proximal anal-fin pterygiophore and gap between the second and the third anal-fin spines, only a subset of DNA-based hypotheses that have included representatives from three or more of the four subfamilies have recovered a monophyletic Carangidae (e.g., Reed et al., 2002; Sanciangco et al., 2016; Betancur-R. et al., 2017). Hypotheses based on DNA-sequence data mostly recover the carangid subfamilies Caranginae and Naucratinae as sister lineages with the remaining carangid subfamilies, Trachinotinae and Scomberoidinae, sister to the Echeneoidea (e.g., Smith and Wheeler, 2006; Near et al., 2012; Mirande, 2016). Given the repeated non-monophyly of Carangidae in recent analyses, we refer to the carangid subfamilies Trachinotinae and Scomberoidinae as members of the "Carangidae" (Figs. 2, 3) as future studies targeting the non-monophyly of Carangidae will likely place these two subfamilies in one (Trachinotidae) or two (Trachinotidae and Scomberoididae) separate families that, combined, are sister to Echeneoidea. The Echeneoidea has long been allied with carangid taxa in morphology-based studies, with Smith-Vaniz (1984) describing three osteological synapomorphies for the Carangoidei as defined above.

Although testing carangid monophyly was not an explicit goal of this study, we recovered the Echeneoidea nested within the Carangidae, sister to a clade of Trachinotinae and Scomberoidinae, in our combined analysis. This relationship

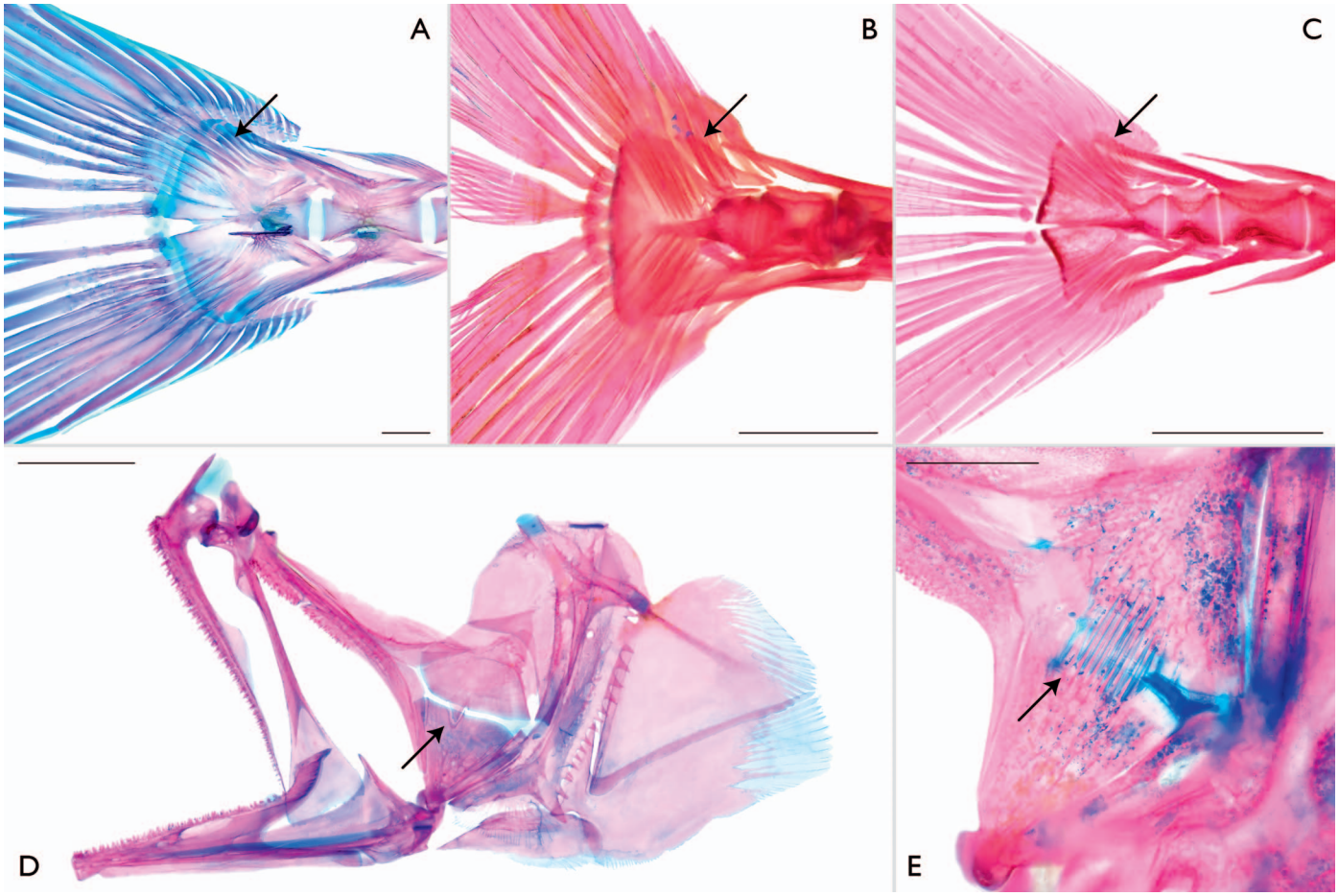

Fig. 10. Representative convergent morphological characters coded in this study. Images of cleared and stained specimens under white or daylight LED light. Presence of hypurostegy (character 190_1)—(A) *Istiophorus platypterus* (SIO 73-269), arrow, right lateral view, scale bar = 1 mm; (B) *Mene maculata* (FMNH 119713), arrow; right lateral view, scale bar = 5 mm; (C) *Scomber japonicus* (KUI uncat.), arrow, right lateral view, scale bar = 5 mm. Presence of interdigitation between metapterygoid and quadrate (character 46_1)—(D) *Polydactylus virginicus* (FMNH 104648), arrow, medial view of right suspensorium, scale bar = 2.5 mm; (E) *Leptobrama muelleri* (KUI 41406), arrow, medial view of right suspensorium, scale bar = 2.5 mm.

is supported by two morphological characters and DNA-sequence data, including the possession of a small supramaxilla (character 25_0) and paired toothplates on basibranchial three (character 73_0). One of these morphological characters is the possession of a small supramaxilla (character 25_0) found in echeneoid and trachinotine taxa examined. This character is coded as inapplicable for *Echeneis* and *Oligoplites*, as the supramaxilla has been lost in these taxa. While we recognize that the size of the supramaxilla varies across many unrelated groups of fishes (e.g., *Lepomis*), the results from our combined analysis suggest that a small supramaxilla supports the relationship among the taxa in the Echeneoidea, Scomberoidinae, and Trachinotinae. Additional investigations are needed into the non-monophyly of Carangidae to fully assess the homology of the characters we highlight above and to test the limits of the family.

Patterns of convergence in relation to carangiform fishes.—The phylogeny of carangiform fishes we recover highlights that morphological characters provide critical insights and help resolve the relationships among these newly recovered DNA-based clades of fishes. The combination of this novel morphological dataset with the topology from the combined analysis depicts a tremendous amount of morphological convergence seen between these and other percomorph fishes that some carangiforms have been historically allied with. For example, it has been hypothesized that Polynemidae and Sciaenidae are closely related based on a number of characters including the interdigitation between the metapterygoid and quadrate (Johnson, 1993; Kang et al., 2017). Many morphological characters were coded similarly between the Polynemidae and Sciaenidae in our dataset, with 22 of 201 characters coded as the same derived character state between these two families. These shared characters include the interdigitation between the metapterygoid and quadrate (Fig. 10D) discussed by previous authors. However, we find that interdigitation between the metapterygoid and quadrate does not support a relationship between Polynemidae and Sciaenidae (character 46), and it is also present in *Leptobrama* (Fig. 10E). Hypotheses based on DNA-sequence data recover Polynemidae and Sciaenidae as divergent lineages, with a number of hypotheses recovering the Pleuronectoideo as the sister group to Polynemidae (e.g., Harrington et al., 2016; Alfaro et al., 2018; Shi et al., 2018; current study). Making a similar comparison between the character states coded for Polynemidae and Psettodidae, only five characters with

derived states are shared between these two lineages. These clades were not considered close allies in previous morphology-based studies. Members of the Pleuronectoideo were traditionally regarded in their own percomorph order due to their highly derived morphology. It is not surprising then that few derived morphological characters are shared between these lineages. However, given our datasets and analysis, the overwhelming morphological similarity between Polynemidae and Sciaenidae is best explained by convergence. Despite this convergence, there are no uniquely derived features shared between the Polynemidae and Sciaenidae in our dataset, and it is only by examining the morphology of these new clades that we recognize the wider distributions of rare features such as the interdigitation of the metapterygoid and quadrate (character 46). In another example, xiphioids have been included within the Scombroidei based on morphological data (Collette et al., 1984; Johnson, 1986) and 13 of 201 characters were coded as having the same derived character state between these groups, highlighting areas of morphological similarity between *Scomber* and Xiphioidea. However, studies based on DNA-sequence data have repeatedly recovered Menidae as the most recent ally of the Xiphioidea (e.g., Betancur-R. and Ortí, 2014; Harrington et al., 2016; Rabosky et al., 2018; Shi et al., 2018). *Mene* has been allied to members of the Carangiformes, specifically Carangidae and Lactariidae, based on morphological data (Leis, 1994). When comparing Menidae and Xiphioidea based on the characters coded in this study, 22 characters support the sister-group relationship between these two lineages despite them not being proposed as allies in previous morphology-based studies. It is noteworthy that eight of these characters are shared among all three lineages—Xiphioidea, *Mene*, and *Scomber*. One possible explanation for these convergences is that all three of these lineages live in similar oceanic environments and are under similar environmental pressures. As such, it is not surprising that these fishes exhibit numerous convergent morphological features (Fig. 10A–C).

The combined morphological and molecular phylogeny presented in this study provides an opportunity to arbitrate the conflict between morphology-based and DNA-based data, test the phylogenetic implications of different traits present in these fishes, and examine the evolution of morphological characters within this newly recovered clade of fishes. We hope that our findings not only highlight the utility of morphological characters as they relate to the evolution of carangiform fishes but that they also invite subsequent authors to test additional evolutionary hypotheses within this clade. Finally, we encourage other authors to integrate morphological characters with DNA-sequence data to further test the relationships of and explore the evolution of the widely diverse percomorph fishes.

NOTE ADDED IN PROOF

During the generation of proofs for this study, Chanet et al. (2020) published a reassessment of the interrelationships among flatfish families by including two explicit carangiform outgroup taxa (*Caranx* and *Lates*) and one extinct flatfish taxon (†*Amphistium*) into Chapleau's (1993) foundational morphological matrix. Chanet et al. (2020) similarly recovered a monophyletic flatfishes and highlighted morphological features that support the relationships they recovered. While their discussion of the relationships within the Pleuronectoideo falls outside of the goals of our study, Chanet et al. (2020) noted morphological similarity in the robustness of the first anal-fin pterygiophore among carangiform taxa they included (their fig. 4). We assessed variation in first anal-fin pterygiophore with respect to the interaction between the first anal-fin pterygiophore and first hemal spine (characters 148, 149), and overall shape of the first anal-fin pterygiophore (character 153), but these features optimized in disparate locations in our resulting phylogeny (Fig. 3, Supplemental Fig. 2; see Data Accessibility). In light of this, we did not find the results of Chanet et al. (2020) to impact the results of our analysis and have not altered our study in light of their findings. However, we value the study by Chanet et al. (2020) as it places the relationships among flatfishes based on morphology in a modern phylogenetic context.

MATERIAL EXAMINED

In the following section, cleared and stained specimens are denoted "CS"; whole ethanol specimens are denoted "ET"; dry osteological preparations and skeletons are denoted "SK." Following the listing of each taxon, an approximate size or range of sizes are listed in mm standard length (SL) for the specimens examined.

OUTGROUP TAXA

Centrarchidae

Lepomis cyanellus: KUI 15906 (6 CS), 43–62 mm SL.

Channidae

Channa micropeltes: CAS 230636 (1 CS; 1 ET), 50–52 mm SL.

Mugilidae

Mugil curema: KUI 15930 (5 CS; 2 ET), 47–75 mm SL.

Nandidae

Nandus nandus: KUI 29103 (1 CS; 1 ET), 79–80 mm SL.

Percidae

Perca flavescens: KUI 16973 (2 CS), 47–60 mm SL.

Polycentridae

Monocirrhus polyacanthus: KUI 23678 (1 CS), 42 mm SL.

Sciaenidae

Micropogonias undulatus: KUI 29204 (2 CS), 33–48 mm SL.

Scombridae

Scomber japonicus: KUI uncataloged (1 CS), 105 mm SL.

CARANGIFORMES

Achiridae

Achirus lineatus: FMNH 113137 (2 CS), 56–58 mm SL.

Carangidae

Caranx hippos: KUI 30383 (1 CS), 58 mm SL.

Naucrates ductor: LACM 8999.012 (1 CS); LACM 50892.001 (1 ET); LACM 56285.017 (1 ET), 64–100 mm SL.

Oligoplites saurus: KUI 17205 (1 CS; 1 ET), 56–62 mm SL.

Trachinotus carolinus: KUI 20087 (1 CS; 2 ET), 72–75 mm SL.

Trachurus trachurus: KUI 19964 (2 CS; 1 ET), 45–70 mm SL.

Centropomidae

Centropomus armatus: CAS 78494 (1 CS; 1 ET); KUI 40318 (1 CS), 35–106 mm SL.

Centropomus undecimalis: AMNH 22051 (2 CS); FMNH 77806 (4 CS), 37–65 mm SL.

Coryphaenidae

Coryphaena hippurus: FMNH 48561 (2 CS), 73–74 mm SL.

Echeneidae

Echeneis naucrates: KUI 10026 (1 CS); KUI 41346 (1 CS), 115–179 mm SL.

Istiophoridae

Istiophorus platypterus: SIO 73-269 (1 CS), 120 mm SL.

Lactariidae

Lactarius lactarius: KUI 41405 (1 CS); LACM 38318.005 (2 ET); USNM 345430 (1 CS), 111–142 mm SL.

Latidae

Lates calcarifer: AMNH 37839 (1 CS; 1 ET), 82–85 mm SL.

Psammoperca waigiensis: FMNH 51826 (1 CS), 96 mm SL.

Leptobramidae

Leptobrama muelleri: AMNH 219223 (1 SK); AMNH 219224 (1 SK); KUI 41406 (1 CS); UW 7204 (1 ET), 113–270 mm SL.

Menidae

Mene maculata: FMNH 119713 (1 CS); KUI 41878 (1 ET); KUI 42175 (2 SK; 1 ET), 110–190 mm SL.

Nematistiidae

Nematistius pectoralis: ANSP 148654 (1 CS); SIO 12-3085 (1 CS, 2 ET), 78–190 mm SL.

Polynemidae

Eleutheronema tetradactylum: AMNH 216773 (1 SK); FMNH 51970 (1 CS), 94–200 mm SL.

Filimanus similis: LACM 38134.017, 90 mm SL.

Polydactylus sexfilis: CAS 50911, 51 mm SL.

Polydactylus virginicus: FMNH 104648 (1 CS; 1 ET), 49–56 mm SL.

Psettodidae

Psettodes erumei: AMNH 214777 (1 SK); ANSP 415349 (1 CS); USNM 282709 (1 CS), 53–290 mm SL.

Rachycentridae

Rachycentron canadum: TU 167726 (2 CS; 5 ET), 38–100 mm SL.

Scophthalmidae

Scophthalmus aquosus: KUI 30388 (3 CS), 47–49 mm SL.

Sphyraenidae

Sphyraena barracuda: FMNH 74209 (1 CS), 110 mm SL.

Sphyraena idiastes: SIO 15–182 (1 CS), 162 mm SL.

Toxotidae

Toxotes blythii: KUI 42173 (2 CS), 36–46 mm SL.

Toxotes jaculatrix: FMNH 69510 (4 CS); KUI 42174 (1 CS), 60–63 mm SL.

Xiphiidae

Xiphias gladius: MCZ 55512 (1 CS), 146 mm SL.

DATA ACCESSIBILITY

Supplemental information is available at https://www.copeiajournal.org/ci-19-320.

ACKNOWLEDGMENTS

We thank R. Smetana and K. Smith for helpful discussions and editing of this manuscript. We thank K. Herzog, K. Jensen, G. Ornay, and R. Timm (KU), A. Alexander (University of Otago), J. Webb (University of Rhode Island), M. Ghedotti (Regis University), and K. Tang (University of Michigan, Flint) for thoughtful discussions of methods and morphology in this study. We thank H. J. Walker (SIO) for examining specimens of *Nematistius* at SIO. We thank J. Sparks and B. Brown (AMNH), M. Sabaj and M. Arce H. (ANSP), L. Rocha and D. Catania (CAS), A. Graham (CSIRO), C. McMahan, S. Mochel, and K. Swagel (FMNH), R. Hanel (ISH), A. Bentley (KUI), C. Thacker and R. Feeney (LACM), G. Dally, M. Hammer, and H. Larson (MAGNT), A. Williston (MCZ), K. Carpenter (ODU), P. Hastings, H. J. Walker, and B. Frable (SIO), H. Bart (TU), G. D. Johnson and J. Williams (USNM), and the crew aboard Delaware II DE 01-11, for providing data, support, and/or access to specimens or tissues from their collections. Research was funded by a Biodiversity Institute Panorama Grant (awarded to M.G.G.), Lerner Gray Grant for Marine Research (awarded to M.G.G.), University of Kansas General Research Fund (2105077 awarded to W.L.S.), and National Science Foundation grants (DEB 1258141 and 1543654 awarded to M.P.D. and W.L.S.), and the University of Kansas.

LITERATURE CITED

Alfaro, M. E., B. C. Faircloth, R. C. Harrington, L. Sorenson, M. Friedman, C. E. Thacker, C. H. Oliveros, D. Černý, and T. J. Near. 2018. Explosive diversification of marine fishes at the Cretaceous-Palaeogene boundary. Nature Ecology and Evolution 2:688–696.

Allis, E. P. 1899. The skull and cranial and first spinal muscles and nerves in *Scomber scomber*. Journal of Morphology 28:45–328.

Amaoka, K. 1969. Studies on the sinistral flounders found in the waters around Japan: taxonomy, anatomy and phylogeny. Journal of the Shimonoseki College of Fisheries 18: 65–340.

Baldwin, C. C., and G. D. Johnson. 1993. Phylogeny of the Epinephelinae (Teleostei: Serranidae). Bulletin of Marine Science 52:240–283.

Baldwin, C. C., and G. D. Johnson. 1996. Aulopiform interrelationships, p. 355–404. *In*: Interrelationships of Fishes. M. L. J. Stiassny, L. R. Parenti, and G. D. Johnson (eds.). Academic Press, San Diego.

Bannikov, A. F. 1987. The phylogenetic relationships of the carangid fishes of the subfamily Caranginae. Paleontological Journal 21:44–53.

Berendzen, P. B., and W. W. Dimmick. 2002. Phylogenetic relationships of Pleuronectiformes based on molecular evidence. Copeia 2002:642–652.

Betancur-R., R., R. E. Broughton, E. O. Wiley, K. Carpenter, J. A. López, C. Li, N. I. Holcroft, D. Arcila, M. Sanciangco, J. C. Cureton II, F. Zhang, T. Buser, M. A. Campbell, J. A. Ballesteros . . . G. Ortí. 2013b. The tree of life and a new classification of bony fishes. PLoS Currents Tree of Life 5.

Betancur-R., R., C. Li, T. A. Munroe, J. A. Ballesteros, and G. Ortí. 2013a. Addressing gene tree discordance and non-stationarity to resolve a multi-locus phylogeny of the flatfishes (Teleostei: Pleuronectiformes). Systematic Biology 62:763–785.

Betancur-R., R., and G. Ortí. 2014. Molecular evidence for the monophyly of flatfishes (Carangimorpharia: Pleuronectiformes). Molecular Phylogenetics and Evolution 73: 18–22.

Betancur-R., R., E. O. Wiley, G. Arratia, A. Acero, N. Bailly, M. Miya, G. Lecointre, and G. Ortí. 2017. Phylogenetic classification of bony fishes. BMC Evolutionary Biology 17: 162.

Bolger, A. M., M. Lohse, and B. Usadel. 2014. Trimmomatic: a flexible trimmer for Illumina sequence data. Bioinformatics 30:2114–2120.

Bräger, Z., and T. Moritz. 2016. A scale atlas for common Mediterranean teleost fishes. Vertebrate Zoology 66:275–386.

Brewster, B. 1987. Eye migration and cranial development during flatfish metamorphosis: a reappraisal (Teleostei, Pleuronectiformes). Journal of Fish Biology 31:805–833.

Bridge, T. W. 1896. The mesial fins of ganoids and teleosts. Journal of the Linnean Society of London, Zoology 25:530–602.

Brill, R. W. 1996. Selective advantages conferred by the high performance physiology of tunas, billfishes, and dolphin fish. Comparative Biochemistry and Physiology, Part A 113:3–15.

Britz, R., and G. D. Johnson. 2012. Ontogeny and homology of the skeletal elements that form the sucking disc of remoras (Teleostei, Echeneoidei, Echeneidae). Journal of Morphology 273:1353–1366.

Byrne, L., F. Chapleau, and S. Aris-Brosou. 2018. How the Central American seaway and an ancient northern passage affected flatfish diversification. Molecular Biology and Evolution 35:1982–1989.

Campbell, M. A., B. Chanet, J.-N. Chen, M.-Y. Lee, and W.-J. Chen. 2019. Origins and relationships of the Pleuronectoidei: molecular and morphological analysis of living and fossil taxa. Zoologica Scripta 48:640–656.

Campbell, M. A., W.-J. Chen, and J. A. López. 2013. Are flatfishes (Pleuronectiformes) monophyletic? Molecular Phylogenetics and Evolution 69:664–673.

Campbell, M. A., W.-J. Chen, and J. A. López. 2014b. Molecular data do not provide unambiguous support for the monophyly of flatfishes (Pleuronectiformes): a reply to Betancur-R. and Ortí. Molecular Phylogenetics and Evolution 75:149–153.

Campbell, M. A., J. A. López, T. P. Satoh, W.-J. Chen, and M. Miya. 2014a. Mitochondrial genomic investigation of flatfish monophyly. Gene 551:176–182.

Carpenter, K. E., B. B. Collette, and J. L. Russo. 1995. Unstable and stable classifications of scombroid fishes. Bulletin of Marine Science 56:379–405.

Carpenter, K. E., F. Krupp, D. A. Jones, and U. Zajonz. 1997. Living marine resources of Kuwait, eastern Saudi Arabia, Bahrain, Qatar, and the United Arab Emirates. Food and Agriculture Organization of the United Nations, Rome.

Chabanaud, P. 1936. Le neurocrane osseux des téléostéens dyssymétriques après la métamorphose. Annales de l'Institut Océanographique 16:223–297.

Chabanaud, P. 1949. Le problème de la phylogénèse des Heterosomata. Bulletin de l'Institut Océanographique 950: 1–24.

Chakrabarty, P., M. P. Davis, W. L. Smith, R. Berquist, K. M. Gledhill, L. R. Frank, and J. S. Sparks. 2011. Evolution of the light organ system in ponyfishes (Teleostei: Leiognathidae). Journal of Morphology 272:704–721.

Chanet, B. 2003. Interrelationships of scophthalmid fishes (Pleuronectiformes: Scophthalmidae). Cybium 27:275–286.

Chanet, B., F. Chapleau, and M. Desoutter. 2004. Intermuscular bones and ligaments in flatfishes [Teleostei: Pleuronectiformes]: phylogenetic interpretations. Cybium 28:9–14.

Chanet, B., J. Mondéjar-Fernández, and G. Lecointre. 2020. Flatfishes interrelationships revisited based on anatomical characters. Cybium 44:9–18.

Chapleau, F. 1993. Pleuronectiform relationships: a cladistic reassessment. Bulletin of Marine Science 52:516–540.

Chen, W.-J., C. Bonillo, and G. Lecointre. 2003. Repeatability of clades as a criterion of reliability: a case study for molecular phylogeny of Acanthomorpha (Teleostei) with larger number of taxa. Molecular Phylogenetics and Evolution 26:262–288.

Chen, W.-J., R. Ruiz-Carus, and G. Ortí. 2007. Relationships among four genera of mojarras (Teleostei: Perciformes: Gerreidae) from the western Atlantic and their tentative placement among percomorph fishes. Journal of Fish Biology 70:202–218.

Chernomor, O., A. von Haeseler, and B. Q. Minh. 2016. Terrace aware data structure for phylogenomic inference from supermatrices. Systematic Biology 65:997–1008.

Cockerell, T. D. A. 1913. Observations on fish scales. Bulletin of the Bureau of Fisheries 779:117–179.

Collette, B. B., T. Potthoff, W. J. Richards, S. Ueyanagi, J. L. Russo, and Y. Nishikawa. 1984. Scombroidei: development and relationships, p. 591–620. *In*: Ontogeny and Systematics of Fishes. H. G. Moser, W. J. Richards, D. M. Cohen, M. P. Fahay, A. W. Kendall, Jr., and S. L. Richardson (eds.). American Society of Ichthyologists and Herpetologists, Special Publication No. 1, Lawrence, Kansas.

Collette, B. B., and J. L. Russo. 1984. Morphology, systematics, and biology of the Spanish Mackerels (*Scomberomorus*, Scombridae). Fishery Bulletin 82:545–692.

Cooper, J. A., and F. Chapleau. 1998. Phylogenetic status of *Paralichthodes algoensis* (Pleuronectiformes: Paralichthodidae). Copeia 1998:477–481.

Cuvier, G., and M. Valenciennes. 1831. Histoire Naturelle des Poisons. Volume 8, Paris.

Datovo, A., and R. P. Vari. 2013. The jaw adductor muscle complex in teleostean fishes: evolution, homologies and revised nomenclature (Osteichthyes: Actinopterygii). PLoS ONE 8:e60846.

Davis, B. D. 2009. Spitting at the dinner table: archerfish (*Toxotes chatareus*) kleptoparasitism and social foraging. Unpubl. Ph.D. diss., Simon Frasier University, Burnaby, British Columbia.

Davis, M. P., J. S. Sparks, and W. L. Smith. 2016. Repeated and widespread evolution of bioluminescence in marine fishes. PLoS ONE 11:e0155154.

de Sylva, D. P. 1984a. Sphyraenoidei: development and relationships, p. 534–540. *In*: Ontogeny and Systematics of Fishes. H. G. Moser, W. J. Richards, D. M. Cohen, M. P. Fahay, A. W. Kendall, Jr., and S. L. Richardson (eds.). American Society of Ichthyologists and Herpetologists, Special Publication No. 1, Lawrence, Kansas.

de Sylva, D. P. 1984b. Polynemoidei: development and relationships, p. 540–541. *In*: Ontogeny and Systematics of Fishes. H. G. Moser, W. J. Richards, D. M. Cohen, M. P. Fahay, A. W. Kendall, Jr., and S. L. Richardson (eds.). American Society of Ichthyologists and Herpetologists, Special Publication No. 1, Lawrence, Kansas.

Dettaï, A., and G. Lecointre. 2004. In search of notothenioid (Teleostei) relatives. Antarctic Science 16:71–85.

Dettaï, A., and G. Lecointre. 2005. Further support for the clades obtained by multiple molecular phylogenies in the acanthomorph bush. Comptes Rendus Biologies 328:674–689.

Dill, L. M. 1977. Refraction and the spitting behavior of the archerfish (*Toxotes chatareus*). Behavioral Ecology and Sociobiology 2:169–184.

Eastman, J. T. 1977. The pharyngeal bones and teeth of catostomid fishes. American Midland Naturalist 97:68–88.

Faircloth, B. C. 2013. Illumiprocessor: a Trimmomatic wrapper for parallel adapter and quality trimming. https://dx.doi.org/10.6079/J9ILL

Faircloth, B. C. 2016. PHYLUCE is a software package for the analysis of conserved genomic loci. Bioinformatics 32:786–788.

Faircloth, B. C., J. E. McCormack, N. G. Crawford, M. G. Harvey, R. T. Brumfield, and T. C. Glenn. 2012. Ultraconserved elements anchor thousands of genetic markers spanning multiple evolutionary timescales. Systematic Biology 61:717–726.

Faircloth, B. C., L. Sorenson, F. Santini, and M. E. Alfaro. 2013. A phylogenomic perspective on the radiation of ray-finned fishes based upon targeted sequencing of ultraconserved elements (UCEs). PLoS ONE 8:e65923.

Feltes, R. M. 1986. A systematic revision of the Polynemidae (Pisces). Unpubl. Ph.D. diss., The Ohio State University, Columbus, Ohio.

Feltes, R. M. 1991. Revision of the polynemid fish genus *Filimanus*, with the description of two new species. Copeia 1991:302–322.

Feltes, R. M. 1993. *Parapolynemus*, a new genus for the polynemid fish previously known as *Polynemus verekeri*. Copeia 1993:207–215.

Fink, W. L. 1981. Ontogeny and phylogeny of tooth attachment modes in actinopterygian fishes. Journal of Morphology 167:167–184.

Fink, W. L. 1985. Phylogenetic interrelationships of the stomiid fishes (Teleostei, Stomiiformes). Miscellaneous Publications Museum of Zoology, The University of Michigan 171:1–125.

Fraser, T. H. 1972. Comparative osteology of the shallow water cardinal fishes (Perciformes: Apogonidae) with references to the systematics and the evolution of the family. Ichthyological Bulletin, No. 34, Ichthyological Bulletin of the J.L.B. Smith Institute of Ichthyology 34:1–105.

Freihofer, W. C. 1978. Cranial nerves of a percoid fish, *Polycentrus schomburgkii* (family Nandidae), a contribution to the morphology and classification of the order Perciformes. Occasional Papers of the California Academy of Sciences 128:1–178.

Fricke, R., W. N. Eschmeyer, and R. van der Laan (Eds.). 2019. Eschmeyer's Catalog of Fishes: Genera, Species, References. http://researcharchive.calacademy.org/research/ichthyology/catalog/fishcatmain.asp. Electronic version accessed 15 October 2019.

Friedman, M. 2008. The evolutionary origin of flatfish asymmetry. Nature 454:209–212.

Friedman, M., Z. Johanson, R. C. Harrington, T. J. Near, and M. R. Graham. 2013. An early fossil remora (Echeneoidea) reveals the evolutionary assembly of the adhesion disc. Proceedings of the Royal Society B: Biological Sciences 280:20131200.

Friedman, M., and G. D. Johnson. 2005. A new species of *Mene* (Perciformes: Menidae) from the Paleocene of South America, with notes on paleoenvironment and a brief review of menid fishes. Journal of Vertebrate Paleontology 25:770–783.

Fujita, K. 1990. The Caudal Skeleton of Teleostean Fishes. Tokai University Press, Tokyo, Japan.

Futch, C. R., R. W. Topp, and E. D. Houde. 1972. Developmental osteology of the lined sole, *Achirus lineatus* (Pisces: Soleidae). Contributions in Marine Science 16:33–58.

Gemballa, S., and R. Britz. 1998. Homology of intermuscular bones in acanthomorph fishes. American Museum Novitates 3241:1–25.

Ghedotti, M. J., J. N. Gruber, R. W. Barton, M. P. Davis, and W. L. Smith. 2018. Morphology and evolution of bioluminescent organs in the glowbellies (Percomorpha: Acropomatidae) with comments on the taxonomy and

phylogeny of Acropomatiformes. Journal of Morphology 279:1640–1653.

Gill, A. C., and J. M. Leis. 2019. Phylogenetic position of the fish genera *Lobotes*, *Datnioides* and *Hapalogenys*, with a reappraisal of acanthuriform composition and relationships based on adult and larval morphology. Zootaxa 4680: 1–81.

Gill, A. C., and R. D. Mooi. 1993. Monophyly of the Grammatidae and of the Notograptidae, with evidence for their phylogenetic positions among perciforms. Bulletin of Marine Science 52:327–350.

Gill, T. N. 1861. Synopsis of the polynematoids. Proceedings of the Academy of Natural Sciences of Philadelphia 13: 271–282.

Girard, M. G., and W. L. Smith. 2016. The phylogeny of marine sculpins of the genus *Icelinus* with comments on the evolution and biogeography of the Pseudoblenninae. Zootaxa 4171:549–561.

Gosline, W. A. 1961. The perciform caudal skeleton. Copeia 1961:265–270.

Gosline, W. A. 1962. Systematic position and relationships of the percesocine fishes. Pacific Science 16:207–217.

Gosline, W. A. 1968. The suborders of perciform fishes. Proceedings of the United States National Museum 124:1–78.

Gosline, W. A. 1971. Functional Morphology and Classification of Teleostean Fishes. University of Hawaii Press, Honolulu, Hawaii.

Graham, J. B., N. C. Wegner, L. A. Miller, C. J. Jew, N. C. Lai, R. M. Berquist, L. R. Frank, and J. A. Long. 2014. Spiracular air breathing in polypterid fishes and its implications for aerial respiration in stem tetrapods. Nature Communications 5:3022.

Grande, T., W. C. Borden, and W. L. Smith. 2013. Limits and relationships of Paracanthopterygii: a molecular framework for evaluating past morphological hypotheses, p. 385–418. *In*: Mesozoic Fishes 5—Global Diversity and Evolution. G. Arratia, H.-P. Schultze, and M. V. H. Wilson (eds.). Verlag Dr. Friedrich Pfeil, München, Germany.

Grande, T. C., W. C. Borden, M. V. H. Wilson, and L. Scarpitta. 2018. Phylogenetic relationships among fishes in the order Zeiformes based on molecular and morphological data. Copeia 106:20–48.

Greenwood, P. H. 1976. A review of the family Centropomidae (Pisces, Perciformes). Bulletin of the British Museum (Natural History) 29:1–81.

Greenwood, P. H., D. E. Rosen, S. H. Weitzman, and G. S. Myers. 1966. Phyletic studies of teleostean fishes, with a provisional classification of living forms. Bulletin of the American Museum of Natural History 131:341–455.

Gregory, W. K. 1933. Fish skulls: a study of the evolution of natural mechanisms. Transactions of the American Philosophical Society 23:75–481.

Gregory, W. K., and G. M. Conrad. 1937. the comparative osteology of the swordfish (*Xiphias*) and the sailfish (*Istiophorus*). American Museum Novitates 952:1–25.

de Groot, S. J. 1971. On the interrelationships between morphology of the alimentary tract, food and feeding behaviour in flatfishes (Pisces: Pleuronectiformes). Netherlands Journal of Sea Research 5:121–196.

Günther, A. 1860. Catalogue of the acanthopterygian fishes in the collection of The British Museum. Volume Two. London.

Gushiken, S. 1988. Phylogenetic-relationships of the perciform genera of the family Carangidae. Japanese Journal of Ichthyology 34:443–461.

Harold, A. S., and S. H. Weitzman. 1996. Interrelationships of stomiiform fishes, p. 333–353. *In*: Interrelationships of Fishes. M. L. J. Stiassny, L. R. Parenti, and G. D. Johnson (eds.). Academic Press, San Diego.

Harrington, R. C., B. C. Faircloth, R. I. Eytan, W. L. Smith, T. J. Near, M. E. Alfaro, and M. Friedman. 2016. Phylogenomic analysis of carangimorph fishes reveals flatfish asymmetry arose in a blink of the evolutionary eye. BMC Evolutionary Biology 16:224.

Harris, R. S. 2007. Improved pairwise alignment of genomic DNA. Unpubl. Ph.D. diss., The Pennsylvania State University, State College, Pennsylvania.

Hensley, D. A., and E. H. Ahlstrom. 1984. Pleuronectiformes: relationships, p. 670–687. *In*: Ontogeny and Systematics of Fishes. H. G. Moser, W. J. Richards, D. M. Cohen, M. P. Fahay, A. W. Kendall, Jr., and S. L. Richardson (eds.). American Society of Ichthyologists and Herpetologists, Special Publication No. 1, Lawrence, Kansas.

Hilton, E. J., and G. D. Johnson. 2007. When two equals three: developmental osteology and homology of the caudal skeleton in carangid fishes (Perciformes: Carangidae). Evolution and Development 9:178–189.

Hilton, E. J., G. D. Johnson, and W. F. Smith-Vaniz. 2010. Osteology and systematics of *Parastromateus niger* (Perciformes: Carangidae), with comments on the carangid dorsal gill-arch skeleton. Copeia 2010:312–333.

Hilton, E. J., N. K. Schnell, and P. Konstantinidis. 2015. When tradition meets technology: systematic morphology of fishes in the early 21st century. Copeia 103:858–873.

Holcroft, N. I., and E. O. Wiley. 2015. Variation in the posttemporal-supracleithrum articulation in euteleosts. Copeia 103:751–770.

Hoshino, K. 2001. Monophyly of the Citharidae (Pleuronectoidei: Pleuronectiformes: Teleostei) with considerations of pleuronectoid phylogeny. Ichthyological Research 48:391–404.

Hoshino, K. 2006. Fixing the confused term "pseudomesial bar" and homologies of pleuronectiform cranial elements, with proposals of new terms. Ichthyological Research 53: 435–440.

Houde, E. D., R. Detwyler, and C. R. Futch. 1970. Development of the lined sole, *Achirus lineatus*, described from laboratory-reared and Tampa Bay specimens. Florida Department of Natural Resources Technical Reports 62:1–43.

Hubbs, C. L. 1944. Fin structure and relationships of the phallostethid fishes. Copeia 1944:69–79.

Hughes, G. M. 1984. General anatomy of the fish gills, p. 1–72. *In*: Fish Physiology. Vol. 10. W. S. Hoar and D. J. Randall (eds.). Academic Press, London.

Hughes, L. C., G. Ortí, Y. Huang, Y. Sun, C. C. Baldwin, A. W. Thompson, D. Arcila, R. Betancur-R., C. Li, L. Becker, N. Bellora, X. Zhao, X. Li, M. Wang . . . Q. Shi. 2018. Comprehensive phylogeny of ray-finned fishes (Actinopterygii) based on transcriptomic and genomic data. Proceedings of the National Academy of Sciences of the United States of America 115:6249–6254.

Johnson, G. D. 1975. The procurrent spur: an undescribed perciform caudal character and its phylogenetic implica-

tions. Occasional Papers of the California Academy of Sciences 121:1–23.

Johnson, G. D. 1980. The limits and relationships of the Lutjanidae and associated families. Bulletin of the Scripps Institution of Oceanography 24:1–112.

Johnson, G. D. 1983. *Niphon spinosus*: a primitive epinepheline serranid, with comments on the monophyly and intrarelationships of the Serranidae. Copeia 1983:777–787.

Johnson, G. D. 1984. Percoidei: development and relationships, p. 464–498. *In*: Ontogeny and Systematics of Fishes. H. G. Moser, W. J. Richards, D. M. Cohen, M. P. Fahay, A. W. Kendall, Jr., and S. L. Richardson (eds.). American Society of Ichthyologists and Herpetologists, Special Publication No. 1, Lawrence, Kansas.

Johnson, G. D. 1986. Scombroid phylogeny: an alternative hypothesis. Bulletin of Marine Science 39:1–41.

Johnson, G. D. 1988. *Niphon spinosus*, a primitive epinepheline serranid: corroborative evidence from the larvae. Japanese Journal of Ichthyology 35:7–18.

Johnson, G. D. 1993. Percomorph phylogeny—progress and problems. Bulletin of Marine Science 52:3–28.

Johnson, G. D., and E. B. Brothers. 1993. *Schindleria*: a paedomorphic goby (Teleostei: Aobioidei). Bulletin of Marine Science 52:441–471.

Johnson, G. D., and C. Patterson. 1993. Percomorph phylogeny: a survey of acanthomorphs and a new proposal. Bulletin of Marine Science 52:554–626.

Kang, S., H. Imamura, and T. Kawai. 2017. Morphological evidence supporting the monophyly of the family Polynemidae (Teleostei: Perciformes) and its sister relationship with Sciaenidae. Ichthyological Research 65:29–41.

Katoh, K., and D. M. Standley. 2013. MAFFT multiple sequence alignment software version 7: improvements in performance and usability. Molecular Biology and Evolution 30:772–780.

Kimura, S., T. Peristiwady, and R. Fricke. 2016. Taxonomic review of the genus *Leptobrama* Steindachner 1878 (Perciformes: Leptobramidae), with the resurrection of *Leptobrama pectoralis* (Ramsay and Ogilby 1887). Ichthyological Research 60:435–444.

Kishinouye, K. 1923. Contributions to the comparative study of the so-called scombroid fishes. Journal of the College of Agriculture, Imperial University of Tokyo 8:293–475.

Kottelat, M., and T. H. Hui. 2018. Three new species of archerfishes from the freshwaters of Southeast Asia (Teleostei: Toxotidae) and notes on Henri Mouhot's fish collections. Ichthyological Exploration of Freshwaters 952:1–19.

Kramer, D. 1960. Development of eggs and larvae of Pacific mackerel and distribution and abundance of larvae 1952–56. United States Fish and Wildlife Service Fisheries Bulletin 60:393–438.

Kusaka, T. 1974. The Urohyal of Fishes. University of Tokyo Press, Tokyo.

Kyle, H. M. 1923. II.—The asymmetry, metamorphosis and origin of flat-fishes. Philosophical Transactions of the Royal Society of London B: Biological Sciences 211:75–129.

Lanfear, R., B. Calcott, D. Kainer, C. Mayer, and A. Stamatakis. 2014. Selecting optimal partitioning schemes for phylogenomic datasets. BMC Evolutionary Biology 14: 82.

Lanfear, R., P. B. Frandsen, A. M. Wright, T. Senfeld, and B. Calcott. 2017. PartitionFinder 2: new methods for selecting partitioned models of evolution for molecular and morphological phylogenetic analyses. Molecular Biology and Evolution 34:772–773.

Lau, S. R., and P. L. Shafland. 1982. Larval development of snook, *Centropomus undecimalis* (Pisces, Centropomidae). Copeia 1982:618–627.

Leis, J. M. 1994. Larvae, adults and relationships of the monotypic perciform fish family Lactariidae. Records of the Australian Museum 46:131–143.

Li, B., A. Dettaï, C. Cruaud, A. Couloux, M. Desoutter-Meniger, and G. Lecointre. 2009. RNF213, a new nuclear marker for acanthomorph phylogeny. Molecular Phylogenetics and Evolution 50:345–363.

Li, C., R. Betancur-R., W. L. Smith, and G. Ortí. 2011. Monophyly and interrelationships of snook and barramundi (Centropomidae *sensu* Greenwood) and five new markers for fish phylogenetics. Molecular Phylogenetics and Evolution 60:463–471.

Lo, P. C., S. H. Liu, N. L. Chao, F. K. E. Nunoo, H. K. Mok, and W. J. Chen. 2015. A multi-gene dataset reveals a tropical New World origin and Early Miocene diversification of croakers (Perciformes: Sciaenidae). Molecular Phylogenetics and Evolution 88:132–143.

Mabee, P. M. 1988. Supraneural and predorsal bones in fishes: development and homologies. Copeia 1988:827–838.

Maddison, W. P., and D. R. Maddison. 2018. Mesquite: a modular system for evolutionary analysis. Version 3.6. http://mesquiteproject.org

Marathe, V. B., and D. V. Bal. 1956. Observations on the development of the caudal skeleton in *Eleutheronema tetradactylum* (Shaw) and *Trichopodus trichopterus* (Pall). Journal of the University of Bombay 25:1–12.

Märss, T., M. V. Wilson, T. Saat, and H. Špilev. 2017. Gill rakers and teeth of three pleuronectiform species (Teleostei) of the Baltic Sea: a microichthyological approach. Estonian Journal of Earth Sciences 66:21–26.

McAllister, D. E. 1968. Evolution of branchiostegals and classification of teleostome fishes. Bulletin of the National Museum of Canada 221:1–239.

McCune, A. R., and R. L. Carlson. 2004. Twenty ways to lose your bladder: common natural mutants in zebrafish and widespread convergence of swim bladder loss among teleost fishes. Evolution and Development 6:246–259.

Meek, S. E., and S. F. Hildebrand. 1923. The marine fishes of Panama Part I. Field Museum of Natural History Publication, Zoological Series 215:1–329.

Meek, S. E., and S. F. Hildebrand. 1925. The marine fishes of Panama Part II. Field Museum of Natural History Publication, Zoological Series 226:331–703.

Mirande, J. M. 2016. Combined phylogeny of ray-finned fishes (Actinopterygii) and the use of morphological characters in large-scale analyses. Cladistics 33:333–350.

Miya, M., M. Friedman, T. P. Satoh, H. Takeshima, T. Sado, W. Iwasaki, Y. Yamanoue, M. Nakatani, K. Mabuchi, J. G. Inoue, J. Y. Poulsen, T. Fukunaga, Y. Sato, and M. Nishida. 2013. Evolutionary origin of the Scombridae (tunas and mackerels): members of a paleogene adaptive radiation with 14 other pelagic fish families. PLoS ONE 8: e73535.

Miya, M., H. Takeshima, H. Endo, N. B. Ishiguro, J. G. Inoue, T. Mukai, T. P. Satoh, M. Yamaguchi, A. Kawaguchi, K. Mabuchi, S. M. Shirai, and M. Nishida. 2003. Major patterns of higher teleostean phylogenies: a new perspective based on 100 complete mitochondrial DNA sequences. Molecular Phylogenetics and Evolution 26:121–138.

Mok, H. K., and S. C. Shen. 1983. Osteology and Phylogeny of Squamipinnes. Taiwan Museum, Taipei.

Mooi, R. D., and A. C. Gill. 1995. Association of epaxial musculature with dorsal-fin pterygiophores in acanthomorph fishes, and its phylogenetic significance. Bulletin of the British Museum Natural History. Zoology 61:121–137.

Moritz, T., J. Buchert, and N. K. Schnell. 2019. Unexpected diversity of median caudal cartilages in teleosts. Zoological Journal of the Linnean Society 7:5–34.

Motomura, H. 2004. Threadfins of the World (Family Polynemidae). An Annotated and Illustrated Catalogue of Polynemid Species Known to Date. FAO Species Catalogue for Fishery Purposes. FAO, Rome.

Muir, B. S., and J. I. Kendall. 1968. Structural modifications in the gills of tunas and some other oceanic fishes. Copeia 1968:388–398.

Munroe, T. A. 2015. Systematic diversity of the Pleuronectiformes, p. 13–51. *In*: Flatfishes: Biology and Exploitation. Second edition. R. N. Gibson, R. D. M. Nash, A. J. Geffen, and H. W. van der Veer (eds.). John Wiley and Sons Ltd, West Sussex.

Myers, G. S. 1928. The systematic position of the phallostethid fishes, with diagnosis of a new genus from Siam. American Museum Novitates 295:1–12.

Myers, G. S. 1935. A new phallostethid fish from Palawan. Proceedings of the Biological Society of Washington 48:5–6.

Nakamura, I. 1983. Systematics of the billfishes (Xiphiidae and Istiophoridae). Publications of the Seto Marine Biological Laboratory 28:255–396.

Near, T. J., A. Dornburg, R. I. Eytan, B. P. Keck, W. L. Smith, K. L. Kuhn, J. A. Moore, S. A. Price, F. T. Burbrink, M. Friedman, and P. C. Wainwright. 2013. Phylogeny and tempo of diversification in the superradiation of spiny-rayed fishes. Proceedings of the National Academy of Sciences of the United States of America 110:12738–12743.

Near, T. J., R. I. Eytan, A. Dornburg, K. L. Kuhn, J. A. Moore, M. P. Davis, P. C. Wainwright, M. Friedman, and W. L. Smith. 2012. Resolution of ray-finned fish phylogeny and timing of diversification. Proceedings of the National Academy of Sciences of the United States of America 109:13698–13703.

Nelson, G. 1969. Gill arches and the phylogeny of fishes, with notes on the classification of vertebrates. Bulletin of the American Museum of Natural History 141:479–535.

Nelson, J. S. 2006. Fishes of the World. Fourth edition. John Wiley and Sons Inc., New York.

Nguyen, L.-T., H. A. Schmidt, A. von Haeseler, and B. Q. Minh. 2015. IQ-TREE: a fast and effective stochastic algorithm for estimating maximum-likelihood phylogenies. Molecular Biology and Evolution 32:268–274.

Nishimoto, H., and F. Ohe. 1982. Teeth of fossil *Sphyraena* of the Miocene Mizunami Group, central Japan. Bulletin of the Mizunami Fossil Museum 9:85–102.

Nixon, K. 2002. WinClada. Version 1.00.08. Published by the author, Ithaca, New York.

Norman, J. R. 1934. A Systematic Monograph of the Flatfishes (Heterostomata), Vol. 1 Psettodidae, Bothidae, Pleuronectidae. Printed by the order of the Trustees of the British Museum, London.

Normark, B. B., A. R. McCune, and R. G. Harrison. 1991. Phylogenetic relationships of neopterygian fishes, inferred from mitochondrial DNA sequences. Molecular Biology and Evolution 8:819–834.

Ogilby, J. D. 1913. Edible fishes of Queensland Part 1—Family Pempheridae. Memoirs of the Queensland Museum 2:60–67.

Olney, J. E., G. D. Johnson, and C. C. Baldwin. 1993. Phylogeny of lampridiform fishes. Bulletin of Marine Science 52:137–169.

Orrell, T. M., B. B. Collette, and G. D. Johnson. 2006. Molecular data support separate scombroid and xiphioid clades. Bulletin of Marine Science 79:505–519.

Otero, O. 2004. Anatomy, systematics and phylogeny of both Recent and fossil latid fishes (Teleostei, Perciformes, Latidae). Zoological Journal of the Linnean Society 141:81–133.

O'Toole, B. 2002. Phylogeny of the species of the superfamily Echeneoidea (Perciformes: Carangoidei: Echeneidae, Rachycentridae, and Coryphaenidae), with an interpretation of echeneid hitchhiking behaviour. Canadian Journal of Zoology 80:596–623.

Parenti, L. R. 1981. A phylogenetic and biogeographic analysis of cyprinodontiform fishes (Teleostei, Atherinomorpha). Bulletin of the American Museum of Natural History 168:335–557.

Parenti, L. R. 1993. Relationships of atherinomorph fishes (Teleostei). Bulletin of Marine Science 52:170–196.

Patterson, C., and G. D. Johnson. 1995. The intermuscular bones and ligaments of teleostean fishes. Smithsonian Contributions to Zoology 559:1–83.

Potthoff, T. 1974. Osteological development and variation in young tunas, genus *Thunnus* (Pisces, Scombridae), from the Atlantic Ocean. Fishery Bulletin 72:563–588.

Potthoff, T. 1975. Development and structure of the caudal complex, the vertebral column, and the pterygiophores in the blackfin tuna (*Thunnus atlanticus*, Pisces, Scombridae). Bulletin of Marine Science 25:205–231.

Potthoff, T. 1984. Clearing and staining techniques, p. 35–37. *In*: Ontogeny and Systematics of Fishes. H. G. Moser, W. J. Richards, D. M. Cohen, M. P. Fahay, A. W. Kendall, Jr., and S. L. Richardson (eds.). American Society of Ichthyologists and Herpetologists, Special Publication No. 1, Lawrence, Kansas.

Potthoff, T., S. Kelley, and J. C. Javech. 1986. Cartilage and bone-development in scombroid fishes. Fishery Bulletin 84:647–678.

Potthoff, T., and J. A. Tellock. 1993. Osteological development of the snook, *Centropomus undecimalis* (Teleostei, Centropomidae). Bulletin of Marine Science 52:669–716.

Prendini, L. 2000. Phylogeny and classification of the superfamily Scorpionoidea Latreille 1802 (Chelicerata, Scorpiones): an exemplar approach. Cladistics 16:1–78.

Prendini, L. 2001. Species or supraspecific taxa as terminals in cladistic analysis? Groundplans versus exemplars revisited. Systematic Biology 50:290–300.

Prokofiev, A. M. 2014. Deepsea herrings (Bathyclupeidae) of the northwestern Pacific ocean. Journal of Ichthyology 54: 137–145.

Rabosky, D. L., J. Chang, P. O. Title, P. F. Cowman, L. Sallan, M. Friedman, K. Kaschner, C. Garilao, T. J. Near, M. Coll, and M. E. Alfaro. 2018. An inverse latitudinal gradient in speciation rate for marine fishes. Nature 559: 392–395.

Rambaut, A. 2012. FigTree v1.4. Molecular evolution, phylogenetics and epidemiology. University of Edinburgh, Institute of Evolutionary Biology, Edinburgh, UK.

Reed, D. L., K. E. Carpenter, and M. J. deGravelle. 2002. Molecular systematics of the jacks (Perciformes: Carangidae) based on mitochondrial cytochrome *b* sequences using parsimony, likelihood, and Bayesian approaches. Molecular Phylogenetics and Evolution 23:513–524.

Regan, C. T. 1912. XXVIII.—The classification of the teleostean fishes of the order Pediculati. Journal of Natural History 9:277–289.

Roberts, C. D. 1993. Comparative morphology of spined scales and their phylogenetic significance in the Teleostei. Bulletin of Marine Science 52:60–113.

Rojo, A. L. 2018. Dictionary of Evolutionary Fish Osteology. CRC Press, Boca Raton, Florida.

Rosen, D. E. 1964. The relationships and taxonomic position of the halfbeaks, killifishes, silversides, and their relatives. Bulletin of the American Museum of Natural History 127: 217–268.

Rosen, D. E. 1973. Interrelationships of higher euteleostean fishes, p. 397–513. *In*: Interrelationships of Fishes. P. H. Greenwood, R. S. Miles, and C. Patterson (eds.). Academic Press, London.

Rosen, D. E. 1982. Teleostean interrelationships, morphological function and evolutionary inference. American Zoologist 22:261–273.

Rosen, D. E., and P. H. Greenwood. 1976. A fourth Neotropical species of synbranchid eel and the phylogeny and systematics of synbranchiform fishes. Bulletin of the American Museum of Natural History 157:1–70.

Rosen, D. E., and L. R. Parenti. 1981. Relationships of *Oryzias*, and the groups of atherinomorph fishes. American Museum Novitates 2719:1–25.

Rosen, D. E., and C. Patterson. 1969. The structure and relationships of the paracanthopterygian fishes. Bulletin of the American Museum of Natural History 141:361–469.

Rosen, D. E., and C. Patterson. 1990. On Müller's and Cuvier's concepts of pharyngognath and labyrinth fishes and the classification of percomorph fishes: with an atlas of percomorph dorsal gill arches. American Museum Novitates 2983:1–50.

Rosenblatt, R. H., and M. A. Bell. 1976. Osteology and relationships of the roosterfish, *Nematistius pectoralis* Gill. Natural History Museum of Los Angeles County Contributions in Science 279:1–23.

Sabaj, M. H. 2016. Standard symbolic codes for institutional resource collections in herpetology and ichthyology: An Online Reference. Version 7.1 (21 March 2019). Electronically accessible at https://www.asih.org, American Society of Ichthyologists and Herpetologists, Washington, D.C.

Sanciangco, M. D., K. E. Carpenter, and R. Betancur-R. 2016. Phylogenetic placement of enigmatic percomorph families (Teleostei: Percomorphaceae). Molecular Phylogenetics and Evolution 94:565–576.

Santini, F., G. Carnevale, and L. Sorenson. 2015. First timetree of Sphyraenidae (Percomorpha) reveals a Middle Eocene crown age and an Oligo–Miocene radiation of barracudas. Italian Journal of Zoology 82:133–142.

Sasaki, K. 1989. Phylogeny of the family Sciaenidae, with notes on its zoogeography (Teleostei, Perciformes). Memoirs of the Faculty of Fisheries Hokkaido University 36:1–137.

Schaefer, S. A. 2003. Relationships of *Lithogenes villosus* Eigenmann, 1909 (Siluriformes, Loricariidae): evidence from high-resolution computed microtomography. American Museum Novitates 3401:1–55.

Schwarzhans, W., H. T. Beckett, J. D. Schein, and M. Friedman. 2018. Computed tomography scanning as a tool for linking the skeletal and otolith-based fossil records of teleost fishes. Palaeontology 61:511–541.

Shi, W., S. Chen, X. Kong, L. Si, L. Gong, Y. Zhang, and H. Yu. 2018. Flatfish monophyly refereed by the relationship of *Psettodes* in Carangimorphariae. BMC Genomics 19:400.

Simpson, J. T., K. Wong, S. D. Jackman, J. E. Schein, S. J. M. Jones, and I. Birol. 2009. ABySS: a parallel assembler for short read sequence data. Genome Research 19:1117–1123.

Smith, C. L., and R. M. Bailey. 1962. The subocular shelf of fishes. Journal of Morphology 110:1–17.

Smith, W. L. 2010. Promoting resolution of the percomorph bush: a reply to Mooi and Gill. Copeia 2010:520–524.

Smith, W. L., C. A. Buck, G. S. Ornay, M. P. Davis, R. P. Martin, S. Z. Gibson, and M. G. Girard. 2018b. Improving vertebrate skeleton images: fluorescence and the non-permanent mounting of cleared-and-stained specimens. Copeia 106:427–435.

Smith, W. L., and M. S. Busby. 2014. Phylogeny and taxonomy of sculpins, sandfishes, and snailfishes (Perciformes: Cottoidei) with comments on the phylogenetic significance of their early-life-history specializations. Molecular Phylogenetics and Evolution 79:332–352.

Smith, W. L., and M. T. Craig. 2007. Casting the percomorph net widely: the importance of broad taxonomic sampling in the search for the placement of serranid and percid fishes. Copeia 2007:35–55.

Smith, W. L., E. Everman, and C. Richardson. 2018a. Phylogeny and taxonomy of flatheads, scorpionfishes, sea robins, and stonefishes (Percomorpha: Scorpaeniformes) and the evolution of the lachrymal saber. Copeia 106:94–119.

Smith, W. L., J. H. Stern, M. G. Girard, and M. P. Davis. 2016. Evolution of venomous cartilaginous and ray-finned fishes. Integrative and Comparative Biology 56:950–961.

Smith, W. L., and W. C. Wheeler. 2006. Venom evolution widespread in fishes: a phylogenetic road map for the bioprospecting of piscine venoms. Journal of Heredity 97: 206–217.

Smith-Vaniz, W. F. 1984. Carangidae: relationships, p. 522–530. *In*: Ontogeny and Systematics of Fishes. H. G. Moser, W. J. Richards, D. M. Cohen, M. P. Fahay, A. W. Kendall, Jr., and S. L. Richardson (eds.). American Society of Ichthyologists and Herpetologists, Special Publication No. 1, Lawrence, Kansas.

Smith-Vaniz, W. F., and J. C. Staiger. 1973. Comparative revision of *Scomberoides*, *Oligoplites*, *Parona* and *Hypacanthus*. Proceedings of the California Academy of Sciences 39: 185–256.

Springer, V. G. 1968. Osteology and classification of the fishes of the family Blenniidae. Bulletin of the United States National Museum 284:1–85.

Springer, V. G., and G. D. Johnson. 2004. Study of the dorsal gill-arch musculature of teleostome fishes with special reference to the Actinopterygii. Bulletin of the Biological Society of Washington 11:1–235.

Springer, V. G., and T. M. Orrell. 2004. Appendix: phylogenetic analysis of 147 families of acanthomorph fishes based primarily on dorsal gill-arch muscles and skeleton. Bulletin of the Biological Society of Washington 11:237–260.

Springer, V. G., and W. F. Smith-Vaniz. 2008. Supraneural and pterygiophore insertion patterns in carangid fishes, with description of a new Eocene carangid tribe, †Paratrachinotini, and a survey of anterior anal-fin pterygiophore insertion patterns in Acanthomorpha. Bulletin of the Biological Society of Washington 16:1–73.

Stamatakis, A. 2014. RAxML version 8: a tool for phylogenetic analysis and post-analysis of large phylogenies. Bioinformatics 30:1312–1313.

Starks, E. C. 1899. The osteological characters of the fishes of the suborder Percesoces. Proceedings of the United States National Museum 22:1–10.

Steindachner, F. 1878. Ichthyologische Beiträge (VII). Sitzungsberichte der Kaiserlichen Akademie der Wissenschaften. Mathematisch-Naturwissenschaftliche Classe 78:377–400.

Stiassny, M. L. J. 1993. What are Grey Mullets? Bulletin of Marine Science 52:197–219.

Tagliacollo, V. A., and R. Lanfear. 2018. Estimating improved partitioning schemes for ultraconserved elements. Molecular Biology and Evolution 35:1798–1811.

Tang, K. L., P. B. Berendzen, E. O. Wiley, J. F. Morrissey, R. Winterbottom, and G. D. Johnson. 1999. The phylogenetic relationships of the suborder Acanthuroidei (Teleostei: Perciformes) based on molecular and morphological evidence. Molecular Phylogenetics and Evolution 11:415–425.

Taniguchi, N. 1969. Comparative osteology of the sciaenid fishes from Japan and its adjacent waters-I. Neurocranium. Japanese Journal of Ichthyology 16:55–67.

Tominaga, Y. 1965. The internal morphology and systematic position of *Leptobrama mülleri*, formerly included in the family Pempheridae. Japanese Journal of Ichthyology 12: 33–56.

Tominaga, Y. 1968. Internal morphology, mutual relationships and systematic position of the fishes belonging to the family Pempheridae. Japanese Journal of Ichthyology 15: 43–95.

Tominaga, Y., K. Sakamoto, and K. Matsuura. 1996. Posterior extension of the swimbladder in percoid fishes, with a literature survey of other teleosts. The University Museum, The University of Tokyo Bulletin 36:1–73.

Travers, R. A. 1981. The interarcual cartilage; a review of its development, distribution and value as an indicator of phyletic relationships in euteleostean fishes. Journal of Natural History 15:853–871.

Tyler, J. C. 1980. Osteology, phylogeny, and higher classification of the fishes of the order Plectognathi (Tetraodontiformes). NOAA Technical Report NMFS Circular 434:1–422.

Tyler, J. C., G. D. Johnson, I. Nakamura, and B. B. Collette. 1989. Morphology of *Luvarus imperialis* (Luvaridae) with a phylogenetic analysis of the Acanthuroidei (Pisces). Smithsonian Contributions to Zoology 1–78.

van der Straten, K. M., B. B. Collette, L. K. P. Leung, and S. D. Johnston. 2006. Sperm morphology of the black marlin (*Makaira indica*) differs from scombroid sperm. Bulletin of Marine Science 79:839–845.

Van Neer, W. 1987. A study on the variability of the skeleton of *Lates niloticus* (Linnaeus, 1758) in view of the validity of *Lates maliensis* Gayet, 1983. Cybium 11:411–425.

Wainwright, P. C., W. L. Smith, S. A. Price, K. L. Tang, J. S. Sparks, L. A. Ferry, K. L. Kuhn, R. I. Eytan, and T. J. Near. 2012. The evolution of pharyngognathy: a phylogenetic and functional appraisal of the pharyngeal jaw key innovation in labroid fishes and beyond. Systematic Biology 61:1001–1027.

Webb, J. F. 1989a. Neuromast morphology and lateral line trunk canal ontogeny in two species of cichlids: an SEM study. Journal of Morphology 202:53–68.

Webb, J. F. 1989b. Gross morphology and evolution of the mechanoreceptive lateral-line system in teleost fishes. Brain, Behavior and Evolution 33:205–222.

Webb, J. F., W. L. Smith, and D. R. Ketten. 2006. The laterophysic connection and swim bladder of butterflyfishes in the genus *Chaetodon* (Perciformes: Chaetodontidae). Journal of Morphology 267:1338–1355.

Weitzman, S. H. 1962. The osteology of *Brycon meeki*, a generalized characid fish, with an osteological definition of the family. Stanford Ichthyological Bulletin 8:1–77.

Weitzman, S. H. 1974. Osteology and evolutionary relationships of the Sternoptychidae. Bulletin of the American Museum of Natural History 153:327–478.

Wiley, E. O., and G. D. Johnson. 2010. A teleost classification based on monophyletic groups, p. 123–182. *In*: Origin and Phylogenetic Interrelationships of Teleosts. J. S. Nelson, H.-P. Schultze, and M. V. H. Wilson (eds.). Verlag Dr. Friedrich Pfeil, München, Germany.

Wiley, E. O., G. D. Johnson, and W. W. Dimmick. 2000. The interrelationships of acanthomorph fishes: a total evidence approach using molecular and morphological data. Biochemical Systematics and Ecology 28:319–350.

Yabe, M. 1985. Comparative osteology and myology of the superfamily Cottoidea (Pisces: Scorpaeniformes) and its phylogenetic classification. Memoirs of the Faculty of Fisheries Hokkaido University 32:1–130.

Yazdani, G. M. 1969. Adaptation in the jaws of flatfish (Pleuronectiformes). Journal of Zoology 159:181–222.

Yeates, D. K. 1995. Groundplans and exemplars: paths to the tree of life. Cladistics 11:343–357.

Zehren, S. J. 1987. Osteology and evolutionary relationships of the boarfish genus *Antigonia* (Teleostei, Caproidae). Copeia 1987:564–592.

APPENDIX 1

Abbreviated descriptions and states for the characters examined

The following are a set of abbreviated character descriptions and states examined in this study. A more detailed version of these character descriptions can be found in Supplemental Appendix. In addition to the literature cited in the main text, the following studies are cited in the supplemental version of the character descriptions: Cuvier and Valenciennes, 1831; Allis, 1899; Kishinouye, 1923; Gregory, 1933; Norman, 1934; Chabanaud, 1936; Marathe and Bal, 1956; Kramer, 1960;

Gosline, 1961; Weitzman, 1962; Muir and Kendall, 1968; Nelson, 1969; Yazdani, 1969; Houde et al., 1970; de Groot, 1971; Fraser, 1972; Futch et al., 1972; Kusaka, 1974; Potthoff, 1974, 1975; Rosen and Greenwood, 1976; Eastman, 1977; Johnson, 1980; Travers, 1981; Lau and Shafland, 1982; Rosen, 1982; Hughes, 1984; Fink, 1985; Brewster, 1987; Zehren, 1987; Webb, 1989b; Fujita, 1990; Rosen and Patterson, 1990; Feltes, 1991, 1993; Baldwin and Johnson, 1993; Potthoff and Tellock, 1993; Cooper and Chapleau, 1998; McCune and Carlson, 2004; Motomura, 2004; Friedman, 2008; Davis, 2009; Wiley and Johnson, 2010; Campbell et al., 2014b; Märss et al., 2017; Rojo, 2018; Moritz et al., 2019.

1. Basisphenoid: 0, basisphenoid present; 1, basisphenoid absent.
2. Prootic excluded from posterior portion of orbit by pterosphenoid contacting parasphenoid (based on Greenwood, 1976, page 20): 0, prootic separating pterosphenoid from parasphenoid; 1, prootic posteriorly displaced such that pterosphenoid contacts parasphenoid.
3. Accessory nasal ossifications (Freihofer, 1978; Smith-Vaniz, 1984 character 1): 0, accessory nasal ossifications absent; 1, accessory nasal ossifications present.
4. Number of accessory nasal ossifications (Smith-Vaniz, 1984 character 3): 0, one ossified accessory nasal element present; 1, two or more ossified accessory nasal element present.
5. Vomerine teeth: 0, vomerine teeth present; 1, vomerine teeth absent.
6. Vomerine tooth patch shape (Van Neer, 1987, page 415): 0, single triangular patch with straight or concave posterior margin; 1, single triangular patch with convex posterior margin. Approaching circular in shape; 2, two circular patches.
7. Foramen near distal margin of lateral ethmoid separated from olfactory foramen (modified from Feltes, 1986 character 31): 0, foramen in distal margin of lateral ethmoid absent; 1, foramen in distal margin of lateral ethmoid present.
8. Prominent dorsal extension of parasphenoid: 0, prominent dorsal expansion of the parasphenoid absent; 1, prominent dorsal expansion of the parasphenoid present.
9. Teeth on posterior portion of parasphenoid (Gosline, 1968, page 10): 0, teeth on posterior portion of parasphenoid absent; 1, teeth on posterior portion of parasphenoid present.
10. Basioccipital foramina: 0, basioccipital foramina absent; 1, basioccipital foramina present.
11. Lateral flaring of parasphenoid (based on Gregory and Conrad, 1937, page 17): 0, parasphenoid largely cylindrical throughout ventral margin; 1, parasphenoid flares abruptly and laterally. Approaching plate-like in appearance.
12. Adipose eyelids (Gushkin, 1988 character 17): 0, adipose eyelids absent; 1, adipose eyelids present.
13. Developed neurocranium (Chapleau, 1993 character 1): 0, symmetrical neurocranium, with one eye on each side of body; 1, asymmetrical neurocranium, with one eye crossing the dorsal midline.
14. Pseudomesial bar (Harrington et al., 2016 character 3): 0, pseudomesial bar absent; 1, pseudomesial bar present.
15. Serration on ventral margin of lachrymal: 0, ventral margin of lachrymal without serrations; 1, ventral margin of lachrymal serrated.
16. Number of circumorbitals including dermosphenotic (modified from O'Toole, 2002 character 56): 0, six or fewer circumorbitals; 1, more than six circumorbitals.
17. Dermosphenotic: 0, dermosphenotic broadening dorsally at lateral-line junction; 1, dermosphenotic cylindrical.
18. Suborbital shelf (based on Smith and Bailey, 1962): 0, suborbital shelf absent; 1, suborbital shelf present.
19. Spination on posterior aspect of preopercle vertical arm: 0, spination on vertical arm of preopercle absent; 1, spination on vertical arm of preopercle present.
20. Spination on angle of posterior aspect of preopercle: 0, spination on posterior angle of preopercle absent; 1, spination on posterior angle of preopercle present.
21. Number of spines on angle of posterior aspect of preopercle: 0, single posterior-facing spine on angle of preopercle; 1, multiple spines facing posteriorly on angle of preopercle.
22. Spination on horizontal arm of preopercle: 0, spination on horizontal arm of preopercle absent; 1, spination on horizontal arm of preopercle present.
23. Number of spines on horizontal arm of preopercle: 0, fewer than six spines on horizontal arm of preopercle; 1, more than six spines on horizontal arm of preopercle.
24. Supramaxilla (O'Toole, 2002 character 36): 0, supramaxilla absent; 1, supramaxilla present.
25. Size of supramaxilla: 0, supramaxilla small; 1, supramaxilla large.
26. Elongated, fang-like teeth in oral jaws: 0, fang-like teeth absent in oral jaws; 1, fang-like teeth present in oral jaws.
27. Oral tooth attachment (based on Fink, 1981): 0, oral tooth separated from oral jaw bone by ring of collagen; 1, oral tooth directly attached to oral jaw bone; ankylosed.
28. Elongated premaxillary bill in adults (Collette et al., 1984 character 13; Johnson, 1986 character 46): 0, elongate premaxillary bill absent; 1, elongate premaxillary bill present.
29. Articular process of premaxilla: 0, articular process of premaxilla present; 1, articular process of premaxilla absent.
30. Interaction between ascending process and articular process of premaxilla: 0, ascending process distinct from articular process of premaxilla; 1, ascending process closely applied or joined to articular process of premaxilla.
31. Foramen in articular process of premaxilla: 0, foramen in articular process of premaxilla absent; 1, foramen in articular process of premaxilla present.
32. Postmaxillary process of premaxilla: 0, postmaxillary process absent; 1, postmaxillary process present.
33. External process on maxilla: 0, external process on maxilla absent; 1, external process on maxilla present.

34. Direction of external process of the maxilla: 0, external process on maxilla laterally directed; 1, external process on maxilla dorsally directed.
35. Size of external process of the maxilla: 0, external process on maxilla small to moderate; 1, external process on maxilla large; 2, external process on maxilla minute.
36. Rostral extension of external process on maxilla: 0, external process on maxilla not rostrally extended; 1, external process on maxilla rostrally extended, shelf-like.
37. Foramen on ventral aspect of internal maxillary process: 0, absence of foramen on ventral aspect of internal maxillary process; 1, one or more foramina on ventral aspect of internal maxillary process.
38. Palatine teeth: 0, palatine teeth present; 1, palatine teeth absent.
39. Endopterygoid teeth: 0, endopterygoid teeth absent; 1, endopterygoid teeth present.
40. Endopterygoid tooth attachment (based on Smith-Vaniz and Staiger, 1973): 0, endopterygoid teeth free-floating in tissue separate from the underlying bone; 1, endopterygoid teeth ankylosed to the underlying bone.
41. Ectopterygoid teeth: 0, ectopterygoid teeth absent; 1, ectopterygoid teeth present.
42. Palatine tooth patch length versus ectopterygoid tooth patch length: 0, ectopterygoid tooth patch longer than palatine tooth patch; 1, palatine tooth patch longer than ectopterygoid tooth patch.
43. Contact at metapterygoid–hyomandibular border (modified from Feltes, 1986 character 4): 0, distinct and separate or abutting, but not overlapping; 1, overlapping but otherwise not interacting; 2, interacting by single pointed process inserting into evagination to moderate amount of suturing between elements.
44. Shape of sympletic: 0, lamellar bone extending dorsally from the dorsal margin of symplectic; 1, symplectic simply shaped and largely tubular.
45. Dorsal aspect of symplectic: 0, symplectic extends dorsally above dorsal margin of quadrate; 1, symplectic extending only to or slightly above dorsal margin of quadrate.
46. Interdigitation between the metapterygoid and quadrate (Kang et al., 2017 character 5): 0, absence of suturing between metapterygoid and quadrate; 1, suturing between metapterygoid and quadrate.
47. Contact between ectopterygoid and quadrate: 0, ectopterygoid and quadrate overlapping but otherwise not interacting; 1, suturing between ectopterygoid and quadrate.
48. Contact between ectopterygoid and metapterygoid: 0, ectopterygoid and metapterygoid distinct and separate or abutting, but not overlapping; 1, ectopterygoid and metapterygoid overlapping but otherwise not interacting; 2, single pointed process to moderate amount of suturing between ectopterygoid and metapterygoid.
49. Contact between ectopterygoid and endopterygoid posteriorly: 0, ectopterygoid and endopterygoid distinct and separate or abutting, but not overlapping; 1, ectopterygoid and endopterygoid overlapping but otherwise not interacting; 2, single pointed process from ectopterygoid enveloped by invagination on endopterygoid.
50. Contact between endopterygoid and metapterygoid: 0, endopterygoid and metapterygoid distinct and separate or abutting, but not overlapping; 1, endopterygoid and metapterygoid overlapping but otherwise not interacting; 2, single pointed process to moderate amount of suturing between endopterygoid and metapterygoid.
51. Position of the retroarticular dorsal tip relative to the articular–quadrate facet (modified from Feltes, 1986 character 18): 0, retroarticular dorsal tip posterior to articulation facet with quadrate; 1, retroarticular dorsal tip anterior to articulation facet with quadrate.
52. Teeth on dentary visible and on external face of bone (modified from Feltes, 1986 character 37): 0, teeth restricted to dorsal margin of dentary; 1, teeth on external face of dentary bone.
53. Number of branchiostegal rays: 0, seven or more branchiostegal rays; 1, fewer than seven branchiostegal rays.
54. Insertion of the fourth branchiostegal ray (modified from Johnson, 1986 character 10): 0, fourth branchiostegal ray inserts on ceratohyal; 1, fourth branchiostegal ray inserts on epihyal; 2, fourth branchiostegal ray inserts on cartilaginous element between the ceratohyal and epihyal.
55. Insertion of the fifth branchiostegal ray (modified from Johnson, 1986 character 10): 0, fifth branchiostegal ray inserts on ceratohyal; 1, fifth branchiostegal ray inserts on cartilaginous element between the ceratohyal and epihyal; 2, fifth branchiostegal ray inserts on epihyal.
56. Insertion of the sixth branchiostegal ray (modified from Johnson, 1986 character 10): 0, sixth branchiostegal ray inserts on epihyal; 1, sixth branchiostegal ray inserts on cartilaginous element between the ceratohyal and epihyal; 2, sixth branchiostegal ray inserts on ceratohyal.
57. Beryciform foramen: 0, beryciform foramen absent; 1, beryciform foramen present.
58. Beryciform foramen size: 0, beryciform foramen small. Diameter less than half of dorsal aspect of ceratohyal; 1, beryciform foramen large. Diameter more than half of dorsal aspect of ceratohyal.
59. Position of ceratohyal–epihyal suture: 0, suturing present medially but absent laterally; 1, suturing present medially and laterally.
60. Interhyal length (modified from O'Toole, 2002 character 62): 0, interhyal moderate to elongate in length; 1, interhyal shortened in length.
61. Lateral shape of urohyal: 0, urohyal wing-like, becoming dorsoventrally deeper caudally; 1, urohyal compressed, largely uniform throughout; 2, urohyal recurved, C shaped.
62. Length of basihyal (O'Toole, 2002 character 69): 0, basihyal shorter than hypobranchial one; 1, basihyal longer than hypobranchial one.
63. Basihyal position: 0, basihyal in anterior position, inserting rostral to rostral and slightly dorsal to basibranchial one and does not cover the entirety of the first basibranchial when viewing the branchial

and hyoid arches dorsally; 1, basihyal in posterior position, inserting dorsally to basibranchial one and covers the entirety of the first basibranchial when viewing the branchial and hyoid arches dorsally.

64. Posterior elevation of basihyal: 0, basihyal largely uniform and flat posteriorly; 1, basihyal plate-like anteriorly with posterior mound-like elevation.
65. Basihyal dentition: 0, no dentition on basihyal; 1, dentition present on basihyal.
66. Basihyal dentition attachment: 0, basihyal dentition not anchored to bone, free floating in tissue; 1, basihyal dentition ankylosed to basihyal.
67. Shape of basihyal dentition: 0, single band or patch of teeth associated with basihyal; 1, multiple separated bands or patches of teeth associated with basihyal.
68. Basibranchial one dentition: 0, no dentition present on basibranchial one; 1, toothplate(s) present on basibranchial one.
69. Shape of basibranchial one dentition: 0, paired toothplates on basibranchial one; 1, multiple bands or plates of teeth on basibranchial one.
70. Basibranchial two dentition: 0, no dentition present on basibranchial two; 1, toothplate(s) present on basibranchial two.
71. Shape of basibranchial two dentition: 0, paired toothplates on basibranchial two; 1, single band or patch of teeth on basibranchial two; 2, multiple bands or plates of teeth on basibranchial two.
72. Basibranchial three dentition: 0, no dentition present on basibranchial three; 1, toothplate(s) present on basibranchial three.
73. Shape of basibranchial three dentition: 0, paired toothplates on basibranchial three; 1, single band or patch of teeth on basibranchial three; 2, multiple bands or plates of teeth on basibranchial three.
74. Basibranchial four dentition: 0, no dentition present on basibranchial four; 1, toothplate(s) present on basibranchial four.
75. Shape of basibranchial four dentition: 0, paired toothplates on basibranchial four; 1, single band or patch of teeth on basibranchial four; 2, multiple bands or plates of teeth on basibranchial four.
76. Lateral process on rostrolateral aspect of hypobranchial one (modified from Feltes, 1986 character 48): 0, projection present on hypobranchial one; 1, no projection present on hypobranchial one.
77. Size of lateral process on rostrolateral aspect of hypobranchial one (modified from Feltes, 1986 character 48): 0, small raised projection on hypobranchial one; 1, large spur-like projection on hypobranchial one.
78. Lateral gill rakers on hypobranchial one: 0, gill rakers present on the lateral aspect of hypobranchial one; 1, gill rakers absent on the lateral aspect of hypobranchial one.
79. Shape of lateral gill rakers on hypobranchial one: 0, all elongated gill rakers on lateral aspect of hypobranchial one; 1, one to a few of the anteriormost lateral gill raker(s) flattened into plates or tubercles on hypobranchial one; 2, all gill rakers flattened into plates on the lateral aspect of hypobranchial one.
80. Lateral gill rakers on branchial arches two through four: 0, gill rakers present on the lateral aspect of branchial arches two through four; 1, gill rakers absent on the lateral aspect of branchial arches two through four.
81. Shape of lateral gill rakers on branchial arches two through four: 0, largely flat gill rakers on the lateral aspect of branchial arches two through four; 1, raised gill rakers on the lateral aspect of branchial arches two through four; 2, elongated gill rakers on the lateral aspect of branchial arches two through four.
82. Dorsal broadening of lateral gill rakers on branchial arches two through four: 0, lateral gill rakers largely uniform throughout margin; 1, lateral gill rakers with dorsal broadening around margin.
83. Accessory gill rakers on lateral aspect of branchial arches two through four: 0, accessory gill rakers absent on the lateral aspect of branchial arches two through four; 1, accessory gill rakers present between gill rakers on the lateral aspect of branchial arches two through four.
84. Medial gill rakers on branchial arches one through four: 0, gill rakers present on the medial aspect of branchial arches one through four; 1, gill rakers absent on the medial aspect of branchial arches one through four.
85. Shape of medial gill rakers on branchial arches one through four: 0, largely flat gill rakers on the medial aspect of branchial arches one through four; 1, raised gill rakers on the medial aspect of branchial arches one through four; 2, elongated gill rakers on the medial aspect of branchial arches one through four.
86. Accessory medial gill rakers on branchial arches one through four: 0, accessory gill rakers absent on the medial aspect of branchial arches one through four; 1, accessory gill rakers present between gill rakers on the medial aspect of branchial arches one through four.
87. Interarcual cartilage: 0, interarcual cartilage short; 1, interarcual cartilage elongate.
88. Articulation of epibranchial one with pharyngobranchial one (based on Hilton et al., 2010): 0, pharyngobranchial one attaches at the distal tip of the medial cartilage of epibranchial one; 1, pharyngobranchial one attaches proximally on the medial cartilage of epibranchial one; 2, pharyngobranchial one attaches proximally to the bone of epibranchial one.
89. Size of dorsal lamellar extension of epibranchial three: 0, small to moderate lamellar expansion on epibranchial three; 1, large lamellar expansion on epibranchial three.
90. Epibranchial two toothplate in serial association with pharyngobranchial two toothplate: 0, epibranchial two toothplate absent; 1, epibranchial two toothplate present.
91. Number of epibranchial toothplates associated with pharyngobranchial two toothplate: 0, one epibranchial two toothplate present; 1, multiple epibranchial two toothplates present.
92. Epibranchial three toothplate in serial association with pharyngobranchial three toothplate: 0, epibranchial three toothplate absent; 1, epibranchial three toothplate present.
93. Attachment of epibranchial three toothplate in serial association with pharyngobranchial three toothplate: 0, epibranchial three toothplate autogenous from

epibranchial three; 1, epibranchial three toothplate ankylosed to epibranchial three.

94. Stay on pharyngobranchial four (Collette et al., 1984 character 3; Johnson, 1986 character 31): 0, stay on pharyngobranchial four absent; 1, stay on pharyngobranchial four present.
95. Gill filament blades interconnected by cartilaginous bridges (Collette et al., 1984 character 6; Johnson, 1986 character 42): 0, gill filament blades not interconnected by cartilaginous bridges; 1, gill filament blades interconnected by cartilaginous bridges.
96. Pseudobranch filaments on inside of opercle: 0, pseudobranch present; 1, pseudobranch absent.
97. Spination on posterior margin of posttemporal: 0, no spination present on posterior margin of posttemporal; 1, one or more spines present on posterior margin of posttemporal.
98. Number of spines on posterior margin of posttemporal: 0, single spine present on posterior margin of posttemporal; 1, two or more spines present on posterior margin of posttemporal.
99. Dorsal laminar expansion on posttemporal: 0, laminar expansion absent; 1, laminar expansion present between the main body and the dorsalmost prong of the posttemporal.
100. Size of dorsal lamina on posttemporal: 0, laminar expansion on posttemporal slight; 1, laminar expansion on posttemporal large and leaf-like.
101. Prongs of the posttemporal (Gregory and Conrad, 1937, page 13; Nakamura, 1983 character 20): 0, two-pronged posttemporal; 1, three-pronged posttemporal.
102. Ossification of lateral-extrascapular tubule: 0, lateral-extrascapular tubule completely ossified; 1, lateral aspect of lateral-extrascapular tubule not completely ossified and open.
103. Medial-extrascapular: 0, medial-extrascapular absent; 1, medial-extrascapular present.
104. Position of medial-extrascapular: 0, medial-extrascapular positioned largely dorsal to lateral-extrascapular; 1, medial-extrascapular anteriorly displaced.
105. Accessory ossifications associated with extrascapular bones of supratemporal canal (modified from O'Toole, 2002 character 0): 0, accessory ossifications associated with extrascapular bones of supratemporal canal absent; 1, accessory ossifications associated with extrascapular bones of supratemporal canal present.
106. Number of accessory ossifications associated with extrascapular bones of supratemporal canal (modified from O'Toole, 2002 character 0): 0, one accessory ossification associated with extrascapular bones of supratemporal canal; 1, more than one accessory ossification associated with extrascapular bones of supratemporal canal.
107. Lateral- and medial-extrascapulars enlarged: 0, lateral and medial extrascapular as independent elements; 1, lateral and medial extrascapular enlarged and appear as single element.
108. Length of supracleithrum (modified from Feltes, 1986 character 2): 0, supracleithrum long; 1, supracleithrum short.
109. Dorsoposterior expansion of cleithrum: 0, expansion merging dorsally with posterior margin of cleithrum; 1, posterior margin of cleithrum confluent; 2, distinct leaf-like expansion present.
110. Postcleithrum/Postcleithra (modified from O'Toole, 2002 character 84): 0, one or more elements of the postcleithrum present; 1, postcleithral elements absent.
111. Number of postcleithra (modified from O'Toole, 2002 character 84): 0, two; 1, one.
112. Shape of dorsalmost element of postcleithrum: 0, dorsalmost element of postcleithrum posteriorly expanded. The element was leaf shaped; 1, dorsalmost element of the postcleithrum not posteriorly expanded throughout margin.
113. Length of coracoid relative to cleithrum: 0, ventral process of the coracoid does not reach same ventral plane as cleithrum; 1, ventral process of the coracoid reaches similar or past the ventral plane of cleithrum.
114. Proximity of ventral aspects of coracoid and cleithrum: 0, coracoid and ventral process of the cleithrum in close proximity or touching at ventral aspect; 1, coracoid and ventral process of the cleithrum are not close in proximity, distinctly separate.
115. Width of the ventral process of the coracoid: 0, ventral process of coracoid tapering to rod-like process; 1, ventral process of coracoid broadened by laminae, not rod-like at ventral aspect.
116. Dorsoposterior process on coracoid: 0, dorsoposterior process on coracoid present; 1, dorsoposterior process on coracoid absent.
117. Dorsoposterior process broadening distally: 0, absent, dorsoposterior process tapered distally; 1, present, dorsoposterior process possesses robust and plate-like expansion.
118. Insertion of scapula relative to the cleithrum (Feltes, 1986 character 1): 0, scapula inserts below angle of cleithrum; 1, scapula inserts at or above angle of cleithrum.
119. Number of foramina on scapula: 0, one scapular foramen present; 1, two scapular foramina present.
120. Position of scapular foramen (modified from Feltes, 1986 character 24): 0, scapular foramen largely equidistant from all margins of scapula; 1, scapular foramen anteriorly displaced, positioned near anterior margin of scapula.
121. Suturing between scapula and coracoid: 0, suturing between scapula and coracoid absent; 1, suturing between scapula and coracoid present.
122. Suturing between cleithrum and coracoid dorsally: 0, suturing between cleithrum and coracoid absent dorsally; 1, suturing between cleithrum and coracoid present dorsally.
123. Interdigitation between second and third pectoral radials: 0, margins of second and third pectoral radials are independent; 1, interdigitation between second and third pectoral radials present.
124. Interdigitation between third and fourth pectoral radials: 0, margins of third and fourth pectoral radials are independent; 1, interdigitation between the third and fourth pectoral radials present.
125. Position of third pectoral radial: 0, third pectoral radial inserts on scapula; 1, third pectoral radial spans

between scapula and coracoid; 2, third pectoral radial inserts on coracoid.

126. Position of fourth pectoral radial: 0, fourth pectoral radial inserts on interspace between scapula and coracoid; 1, fourth pectoral radial inserts on coracoid; 2, fourth pectoral radial inserts partially on both interspace and coracoid; 3, fourth pectoral radial inserts partially on scapula, interspace, and coracoid.
127. Longest pectoral radial (modified from Feltes, 1986 character 9): 0, fourth pectoral radial most elongate; 1, third pectoral radial most elongate.
128. Fourth pectoral radial (modified from Feltes, 1986 character 30): 0, fourth pectoral radial simple; does not possess any foramina or reinforced structures; 1, fourth pectoral radial with foramina and strut-like bone.
129. Free pectoral-fin rays on lower part of pectoral fin: 0, all pectoral-fin rays within membrane; 1, lowermost pectoral-fin rays thread-like and free from membrane.
130. Attachment of pelvic girdle: 0, pelvic girdle suspended from cleithrum or coracoid; 1, pelvic girdle suspended from postcleithra; 2, pelvic girdle free floating.
131. Supraneural elements (Smith-Vaniz, 1984 character 11): 0, supraneural elements present; 1, supraneural elements absent.
132. Spinous dorsal fin: 0, spines present in dorsal fin; 1, spines absent in dorsal fin.
133. Spinous and soft dorsal-fin arrangement: 0, dorsal fin arranged as one continuous fin consisting of spinous and soft dorsal-fin elements; 1, dorsal fin arranged into two dorsal fins. The first element completely spinous and the second element with one or more spines on principal element(s); 2, dorsal fin arranged into two dorsal fins. The first element completely spinous and the second element consisting of soft dorsal-fin rays.
134. Epicranial section of dorsal fin (Chapleau, 1993 character 2): 0, dorsal fin without epicranial section; 1, dorsal fin with an epicranial section.
135. Spine(s) on anteriormost dorsal pterygiophore: 0, dorsal spine present on anteriormost proximal-middle pterygiophore of spinous dorsal fin; 1, dorsal spine absent on anteriormost proximal-middle pterygiophore of spinous dorsal fin.
136. Number of dorsal-fin spines associated with anteriormost dorsal pterygiophore (modified from Johnson, 1986 characters 2 and 48): 0, two or more supernumerary spines associated with anteriormost dorsal pterygiophore; 1, single spine in serial correspondence associated with anteriormost dorsal pterygiophore.
137. Development of anteriormost proximal-middle pterygiophore of spinous dorsal fin (modified from Johnson, 1986 character 20): 0, anteriormost pterygiophore of spinous dorsal slender or moderately developed; 1, anteriormost pterygiophore of spinous dorsal greatly enlarged.
138. Anterior process on anteriormost proximal-middle pterygiophore of spinous dorsal fin: 0, anterior process on anteriormost proximal-middle pterygiophore of spinous dorsal fin absent; 1, anterior process on anteriormost proximal-middle pterygiophore of spinous dorsal fin present.
139. Shape of anterior process on first proximal-middle pterygiophore of spinous dorsal fin: 0, anterior process connected by lamellar bone to vertical part of pterygiophore; 1, anterior process free from lamellar bone.
140. Lateral expansion of distal radials of spinous dorsal fin (modified from Bridge, 1896 and Johnson and Patterson, 1993 character 22): 0, distal radials of spinous dorsal fin simple, without lateral expansions; 1, distal radials of spinous dorsal fin laterally expanded.
141. Shape of lateral expansion of distal radials of spinous dorsal fin (modified from Bridge, 1896 and Johnson and Patterson, 1993 character 22): 0, slight lateral expansion of distal radials of spinous dorsal fin; 1, lateral expansion of distal radials of spinous dorsal fin wing-like, forming a bony dorsal groove surrounding spinous dorsal fin.
142. Tripartite pterygiophores in posteriormost elements of soft dorsal fin (modified from Otero, 2004 character 20): 0, posteriormost pterygiophores of soft dorsal fin bipartite; 1, one or more tripartite pterygiophores in posteriormost elements of soft dorsal fin.
143. Number of tripartite pterygiophores in posteriormost elements of soft dorsal fin: 0, multiple tripartite pterygiophores in posteriormost elements of soft dorsal fin; 1, tripartite pterygiophore restricted to terminal pterygiophore of soft dorsal fin.
144. Detached dorsal and anal finlets supported by pterygiophores: 0, finlets absent; 1, finlets present.
145. Dorsal- and anal-fin pterygiophore stays (Smith-Vaniz, 1984 character 4): 0, dorsal- and anal-fin pterygiophore stays present; 1, dorsal- and anal-fin pterygiophore stays absent.
146. Posterior elongation of dorsal- and anal-fin pterygiophore stays: 0, dorsal- and anal-fin pterygiophore stays smaller, square-like elements; 1, dorsal- and anal-fin pterygiophore stays elongate, extending posteriorly toward the caudal fin.
147. Number of anal-fin pterygiophores anterior to first hemal spine (modified from Johnson, 1984; Smith-Vaniz, 1984 character 12; O'Toole, 2002 character 112): 0, one anal-fin pterygiophore anterior to first hemal spine; 1, two anal-fin pterygiophores anterior to first hemal spine; 2, more than two anal-fin pterygiophores anterior to first hemal spine.
148. Anal-fin pterygiophore(s) relationship to first hemal spine: 0, anal-fin pterygiophore(s) and first hemal spine closely applied or in contact; 1, anal-fin pterygiophore(s) and first hemal spine well separated.
149. Strength of connection between first anal-fin pterygiophore and first hemal spine (modified from Smith-Vaniz, 1984; Bannikov, 1987; Springer and Smith-Vaniz, 2008 character 11): 0, weak connection between first anal-fin pterygiophore and first hemal spine; 1, strong connection between first anal-fin pterygiophore and first hemal spine.
150. Anal-fin spines: 0, spinous element(s) of the anal fin present; 1, spinous element(s) of the anal fin absent.

151. Number of anal-fin spines associated with first anal-fin pterygiophore: 0, two supernumerary anal-fin spines on first anal-fin pterygiophore; 1, single spine in serial correspondence on first anal-fin pterygiophore.
152. Separation between second and third anal spines (Smith-Vaniz, 1984 character 14): 0, second and third anal spines closely applied; 1, second and third anal spines separated.
153. Angle of first anal-fin pterygiophore: 0, anteriormost anal-fin pterygiophore positioned at oblique angle; 1, anteriormost anal-fin pterygiophore sweeping rostrally, largely shaped like a C; 2, anteriormost anal-fin pterygiophore strut-like and largely vertical.
154. Epicentral bone on first abdominal vertebra: 0, epicentral bone on first abdominal vertebra present; 1, epicentral bone on first abdominal vertebra absent.
155. Insertion of epicentral bone on first abdominal vertebra (modified from O'Toole, 2002 character 116): 0, epicentral element on first abdominal vertebra inserts on neural arch; 1, epicentral element on first abdominal vertebra inserts on parapophysis.
156. Insertion of epicentral bone on second abdominal vertebra (modified from O'Toole, 2002 character 116): 0, epicentral element on second abdominal vertebra inserts on neural arch; 1, epicentral element on second abdominal vertebra inserts on parapophysis; 2, epicentral element on second abdominal vertebra inserts on vertebral centrum.
157. Anteriormost pleural rib borne on parapophysis: 0, pleural rib on third vertebra is first to be borne on a parapophysis; 1, pleural rib on fourth vertebra is first to be borne on a parapophysis; 2, pleural rib on vertebra five or posterior to fifth vertebra is first to be borne on a parapophysis.
158. Ossified epicentrals on caudal vertebrae: 0, ossified epicentrals on caudal vertebrae absent; 1, ossified epicentrals on caudal vertebrae present.
159. Configuration of the first hemal spine (modified from Otero, 2004 character 19): 0, first hemal spine with simple configuration, similar to more posterior hemal spines; 1, first hemal spine with trifid configuration.
160. Pleural ribs on terminal abdominal vertebrae: 0, pleural ribs associated with terminal abdominal vertebrae; 1, no pleural ribs associated with terminal abdominal vertebrae.
161. Shape of pleural rib on last abdominal vertebra: 0, pleural rib on terminal abdominal vertebra simple and largely linear; 1, pleural rib on terminal abdominal vertebra recurved.
162. Enlargement of the second abdominal neural spine: 0, second neural spine enlarged, often contacting all or part of the posterior margin of the neural arch on the first abdominal vertebra; 1, second neural spine similar-sized as surrounding neural spines. First and second neural spines may contact but not due to enlargement of the second neural spine.
163. Distal tips of posterior abdominal parapophyses: 0, distal tips of parapophyses separated in all abdominal vertebrae; 1, distal tips of posterior abdominal parapophyses directed medially and joined with the opposite parapophysis, often forming a single spine-like projection with a bifurcating distal tip.
164. Dorsally orientated horizontal bar between separated abdominal parapophyses (modified from Otero, 2004 character 19): 0, distal tips of posterior abdominal parapophyses not connected throughout their length; 1, distal tips of posterior abdominal parapophyses linked by a dorsally orientated transverse bridge.
165. Anal-fin ray count versus dorsal-fin ray count: 0, more dorsal-fin rays than anal-fin rays; 1, equal or more anal-fin rays than dorsal-fin rays.
166. Anterior neural zygapophyses on caudal vertebrae: 0, anterior neural zygapophyses largely oblique on caudal vertebrae; 1, anterior neural zygapophyses largely horizontal on caudal vertebrae.
167. Anterior hemal zygapophyses on caudal vertebrae: 0, anterior hemal zygapophyses largely oblique on caudal vertebrae; 1, anterior hemal zygapophyses largely horizontal on caudal vertebrae.
168. Posterior hemal zygapophyses on caudal vertebrae: 0, posterior hemal zygapophyses largely oblique on caudal vertebrae; 1, posterior hemal zygapophyses largely horizontal on caudal vertebrae.
169. Length of the neural spine on preural centrum two (modified from O'Toole, 2002 character 123): 0, neural spine of second preural centrum reduced, not extending posteriorly to the bend of the ural centrum; 1, neural spine of second preural centrum short, extending posteriorly to or slightly past the bend of the ural centrum; 2, neural spine of second preural centrum similar in length to neural spines on more anteriorly positioned caudal vertebrae.
170. Length of the neural spine on preural centrum three (modified from O'Toole, 2002 character 124): 0, neural spine on third preural centrum long, extends posteriorly past the hypurapophysis; 1, neural spine on third preural centrum short, extending at most to the anterior edge of the ural centrum.
171. Fusion of hemal arch on preural centrum three (O'Toole, 2002 character 125): 0, hemal arch autogenous from preural centrum three; 1, hemal arch fused to preural centrum three.
172. Foramen on proximal aspect of hemal spine associated with preural centrum two: 0, proximal aspect of hemal spine associated with preural centrum two without one or more foramina; 1, proximal aspect of hemal spine associated with preural centrum two with one or more foramina.
173. Parhypural and centrum of urostyle (Chapleau, 1993 character 35): 0, parhypural closely applied and articulating with centrum of urostyle; 1, parhypural forms a plate totally free of urostyle.
174. Radial cartilage located near the distal tip of fifth hypural: 0, radial cartilage near distal tip of the fifth hypural; 1, no radial cartilage near distal tip of the fifth hypural.
175. Radial cartilage between the distal tips of the parhypural and hemal spine of preural two: 0, radial cartilage situated between distal tips of the parhypural and hemal spine associated with the second preural centrum; 1, no radial cartilage situated between distal tips of the parhypural and hemal spine associated with the second preural centrum.

176. Radial cartilage between distal tips of preural two hemal spine and preural three hemal spine: 0, radial cartilage situated between distal tips of the second and third preural hemal spines; 1, no radial cartilage element situated between distal tips of the second and third preural hemal spines.
177. Number of radial cartilage segments between distal tips of preural two hemal spine and preural three hemal spine: 0, single radial cartilage situated between distal tips of the second and third preural hemal spines; 1, two elements of radial cartilage situated between distal tips of the second and third preural hemal spines.
178. Radial cartilage posterior to distal tip of neural spine of preural three: 0, radial cartilage posterior to distal tip of third preural neural spine; 1, no radial cartilage posterior to distal tip of third preural neural spine.
179. Radial cartilage anterior to distal tip of neural and hemal spines on preural three (based on Leis, 1994 character 14): 0, no radial cartilage anterior to the distal tip of the neural and hemal spines on the third preural centrum; 1, radial cartilage anterior to the distal tip of the neural and hemal spines on the third preural centrum.
180. Epural count (modified from Collette et al., 1984 character 7; Johnson, 1986 character 36): 0, two epurals present; 1, three epurals present; 2, one epural present.
181. Uroneural one (modified from Collette et al., 1984 character 30; Johnson, 1986 character 34; Otero, 2004 character 24): 0, uroneural one present; 1, uroneural one absent.
182. Uroneural two (modified from Collette et al., 1984 character 30; Johnson, 1986 character 34; Otero, 2004 character 24): 0, uroneural two present; 1, uroneural two absent.
183. Fusion of hypurals one and two (modified from Collette et al., 1984 character 35): 0, hypurals one and two autogenous from each other throughout margin; 1, hypurals one and two fused to each other along all or part of the margin.
184. Fusion of hypurals three and four (modified from Collette et al., 1984 character 32): 0, hypurals three and four autogenous from each other throughout margin; 1, hypurals three and four fused along all or part of the margin.
185. Fusion of hypurals two and three (modified from Otero, 2004 character 25): 0, hypurals two and three autogenous from each other throughout margin; 1, hypurals two and three fused along all or part of the margin.
186. Fusion of hypurals one and two to urostyle (modified from Otero, 2004 character 25): 0, hypurals one and two autogenous from urostyle; 1, hypurals one and two fused to urostyle.
187. Fusion of hypurals three and four to urostyle (modified from, Otero, 2004 character 25): 0, hypurals three and four autogenous from urostyle; 1, hypurals three and four fused to urostyle.
188. Procurrent spur on ventral aspect of lower procurrent caudal-fin ray (Johnson, 1975): 0, procurrent spur absent; 1, procurrent spur present.
189. Proximal base of caudal-fin ray preceding procurrent ray shortened (Johnson, 1975): 0, proximal base of caudal-fin ray preceding procurrent ray not shortened; 1, proximal base of caudal-fin ray preceding procurrent ray shortened.
190. Hypurostegy (Collette et al., 1984 character 14; Johnson, 1986 character 33): 0, hypurostegy absent; 1, hypurostegy present. Proximal bases of caudal-fin rays partially or completely cover hypurals.
191. Caudal-peduncle keel (modified from Nakamura, 1983 character 12): 0, caudal peduncle keel absent; 1, caudal peduncle keel present.
192. Gas bladder: 0, gas bladder absent; 1, gas bladder present.
193. Gas bladder shape: 0, gas bladder without anterior extensions; 1, gas bladder with anterior extensions.
194. Position of anterior gas bladder extensions: 0, anterior gas bladder extensions positioned laterally between base of neurocranium and shoulder girdle; 1, anterior gas bladder extensions inserting into basioccipital foramina.
195. Posterior extension(s) of gas bladder: 0, gas bladder terminates in body cavity anterior to anal-fin origin; 1, gas bladder posteriorly extending, extending caudally at least to the first hemal arch.
196. Lateral-line scales extend onto caudal fin: 0, pored lateral-line scales absent from caudal fin; 1, pored lateral-line scales extending onto caudal fin.
197. Enlarged pelvic-fin axial 'scale': 0, pelvic axial 'scale' not enlarged at the point of insertion of the pelvic fin; 1, pelvic axial 'scale' enlarged at the point of insertion of the pelvic fin.
198. Lateral external pigmentation (Harrington et al., 2016 character 4): 0, symmetrical pigmentation between left and right sides; 1, asymmetrical pigmentation between left and right sides.
199. Scale type (based on descriptions by Johnson, 1984; Roberts, 1993; Bräger and Moritz, 2016 fig. 5): 0, scales cycloid type; 1, scales transforming ctenoid type; 2, scales whole ctenoid type; 3, scales peripheral ctenoid type; 4, scales spinoid type; 5, scales crenate type.
200. Scale shape: 0, scales largely rounded; 1, scales elongate.
201. Scutes (Gushiken, 1988 character 8): 0, scutes absent; 1, scutes present.